First Dark Matter Results from the LUX Experiment at SURF

arXiv:1310.8214 Submitted to PRL October 30, 2013

Berkeley Lab

LUX

Sanford Underground Research Facility

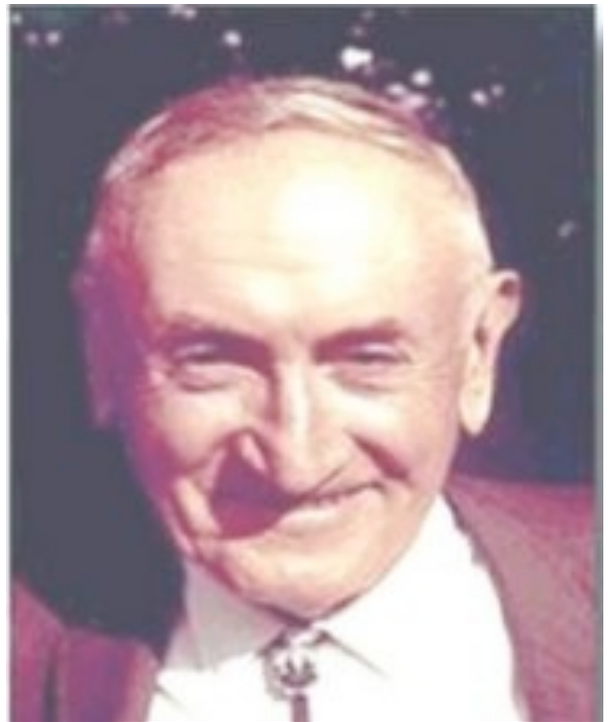

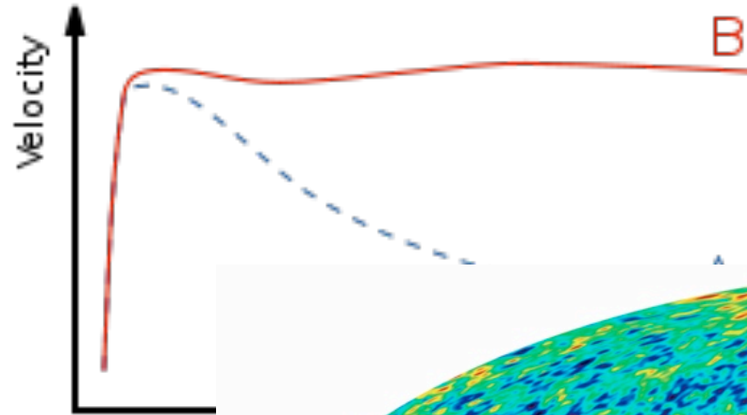
Velocity
B

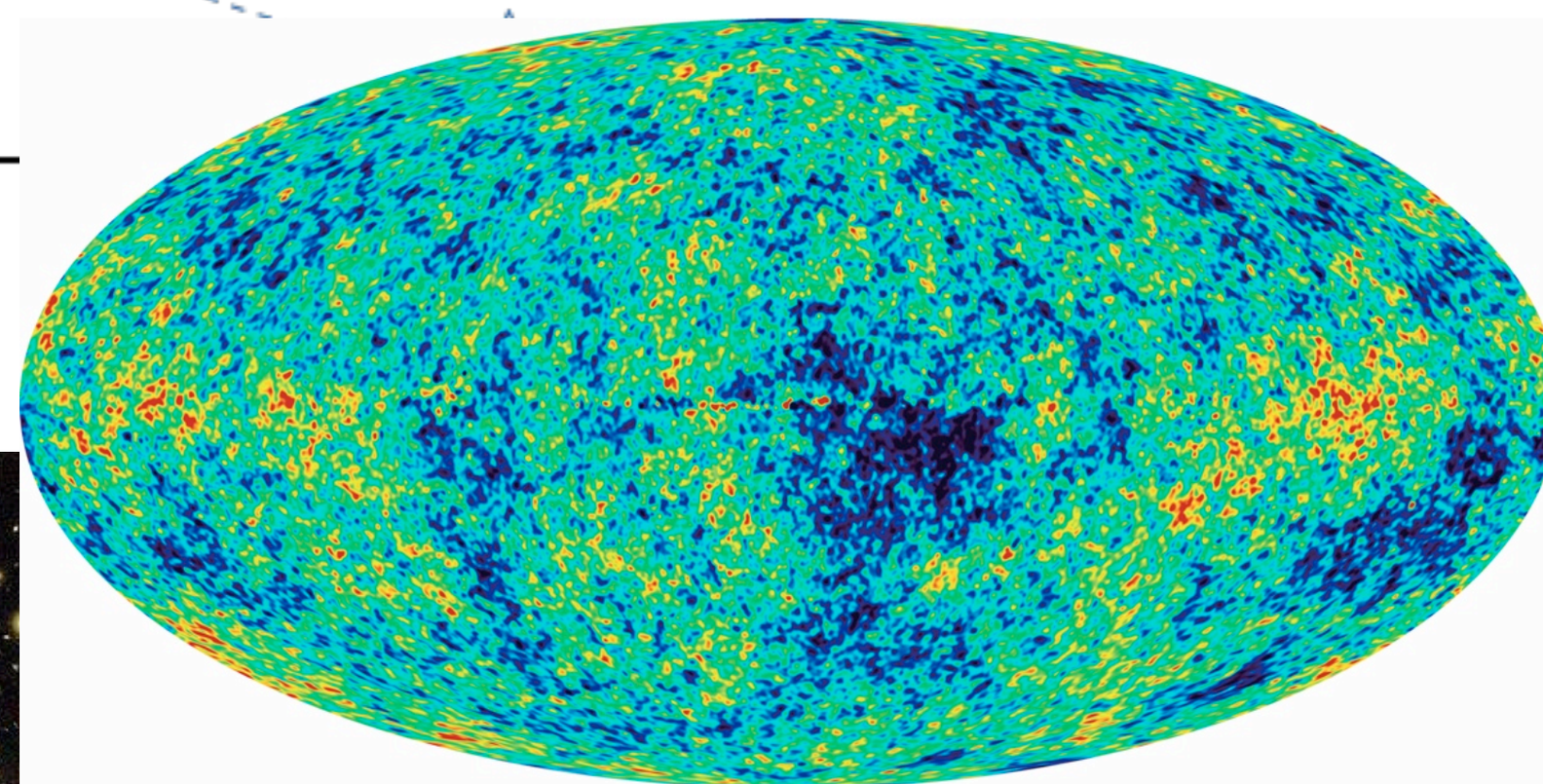

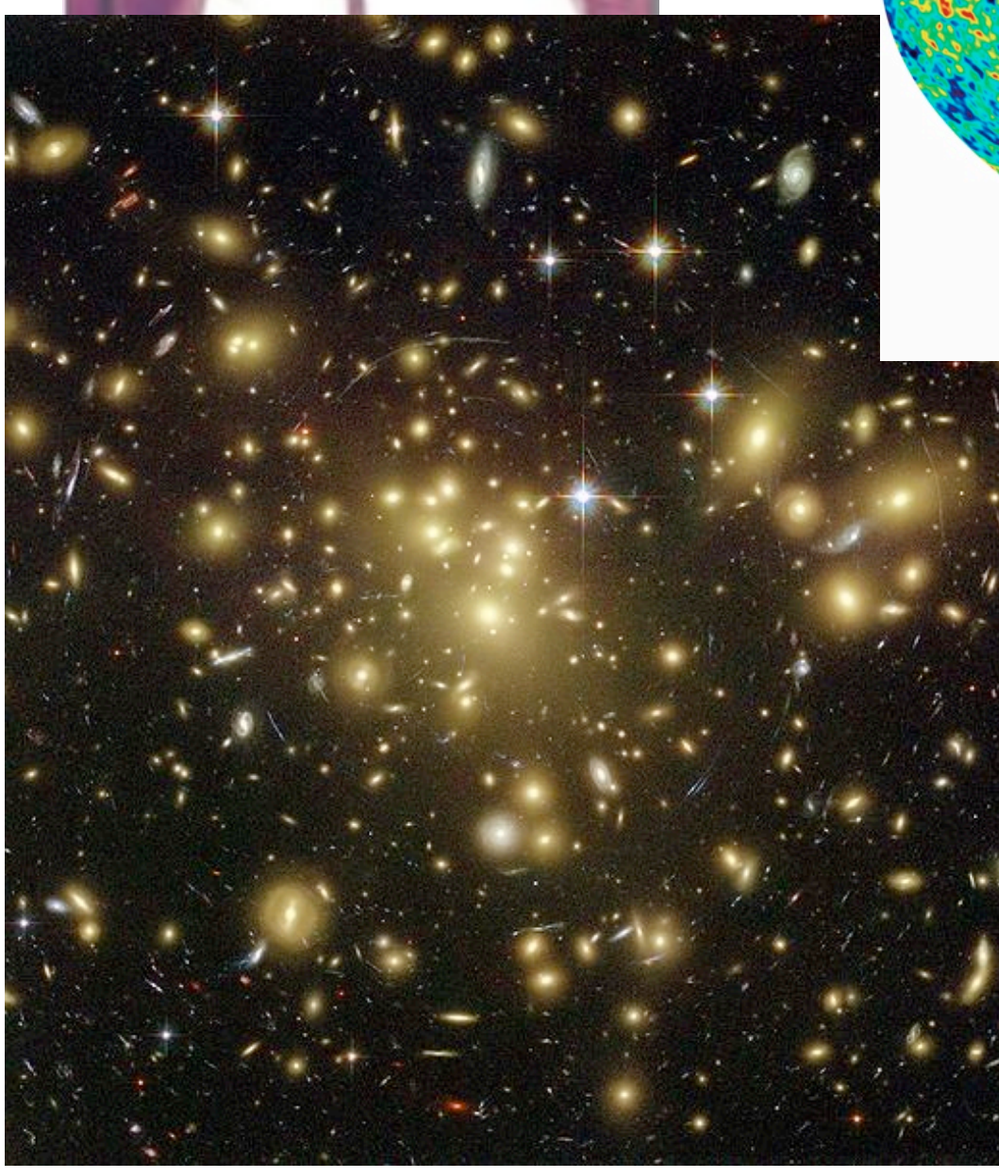

But we don't really know what it is...

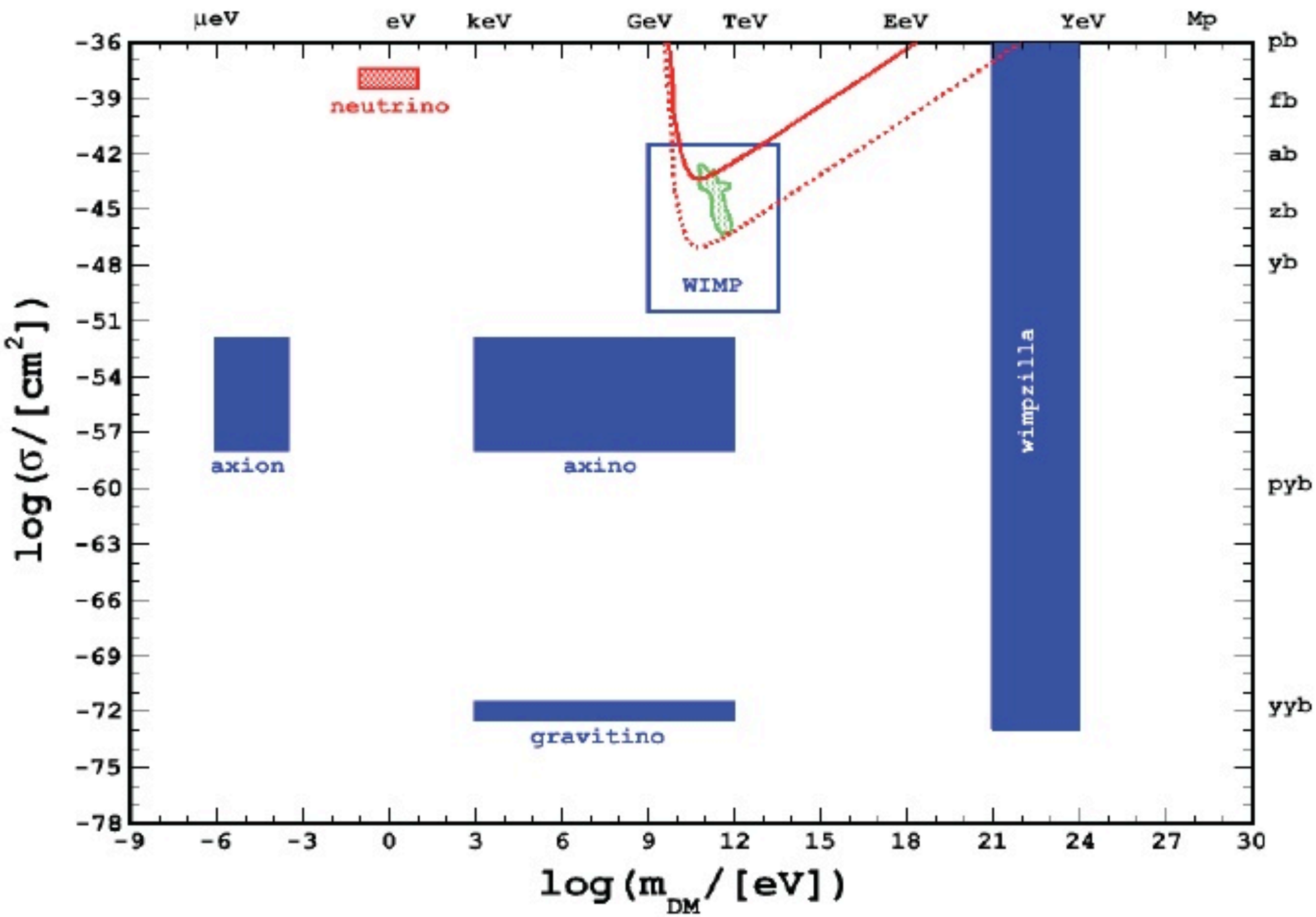

Karen Gibson

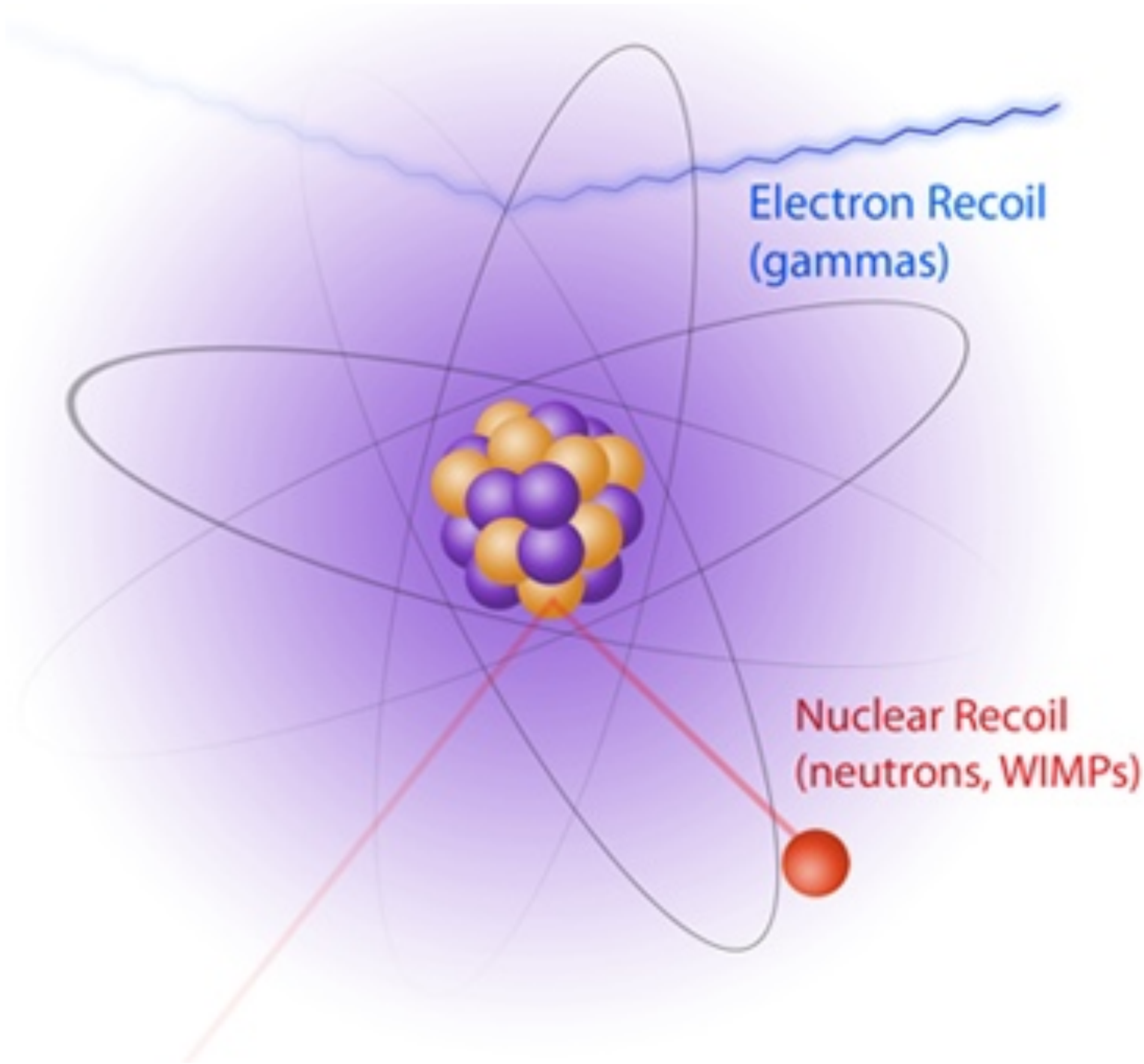
Electron Recoil
(gammas)
Nuclear Recoil
(neutrons, WIMPs)

Experimental Approaches

Direct Detection Techniques

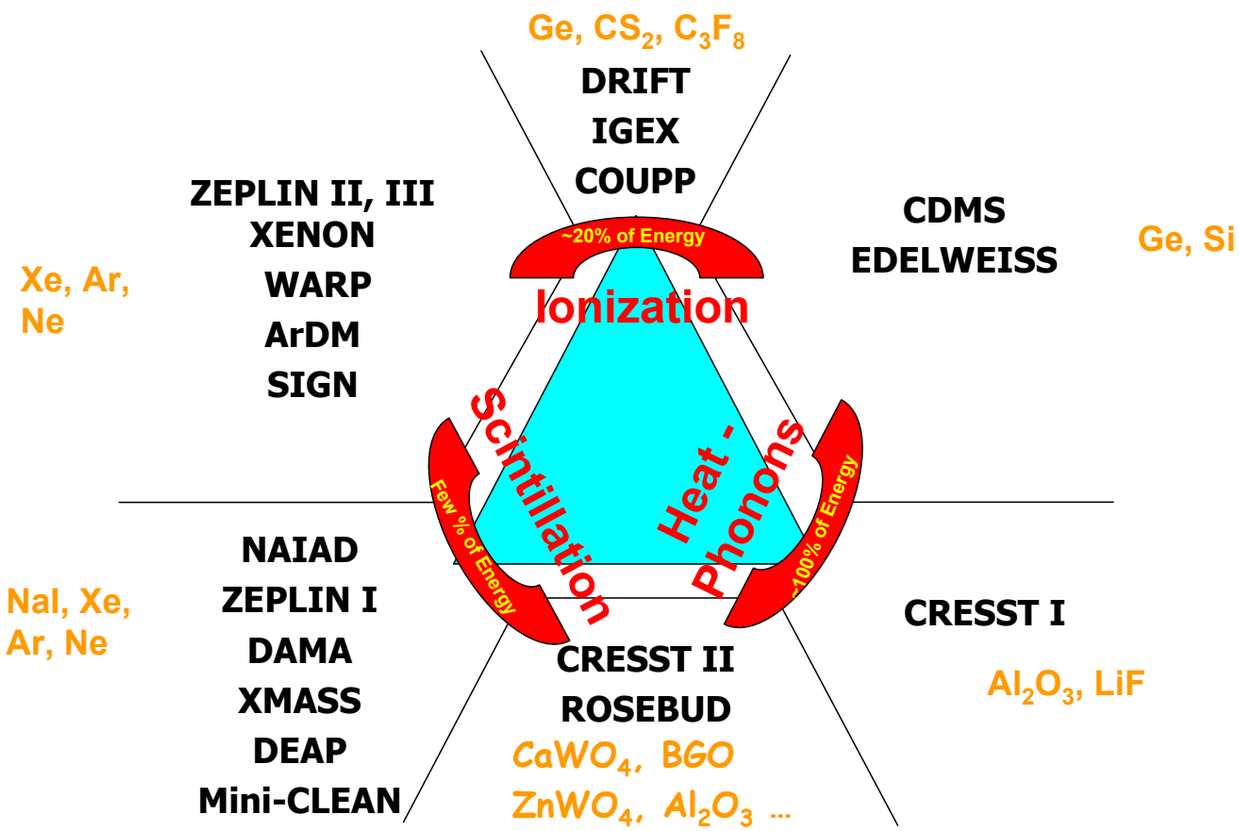

As large an amount of information and a signal to noise ratio as possible

An expanding community

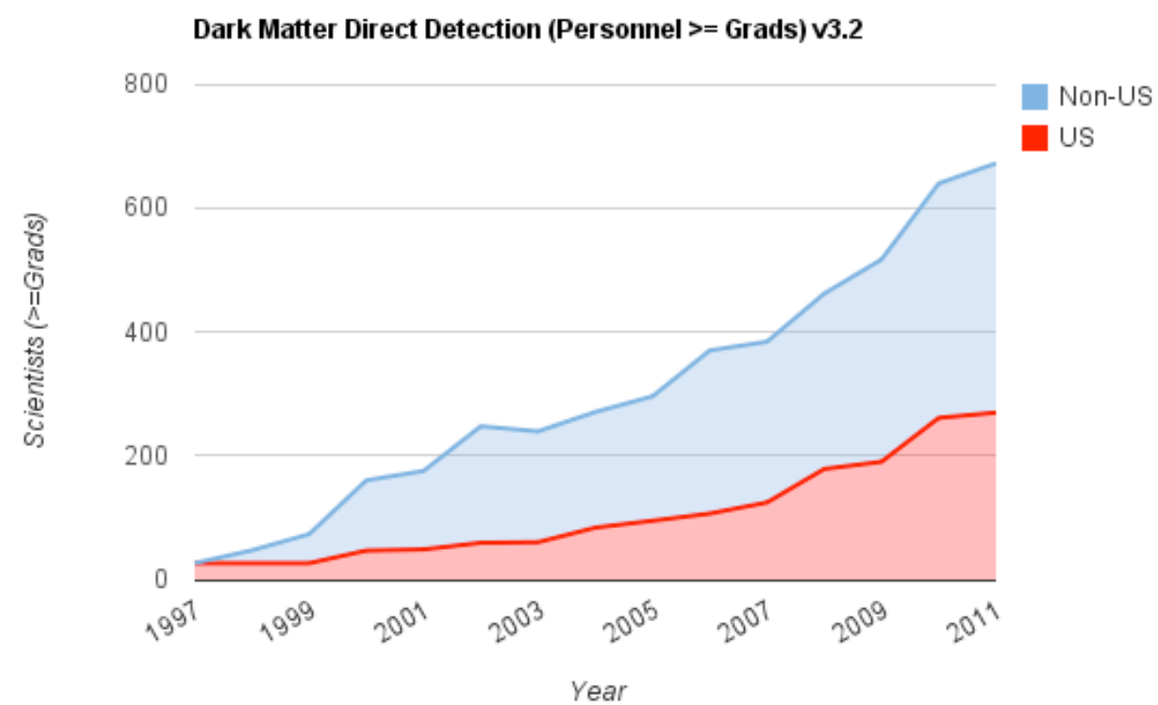

At least two pieces of information in order to
- recognize nuclear recoil
- extract rare events from background (self consistency)
- + fiducial cuts (self shielding, bad regions)

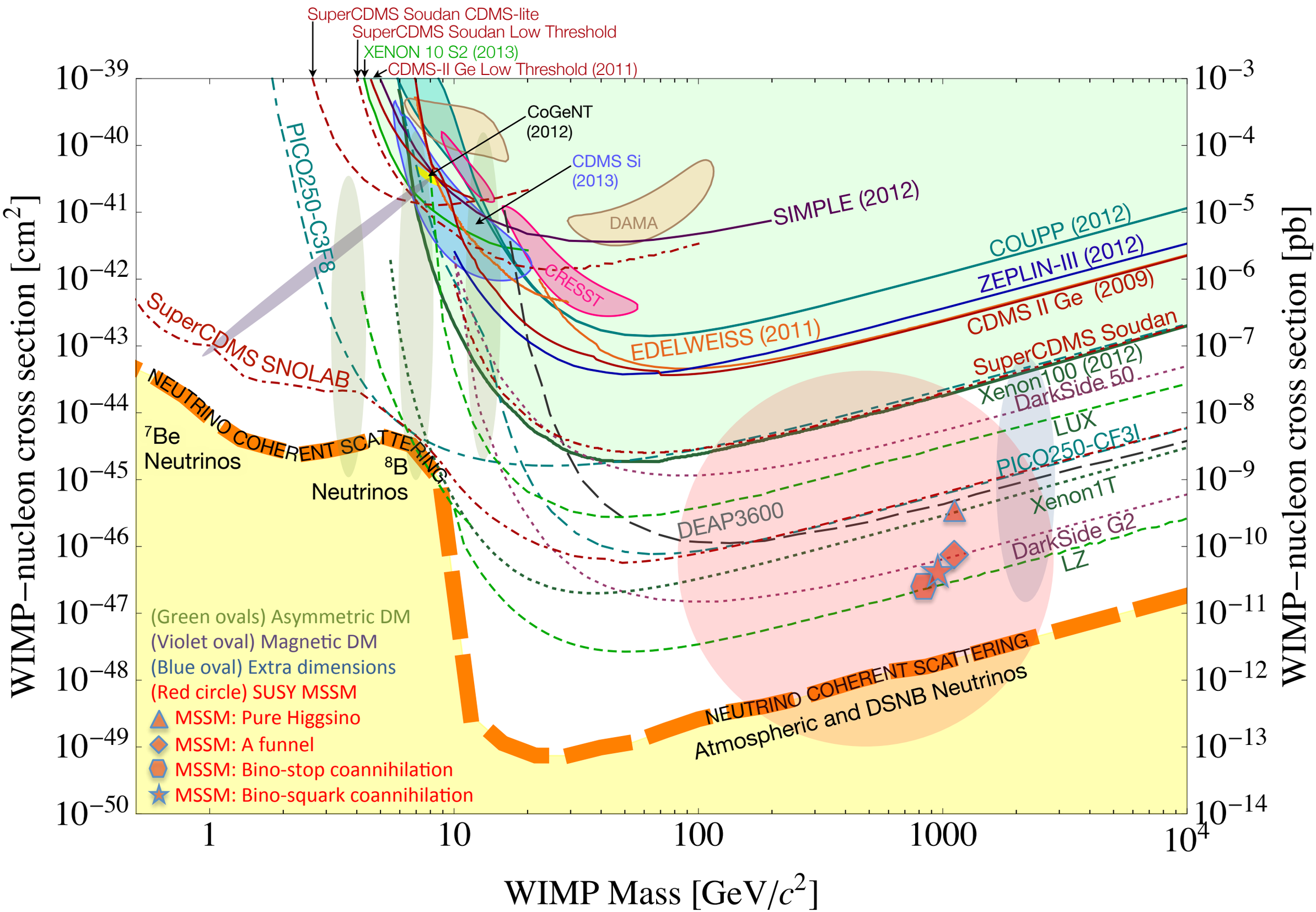
SuperCDMS Soudan CDMS-lite
SuperCDMS Soudan Low Threshold
XENON 10 S2 (2013)
CDMS-II Ge Low Threshold (2011)
CoGeNT (2012)
CDMS Si (2013)
DAMA
SIMPLE (2012)
COUPP (2012)
ZEPLIN-III (2012)
CDMS II Ge (2009)
SuperCDMS Soudan
Xenon100 (2012)
DarkSide 50
LUX
PICO250-CF3I
Xenon1T
DarkSide G2
LZ
DEAP3600
EDELWEISS (2011)
CRESST
PICO250-C3F8
SuperCDMS SNOLAB
NEUTRINO COHERENT SCATTERING
^{7}Be Neutrinos
^{8}B Neutrinos
NEUTRINO COHERENT SCATTERING
Atmospheric and DSNB Neutrinos
(Green ovals) Asymmetric DM
(Violet oval) Magnetic DM
(Blue oval) Extra dimensions
(Red circle) SUSY MSSM
MSSM: Pure Higgsino
MSSM: A funnel
MSSM: Bino-stop coannihilation
MSSM: Bino-squark coannihilation
WIMP–nucleon cross section [cm^2]
WIMP–nucleon cross section [pb]
WIMP Mass [GeV/c^2]
10^{-39}
10^{-40}
10^{-41}
10^{-42}
10^{-43}
10^{-44}
10^{-45}
10^{-46}
10^{-47}
10^{-48}
10^{-49}
10^{-50}
10^{-3}
10^{-4}
10^{-5}
10^{-6}
10^{-7}
10^{-8}
10^{-9}
10^{-10}
10^{-11}
10^{-12}
10^{-13}
10^{-14}
1
10
100
1000
10^4

WIMP direct detection signal in liquid Xenon

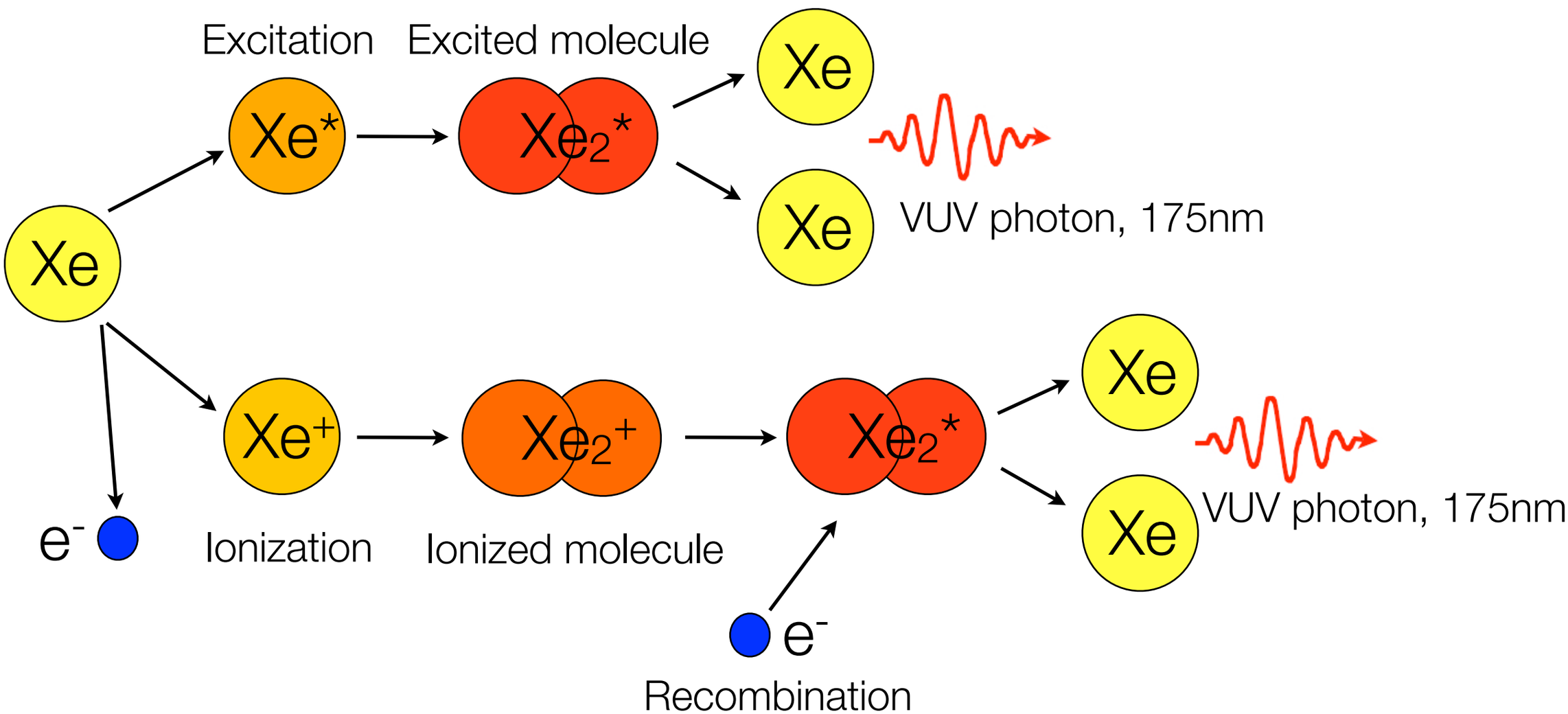

Two-phase Xenon WIMP Detectors

Z position from S1 – S2 timing
X-Y positions from S2 light pattern

Excellent 3D imaging (~mm resolution)
- eliminates edge events
- rejects multiple scatters

Gamma ray, neutron backgrounds reduced by self-shielding

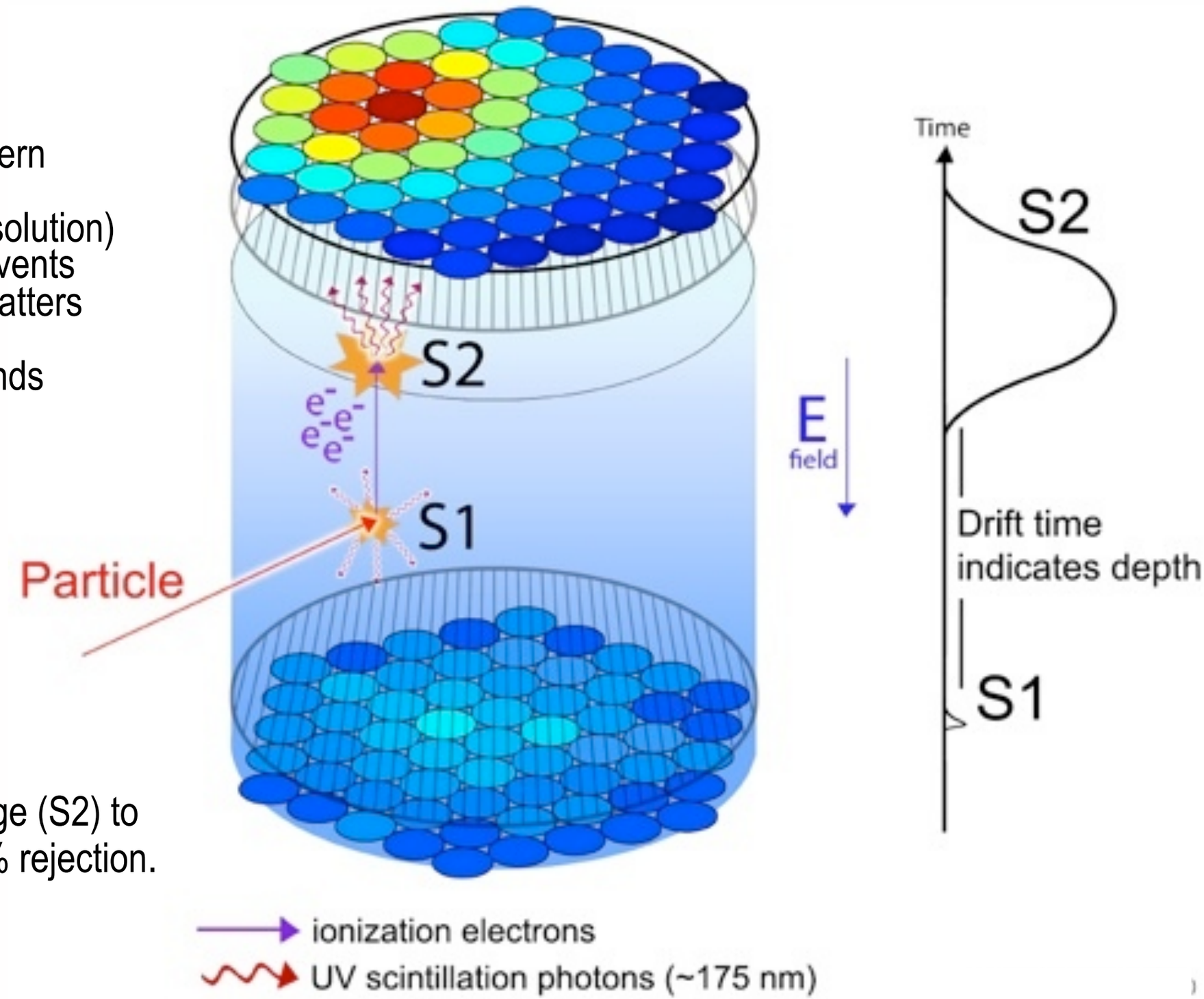

Reject gammas, betas by charge (S2) to light (S1) ratio. Expect > 99.5% rejection.

Light to charge ratio separates nuclear and electronic recoils

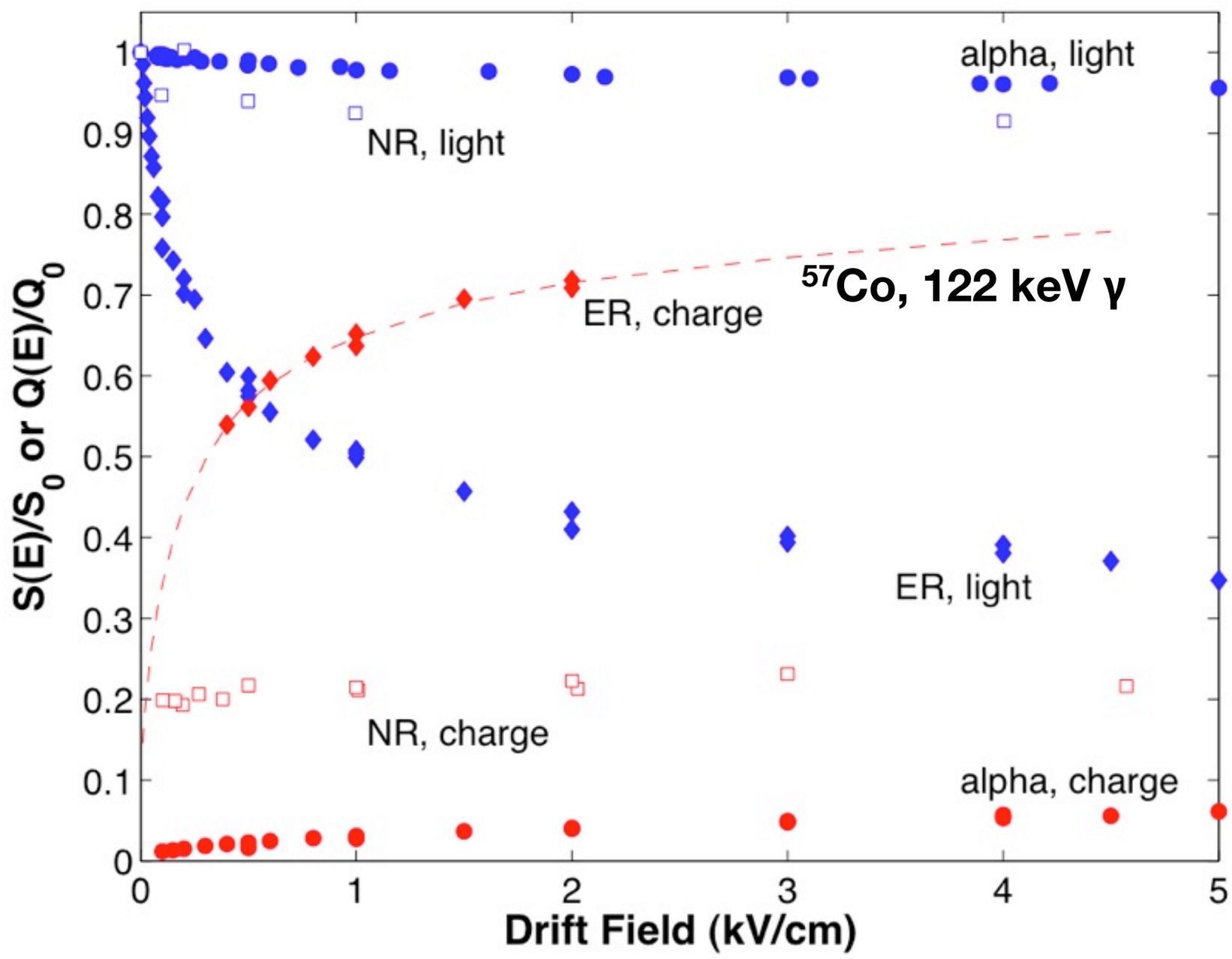

E. Aprile et al., Phys. Rev. Lett. **97**, 081302 (2006)

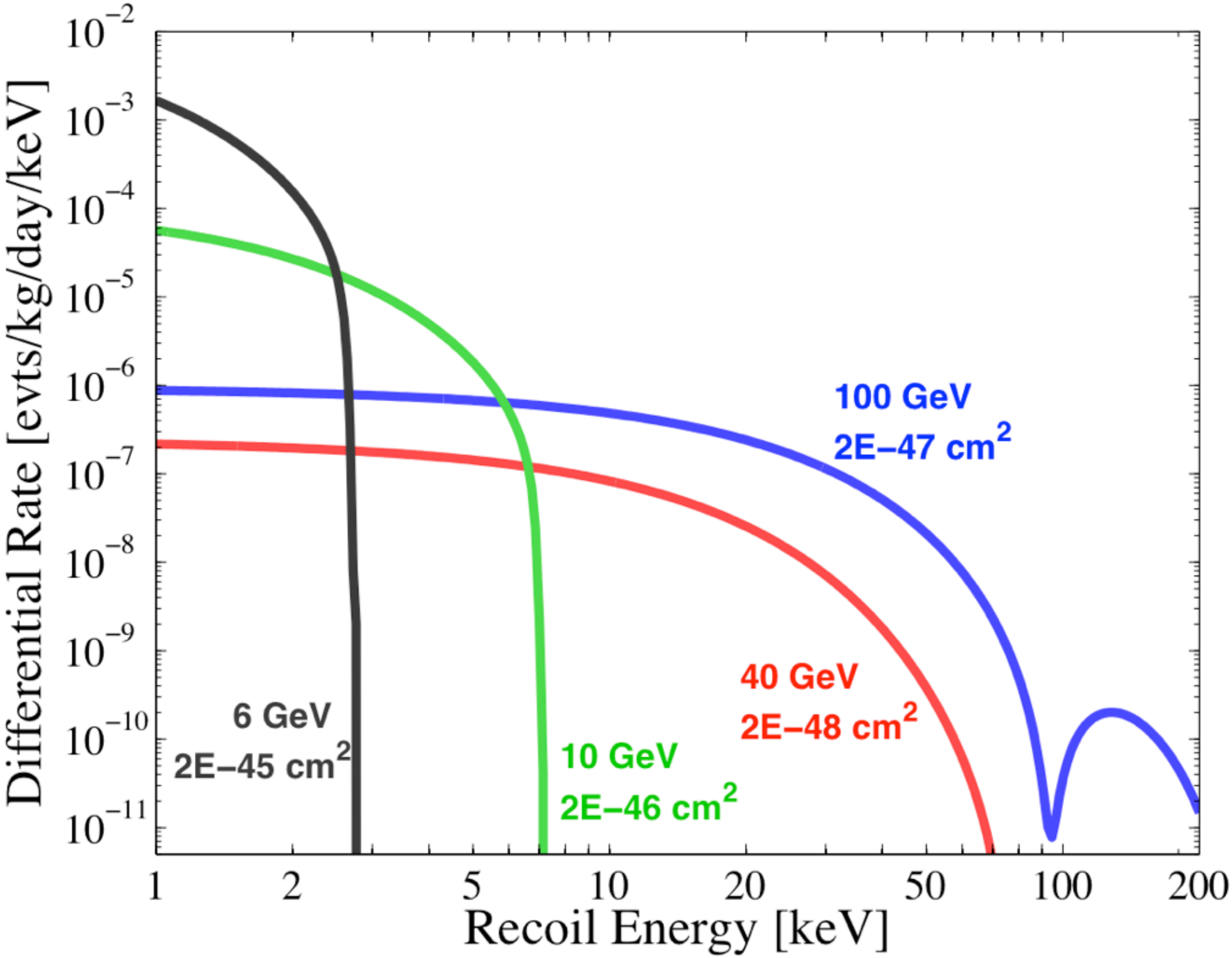
Differential Rate [evts/kg/day/keV]
10^{-2}
10^{-3}
10^{-4}
10^{-5}
10^{-6}
10^{-7}
10^{-8}
10^{-9}
10^{-10}
10^{-11}
1
2
5
10
20
50
100
200
Recoil Energy [keV]
100 GeV
2E−47 cm^2
40 GeV
2E−48 cm^2
10 GeV
2E−46 cm^2
6 GeV
2E−45 cm^2

Noble Element Scintillation Technique (NEST)

$$E_{ee} = (n_\gamma + n_e)W$$

$$E_{nr} = \mathcal{L}^{-1}(n_\gamma + n_e)W$$

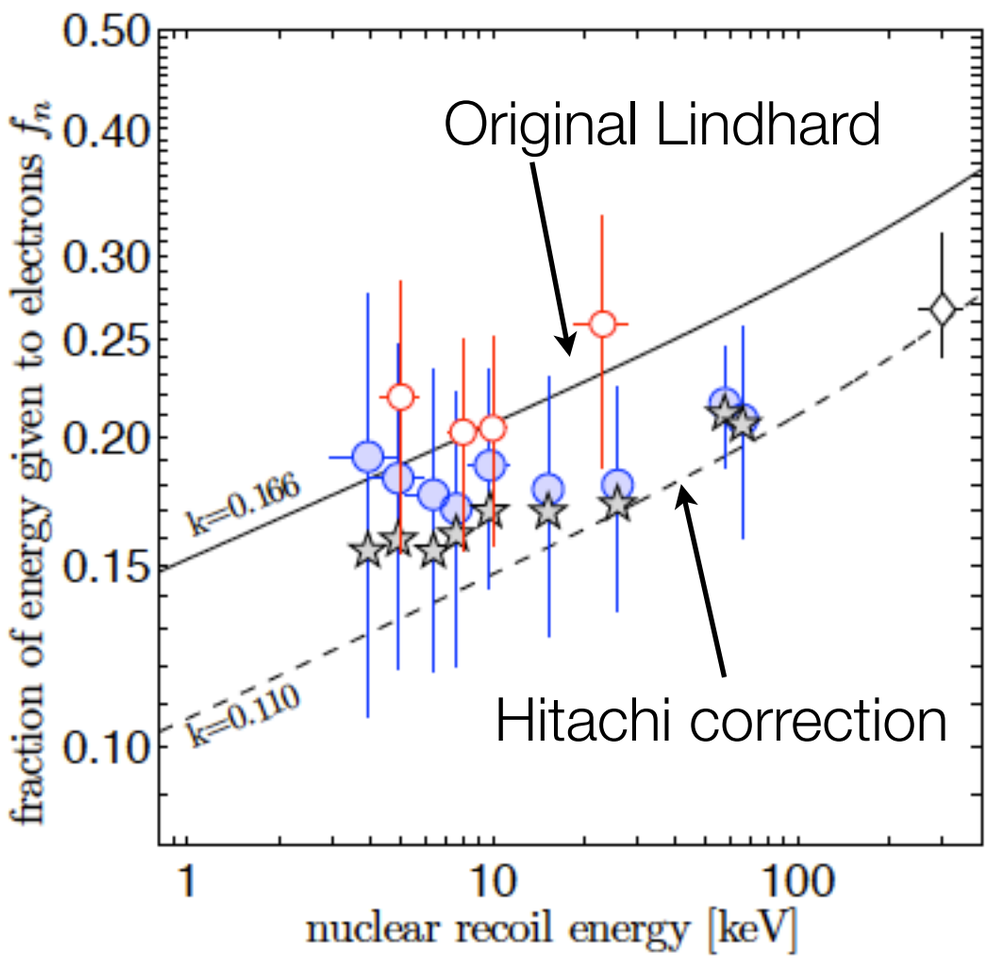

Uses full Lindhard model with Hitachi linear energy transfer (LET)

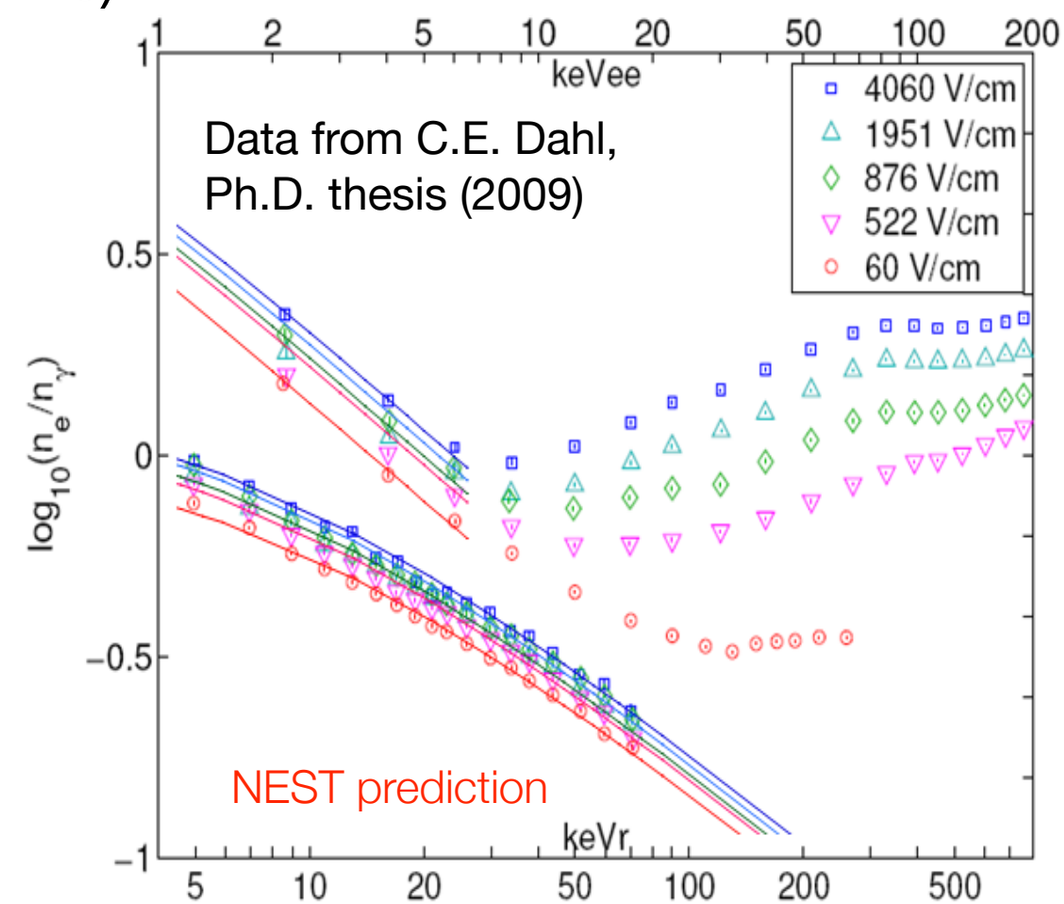

Reproduces NR discrimination data

P. Sorensen and C.E. Dahl, Phys. Rev. D **83**, 063501 (2011)

M. Szydagis et al., JINST 6, p10002 (2011)

Light and Charge Yields

- LUX imposes cutoff in light and charge yields below 3 keVnr, to be conservative.
- Includes predicted electric field quenching of light signal, to 77-82% of the zero-field light yield

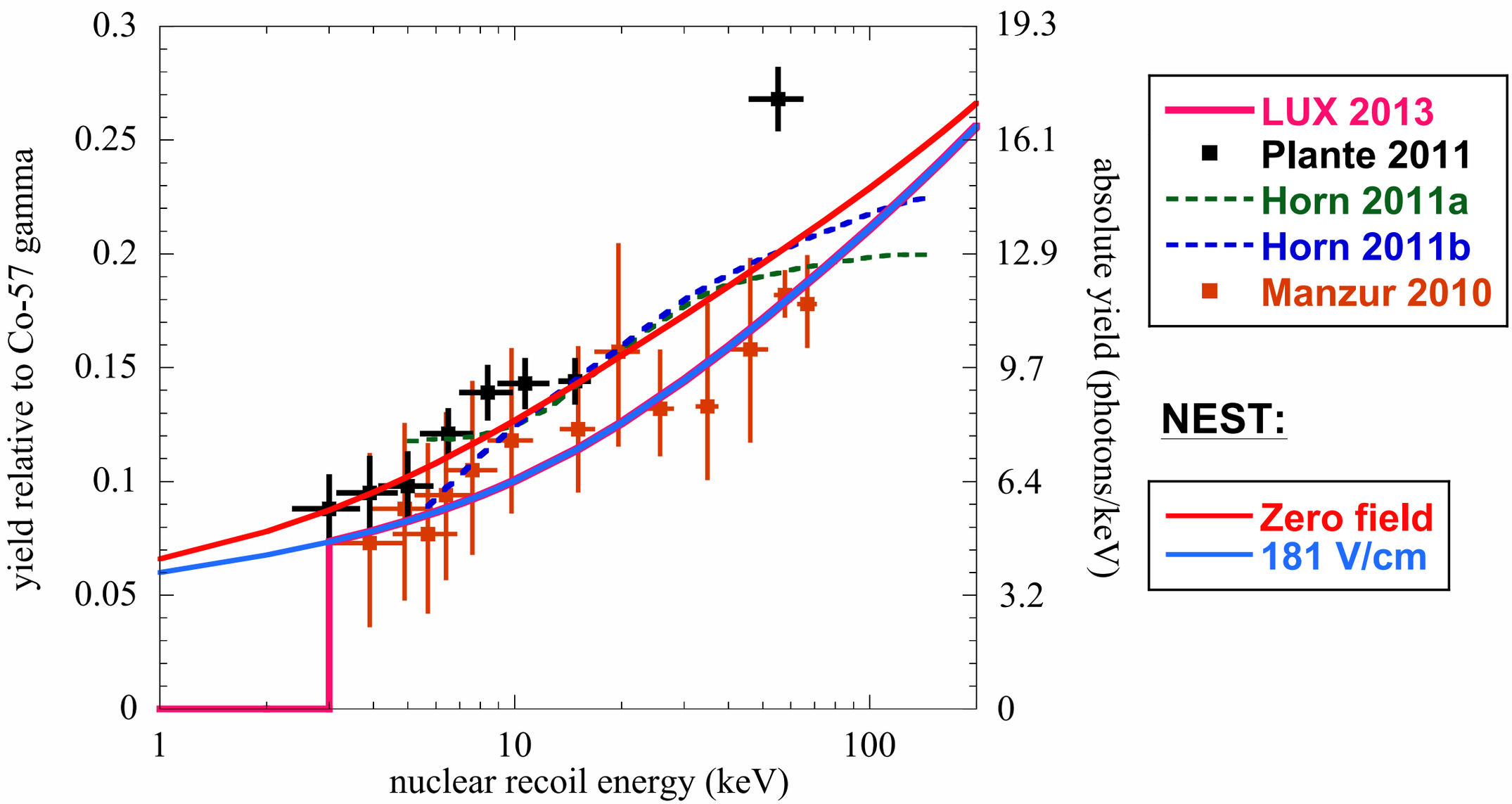

The LUX Collaboration: ~100 researchers from 17 institutions

Collaboration Meeting, Sanford Lab, April 2013

Brown

Richard Gaitskell	PI, Professor
Simon Fiorucci	Research Associate
Monica Pangilinan	Postdoc
Jeremy Chapman	Graduate Student
David Malling	Graduate Student
James Verbus	Graduate Student
Samuel Chung Chan	Graduate Student
Dongqing Huang	Graduate Student

Case Western

Thomas Shutt	PI, Professor
Dan Akerib	PI, Professor
Karen Gibson	Postdoc
Tomasz Biesiadzinski	Postdoc
Wing H To	Postdoc
Adam Bradley	Graduate Student
Patrick Phelps	Graduate Student
Chang Lee	Graduate Student
Kati Pech	Graduate Student

Imperial College London

Henrique Araujo	PI, Reader
Tim Sumner	Professor
Alastair Currie	Postdoc
Adam Bailey	Graduate Student

Lawrence Berkeley + UC Berkeley

Bob Jacobsen	PI, Professor
Murdock Gilchriese	Senior Scientist
Kevin Lesko	Senior Scientist
Carlos Hernandez Faham	Postdoc
Victor Gehman	Scientist
Mia Ihm	Graduate Student

Lawrence Livermore

Adam Bernstein	PI, Leader of Adv. Detectors Group
Dennis Carr	Mechanical Technician
Kareem Kazkaz	Staff Physicist
Peter Sorensen	Staff Physicist
John Bower	Engineer

LIP Coimbra

Isabel Lopes	PI, Professor
Jose Pinto da Cunha	Assistant Professor
Vladimir Solovov	Senior Researcher
Luiz de Viveiros	Postdoc
Alexander Lindote	Postdoc
Francisco Neves	Postdoc
Claudio Silva	Postdoc

SD School of Mines

Xinhua Bai	PI, Professor
Tyler Liebsch	Graduate Student
Doug Tiedt	Graduate Student

SDSTA

David Taylor	Project Engineer
Mark Hanhardt	Support Scientist

Texas A&M

James White †	PI, Professor
Robert Webb	PI, Professor
Rachel Mannino	Graduate Student
Clement Sofka	Graduate Student

UC Davis

Mani Tripathi	PI, Professor
Bob Svoboda	Professor
Richard Lander	Professor
Britt Holbrook	Senior Engineer
John Thomson	Senior Machinist
Ray Gerhard	Electronics Engineer
Aaron Manalaysay	Postdoc
Matthew Szydagis	Postdoc
Richard Ott	Postdoc
Jeremy Mock	Graduate Student
James Morad	Graduate Student
Nick Walsh	Graduate Student
Michael Woods	Graduate Student
Sergey Uvarov	Graduate Student
Brian Lenardo	Graduate Student

UC Santa Barbara

Harry Nelson	PI, Professor
Mike Witherell	Professor
Dean White	Engineer
Susanne Kyre	Engineer
Carmen Carmona	Postdoc
Curt Nehrkorn	Graduate Student
Scott Haselschwardt	Graduate Student

University College London

Chamkaur Ghag	PI, Lecturer
Lea Reichhart	Postdoc

University of Edinburgh

Alex Murphy	PI, Reader
Paolo Beltrame	Research Fellow
James Dobson	Postdoc

University of Maryland

Carter Hall	PI, Professor
Attila Dobi	Graduate Student
Richard Knoche	Graduate Student
Jon Balajthy	Graduate Student

University of Rochester

Frank Wolfs	PI, Professor
Wojtek Skutski	Senior Scientist
Eryk Druszkiewicz	Graduate Student
Mongkol Moongweluwan	Graduate Student

University of South Dakota

Dongming Mei	PI, Professor
Chao Zhang	Postdoc
Angela Chiller	Graduate Student
Chris Chiller	Graduate Student
Dana Byram	*Now at SDSTA

Yale

Daniel McKinsey	PI, Professor
Peter Parker	Professor
Sidney Cahn	Lecturer/Research Scientist
Ethan Bernard	Postdoc
Markus Horn	Postdoc
Blair Edwards	Postdoc
Scott Hertel	Postdoc
Kevin O'Sullivan	Postdoc
Nicole Larsen	Graduate Student
Evan Pease	Graduate Student
Brian Tennyson	Graduate Student
Ariana Hackenburg	Graduate Student
Elizabeth Boulton	Graduate Student

LUX Benefits from an Exceptional Lab and Exceptional Lab Support

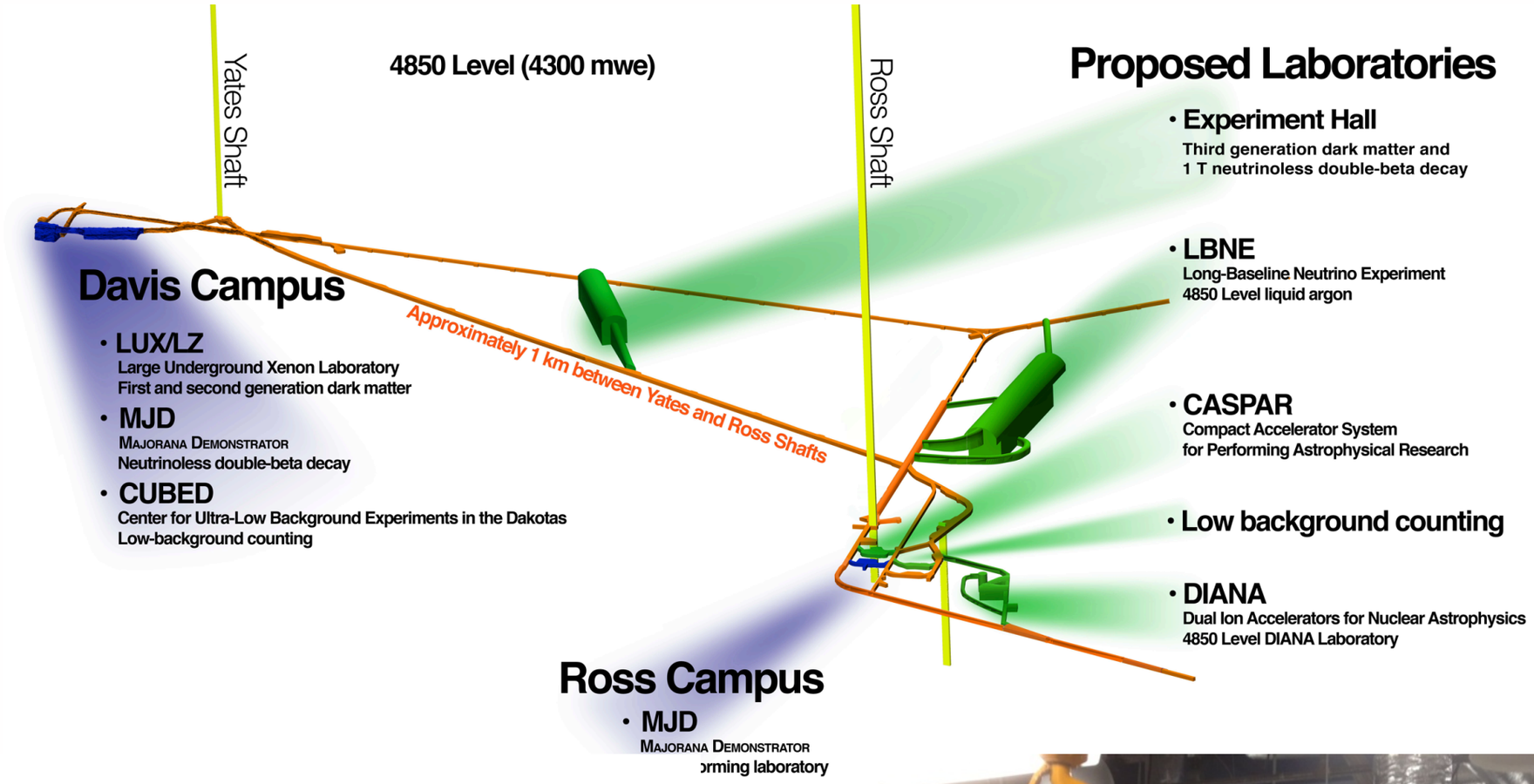

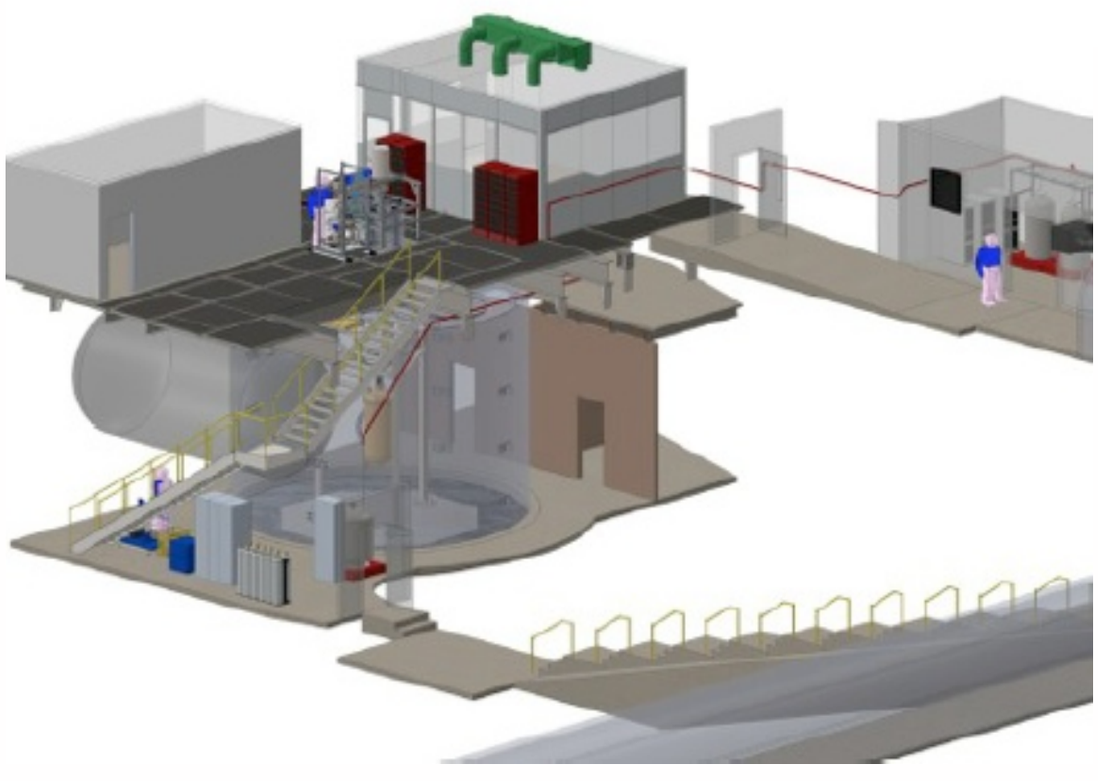

The LUX Detector

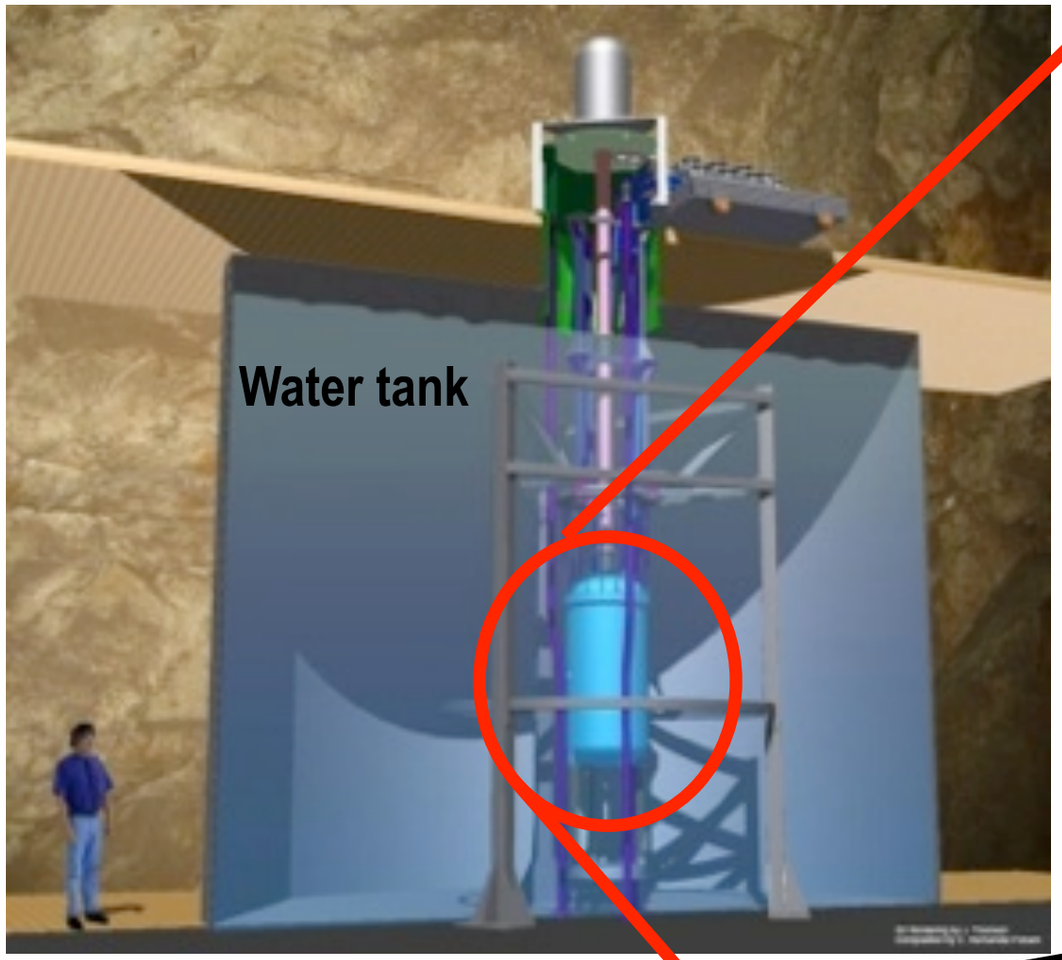

Low-radioactivity
Titanium Cryostat

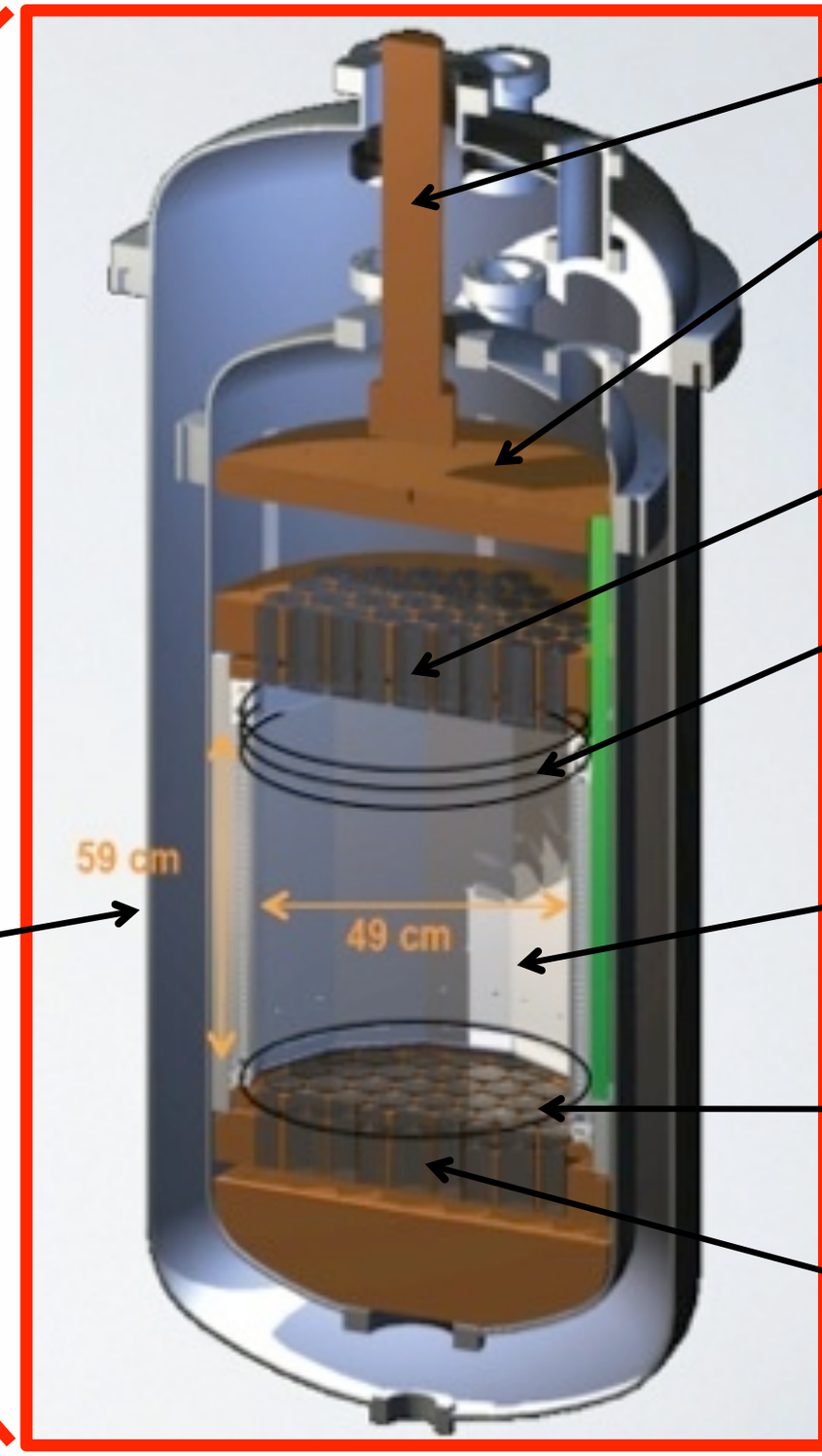

Thermosyphon

Copper shield

Top PMT array

Anode grid

PTFE reflector panels and field cage

Cathode grid

Bottom PMT array

370 kg total xenon mass
250 kg active liquid xenon
118 kg fiducial mass

LUX – the Instrument

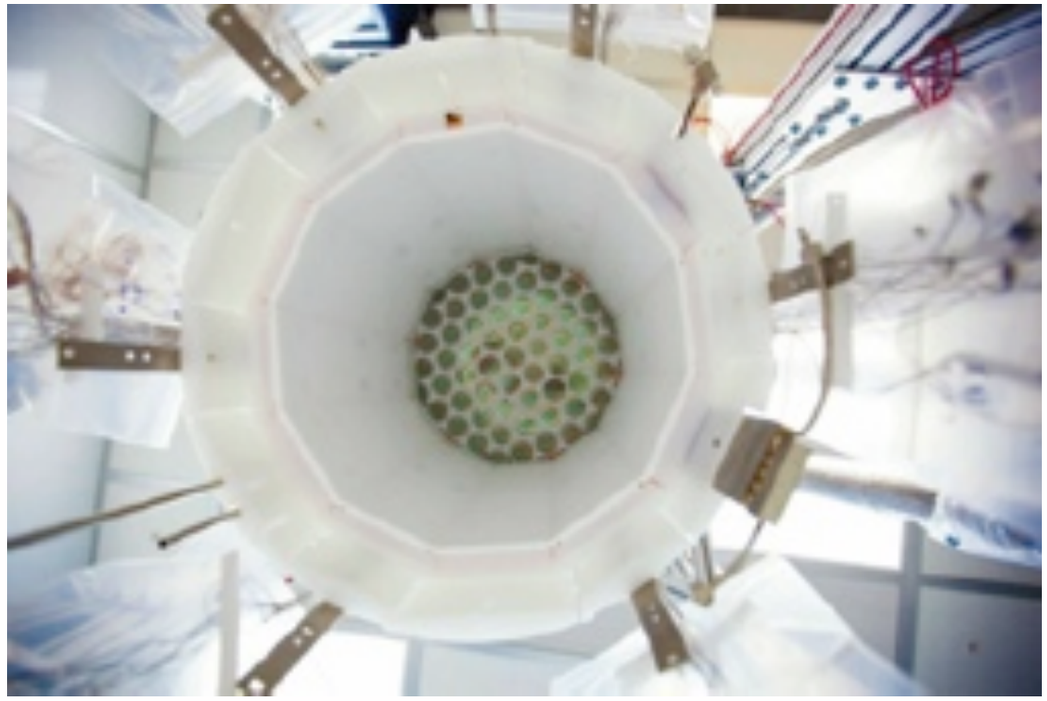

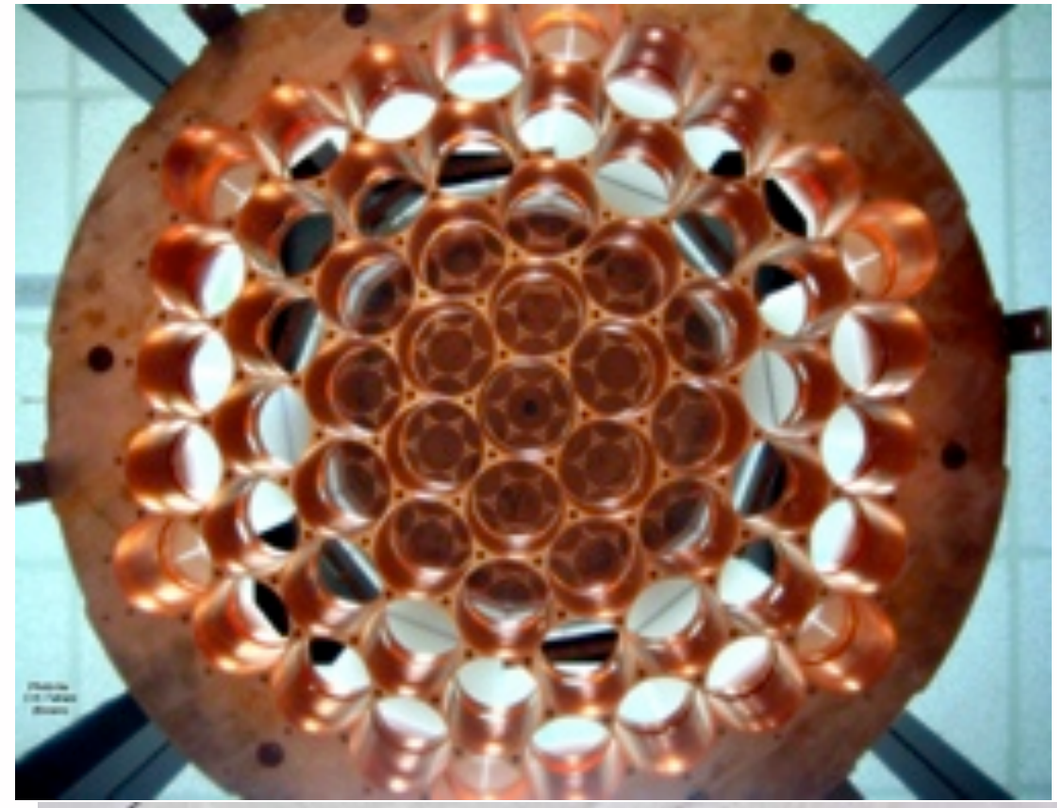

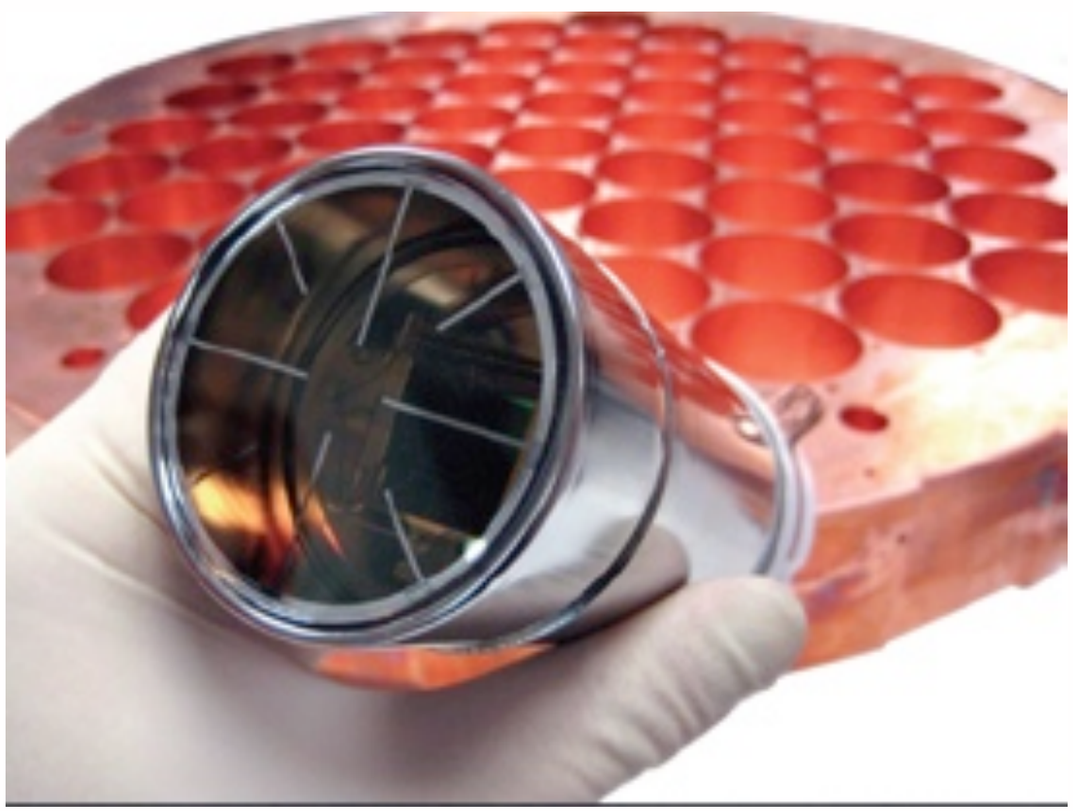

LUX – Supporting Systems

Xenon gas handling and sampling

Cathode HV feedthrough

Thermosyphon cryogenics

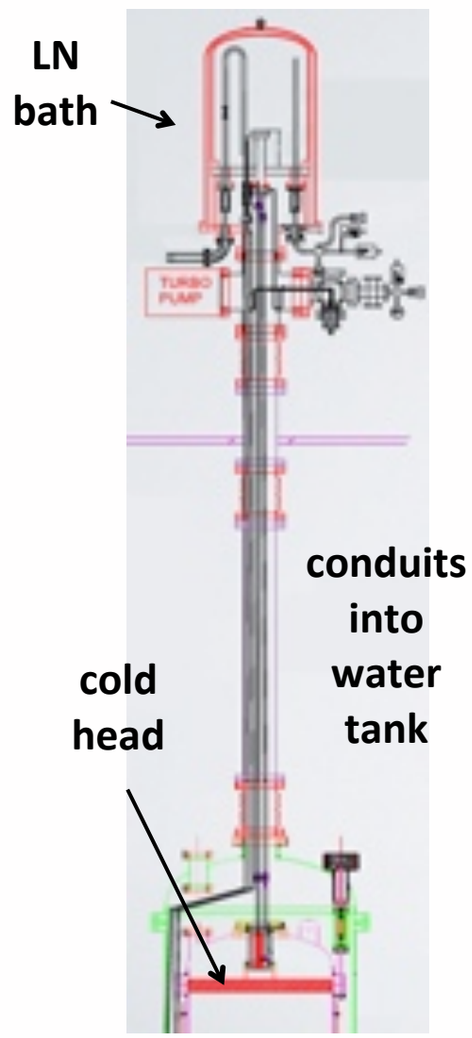

LUX Thermosyphon

Xe storage and recovery

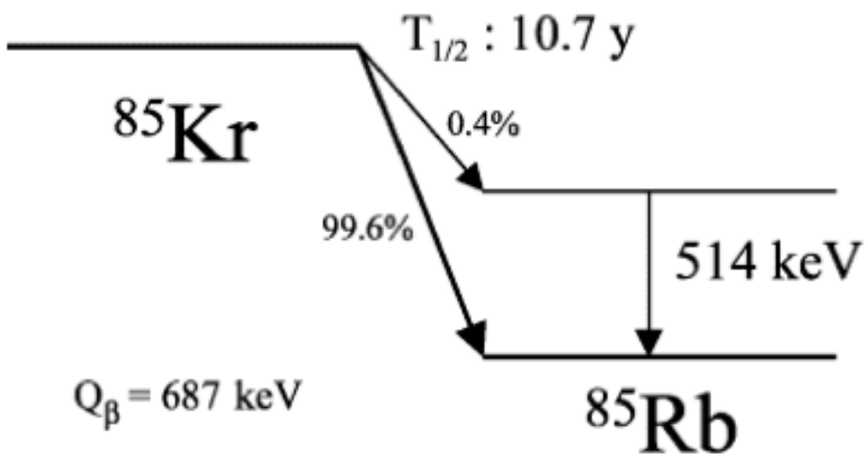

- Krypton-85 is the most important source of internal radioactivity
- Vendor-supplied xenon contains residual krypton at a relative concentration of ~10^{-7}
- LUX goal: reduce Krypton concentration to ~5 x 10^{-12}

complete spectra

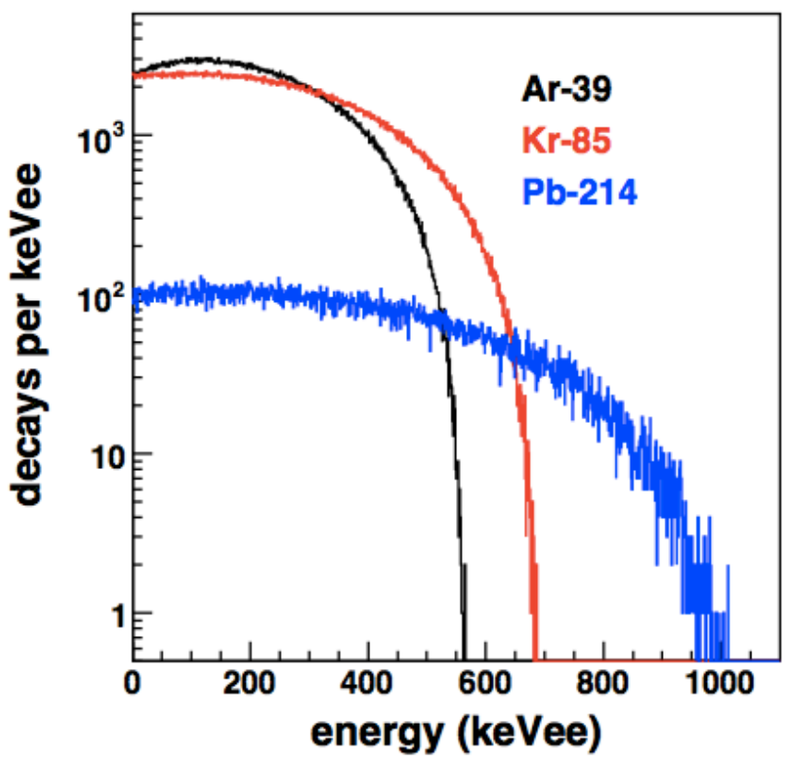

low energy zoom

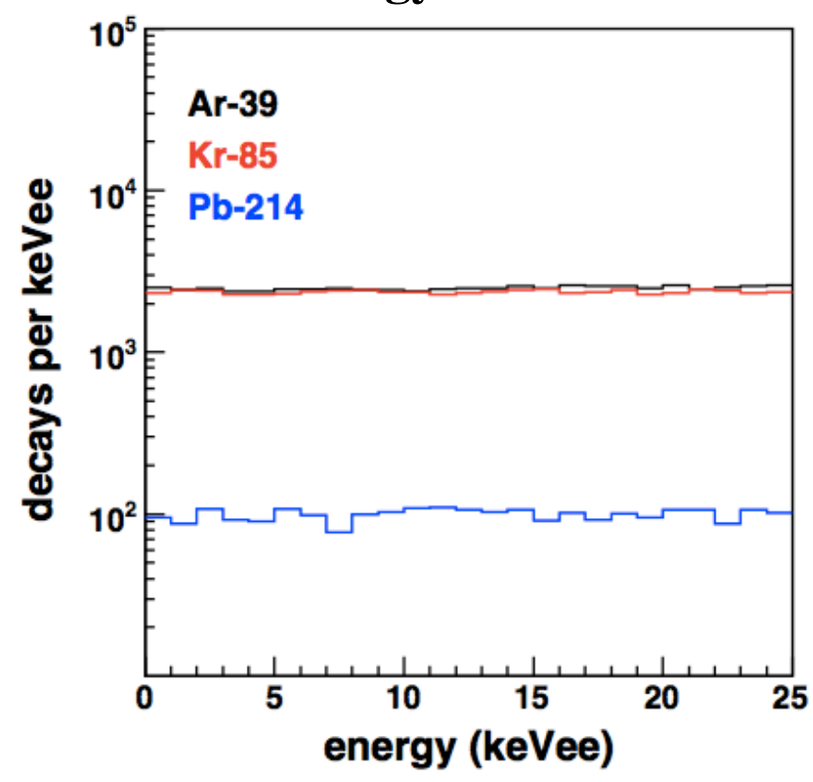

LUX Krypton Removal System

arXiv:1103.2714

- ^{85}Kr - beta decay – intrinsic background in liquid Xe
  - Research grade Xenon: ~100 ppb Kr => 10^4 - 10^5 reduction needed
- August 2012 - January 2013: Kr removal at dedicated facility
  - Chromatographic separation system
- Kr concentration reduced from 130 ppb to 3.5 ± 1 ppt, (factor of 35000)
  - 1 ppt is achievable (useful for next-generation detectors)

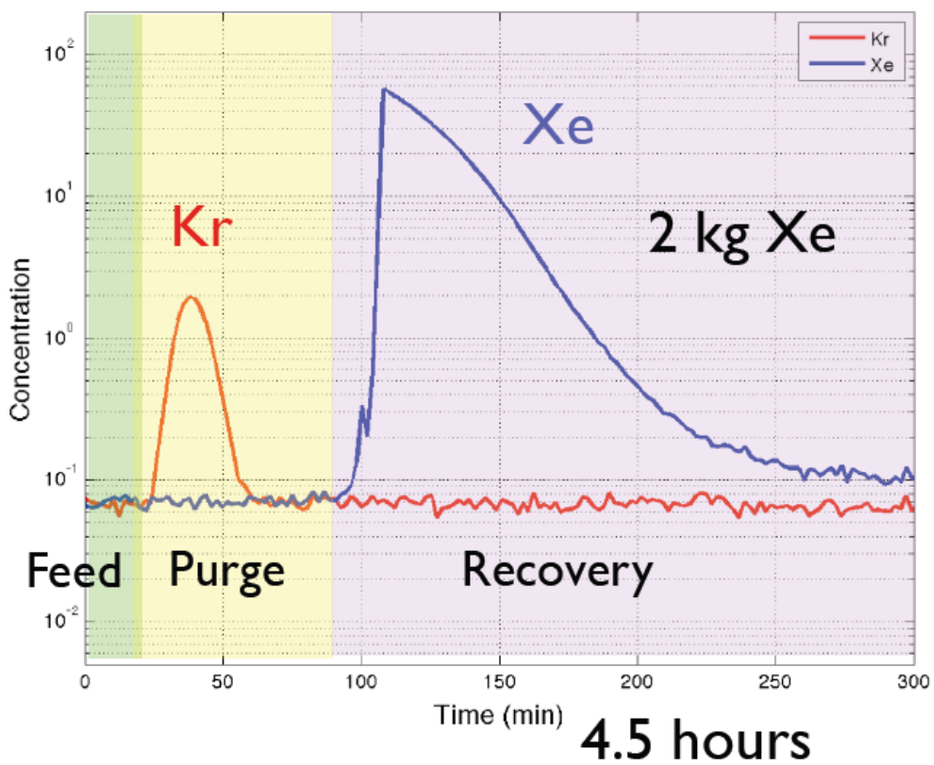

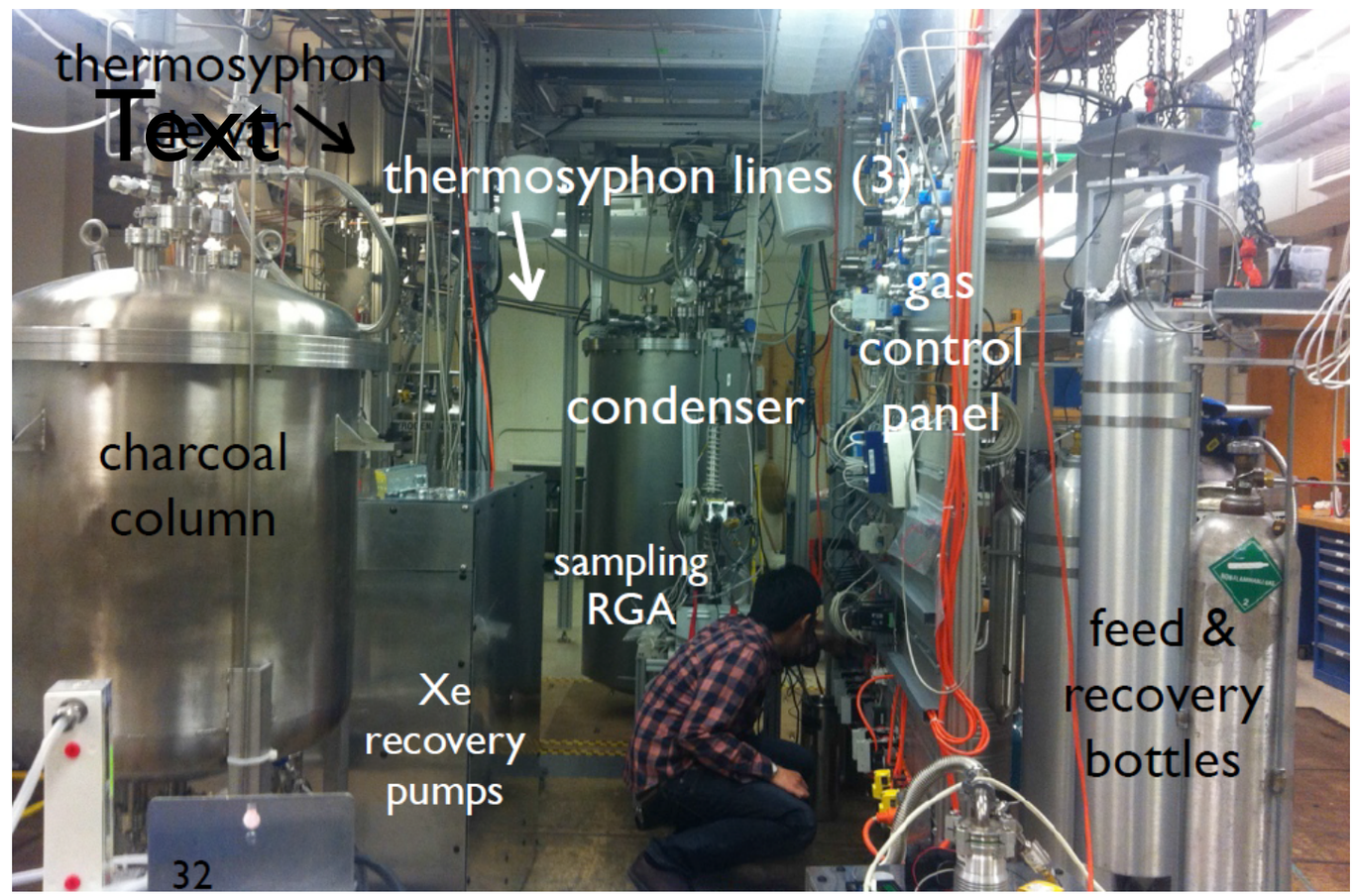

Surface Lab – March to July 2012

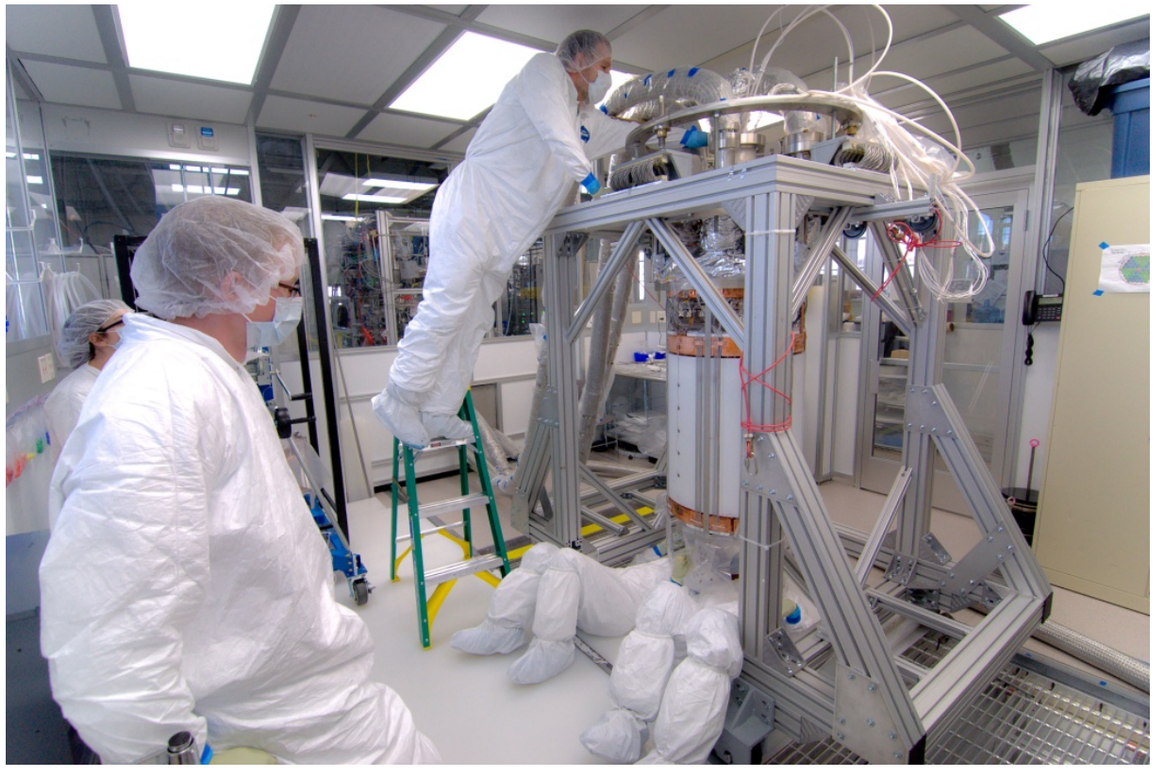

LUX underwater, and a mile underground, at SURF - September 2012

LUX Timeline

LUX funded in 2008 by DOE and NSF

Above-ground laboratory completed at SURF in 2011
LUX assembled; above-ground commissioning runs completed

Underground laboratory completed at SURF in 2012.
LUX moves underground in July to its new home in the Davis cavern.

Detector cool-down and gas phase testing completed early February 2013

Xenon condensation completed mid February 2013

Detector commissioning completed April 2013

Initial (3-month) WIMP search. First results presented 10/30!

Full year-long WIMP search to begin in 2014. Result expected in 2015

Typical Event in LUX

1.5 keV gamma ray scattering event

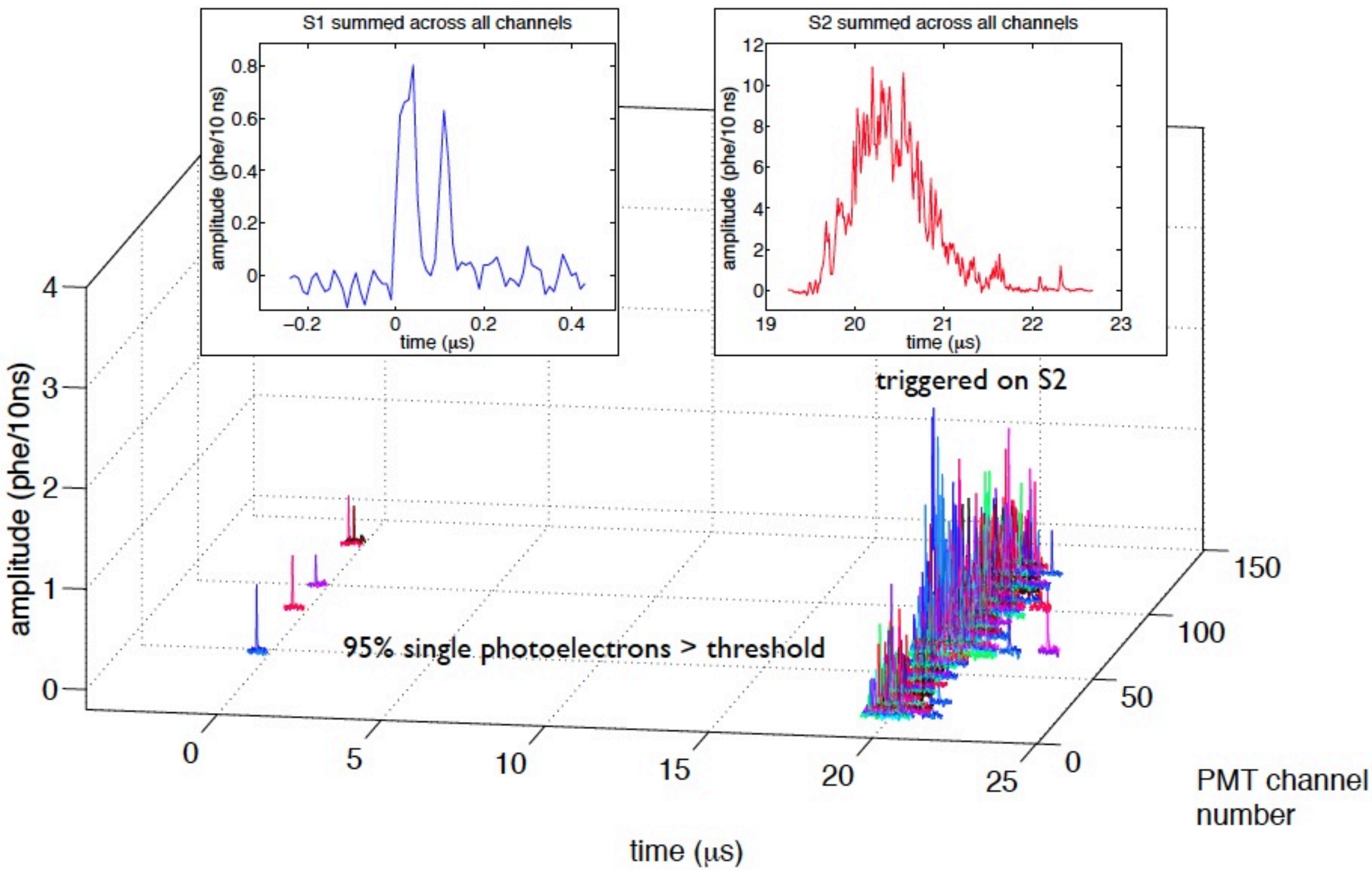

XYZ Position Reconstruction

Z coordinate is determined by the time between S1 and S2 (electron drift speed of 1.51 mm/microsecond)

Light Response Functions (LRFs) are found by iteratively fitting the distribution of S2 signal for each PMT.

XY position is determined by fitting the S2 hit pattern relative to the LRFs.

Reconstruction of XY from events near the anode grid resolves grid wires with 5 mm pitch.

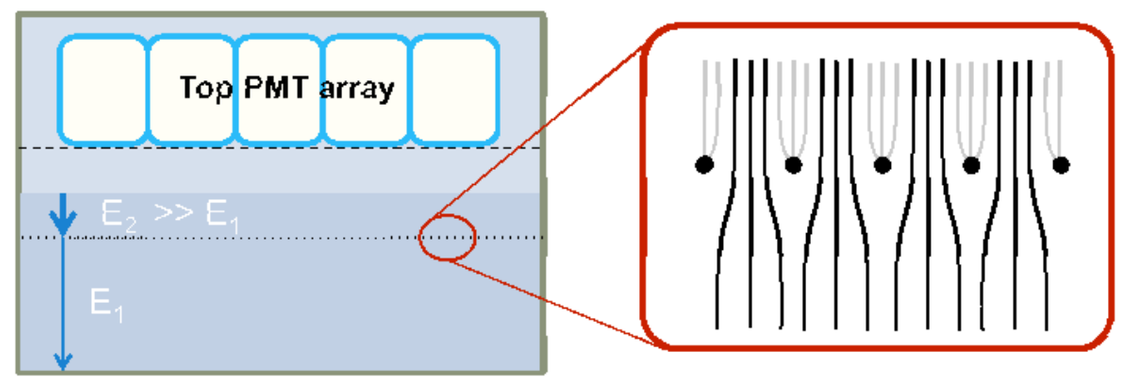

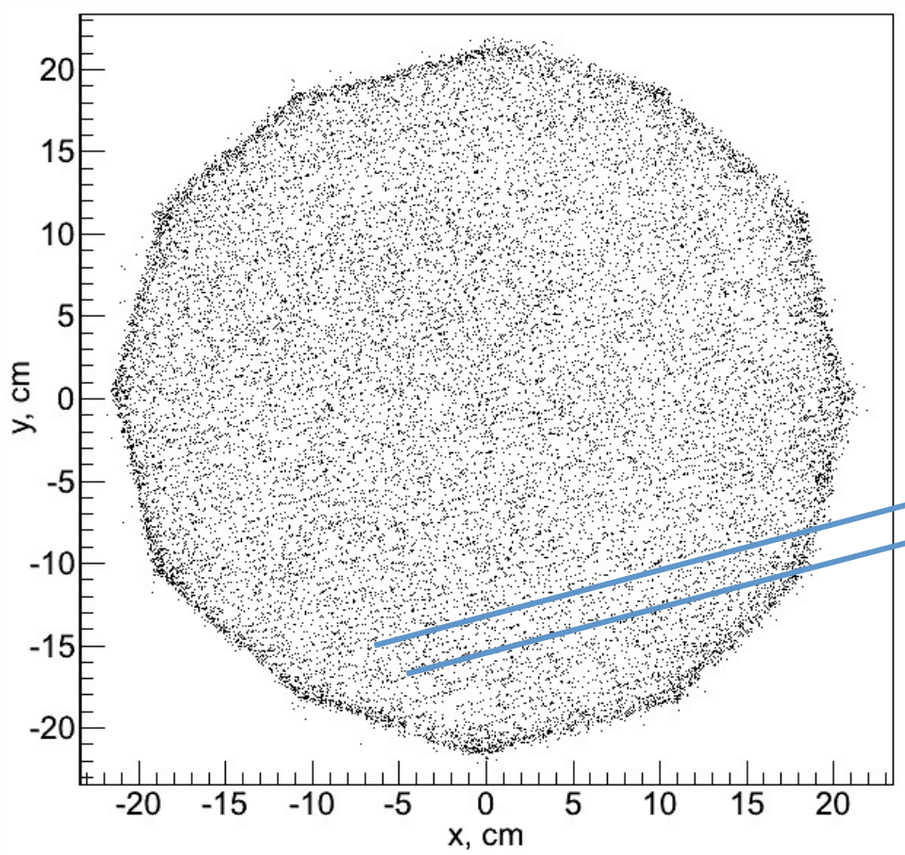

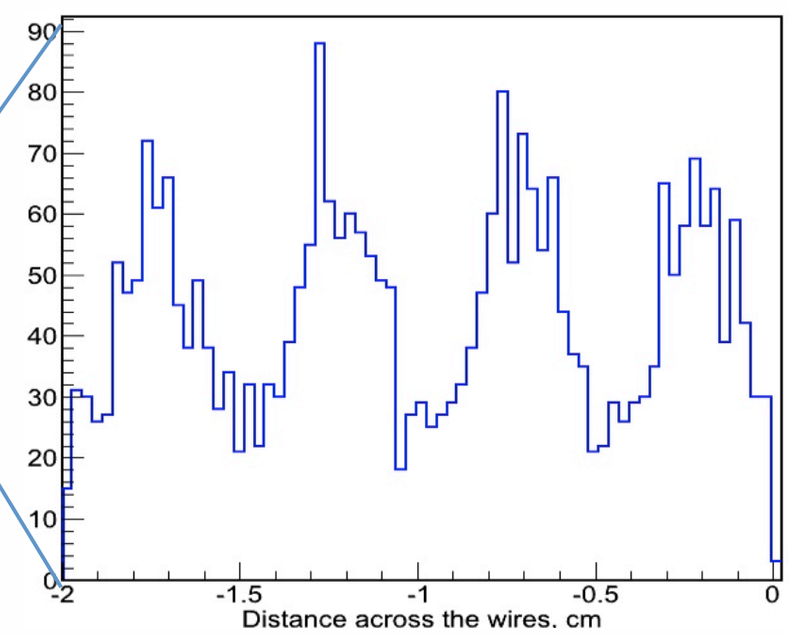

^{83m}Kr Calibration

- ^{83}Rb produces ^{83m}Kr when it decays; this krypton gas can then be flushed into the LUX gas system to calibrate the detector as a function of position.
- Provides reliable, efficient, homogeneous calibration of both S1 and S2 signals, which then decays away in a few hours, restoring low-background operation.

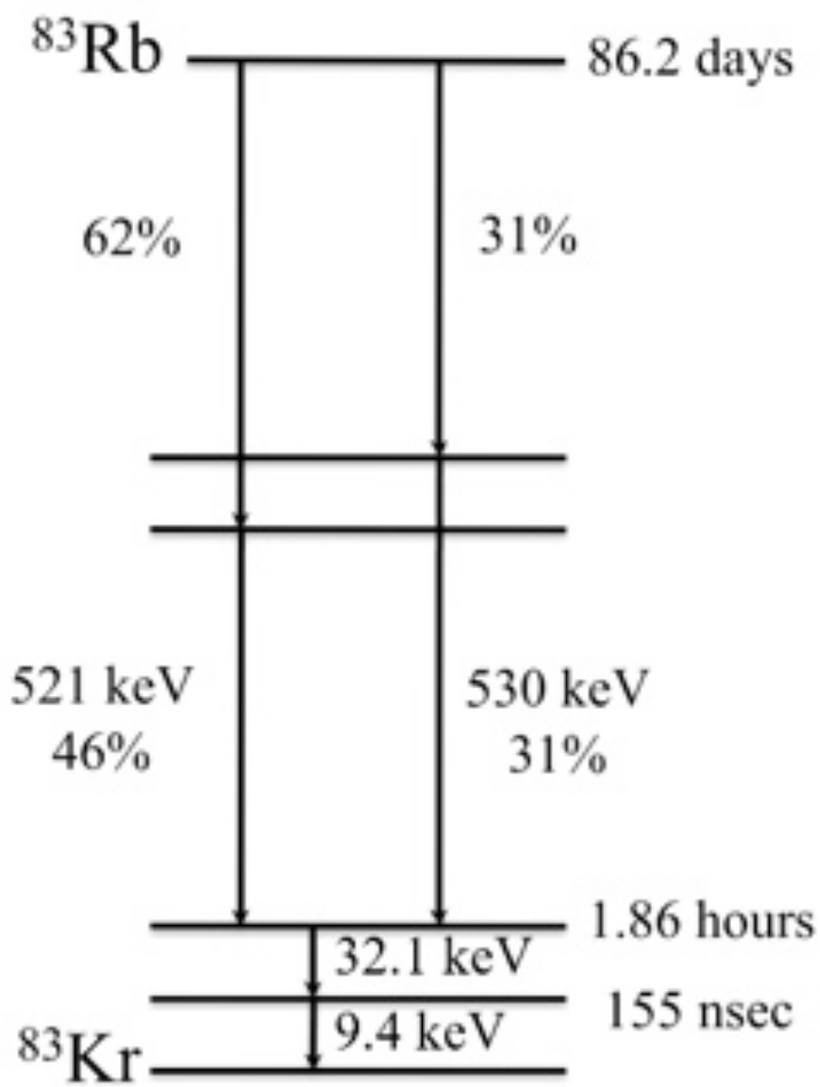

^{83m}Kr source (^{83}Rb coated on charcoal, within xenon gas plumbing)

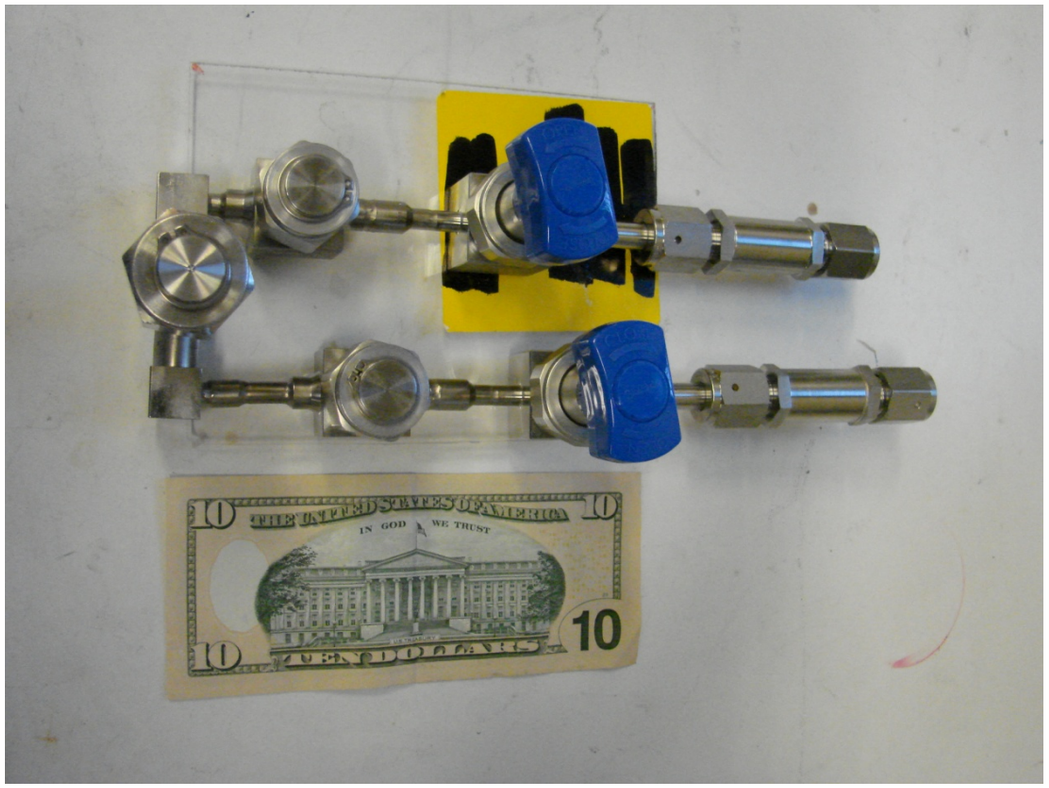

^{83m}Kr Calibration

- Over 1 million ^{83m}Kr events, spread uniformly through the detector.

Fiducial volume determination

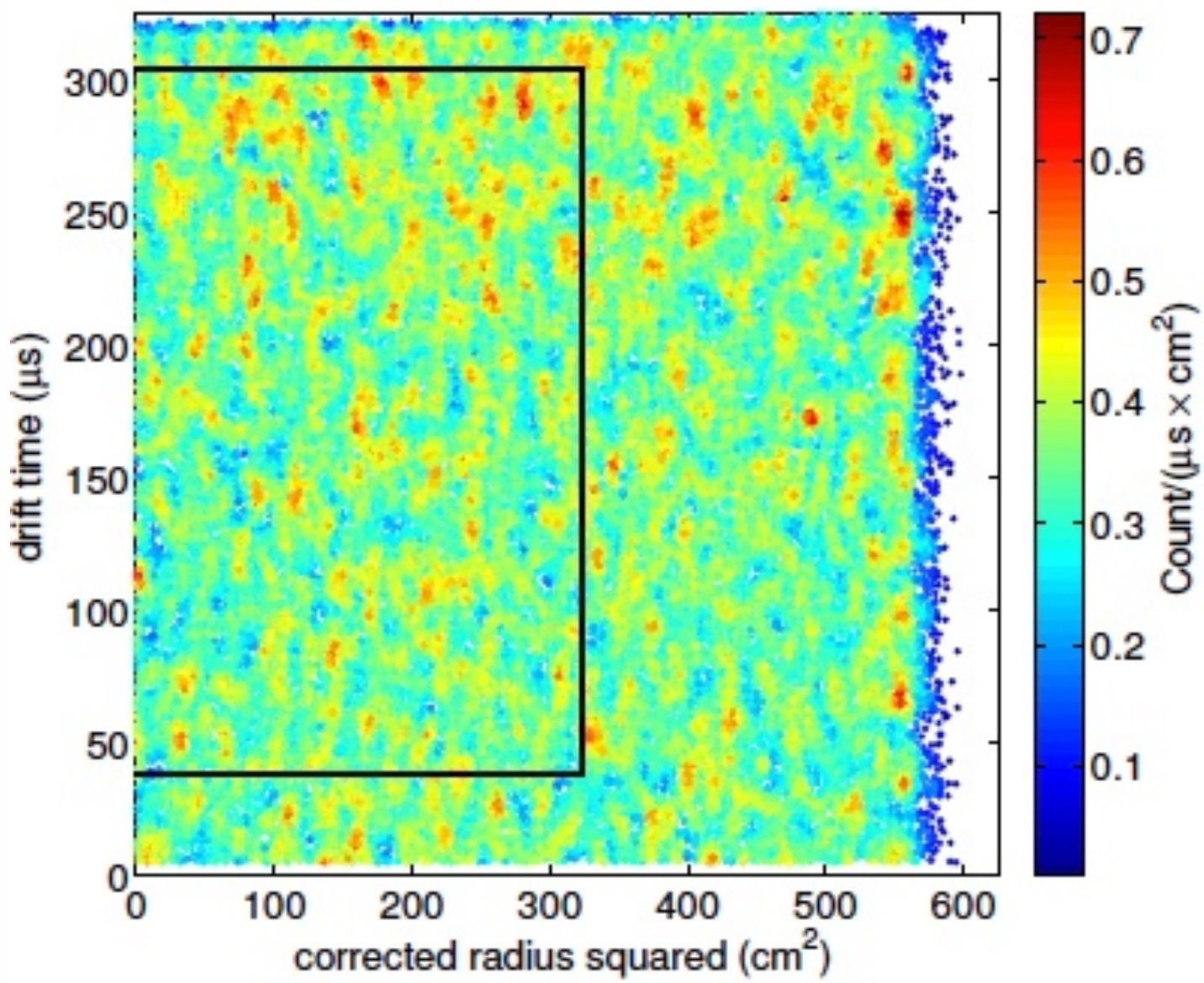

Position-based S1 corrections

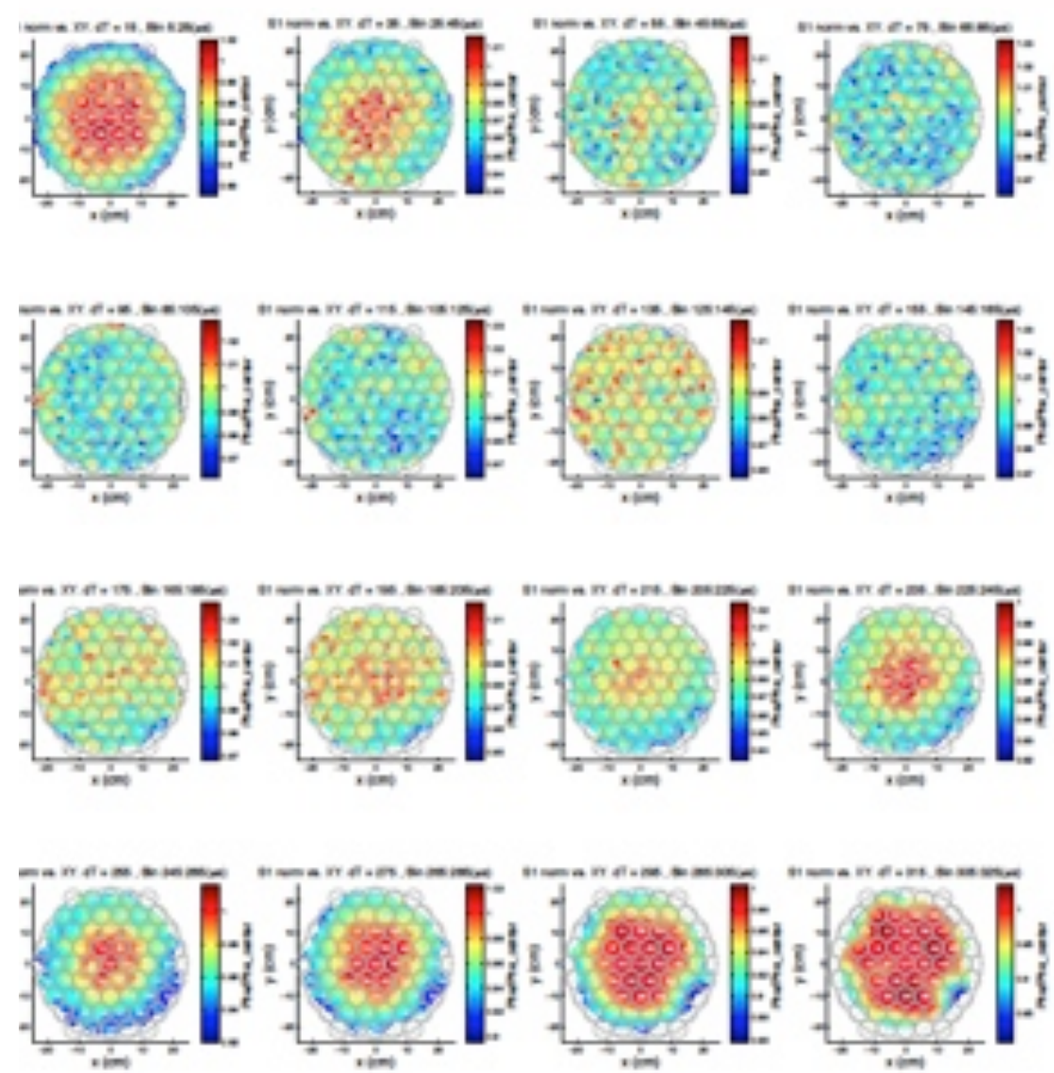

Tritiated Methane Calibration

- LUX uses tritiated methane, doped into the detector, to accurately calibrate the efficiency of background rejection.
- This beta source (endpoint energy 18 keV) allows electron recoil S2/S1 band calibration with unprecedented accuracy
- The tritiated methane is then fully removed by circulating the xenon through the getter
- Parametrization of the electron recoil band from the high-statistics tritiated methane data is then used to characterize the background model.

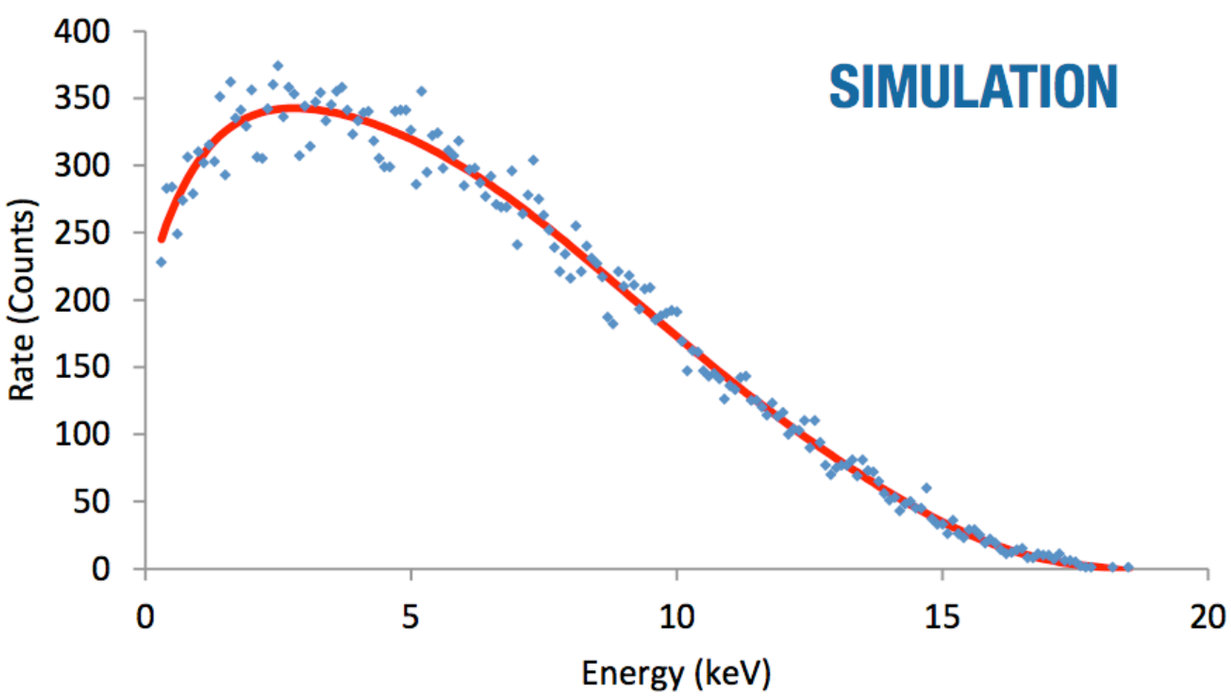

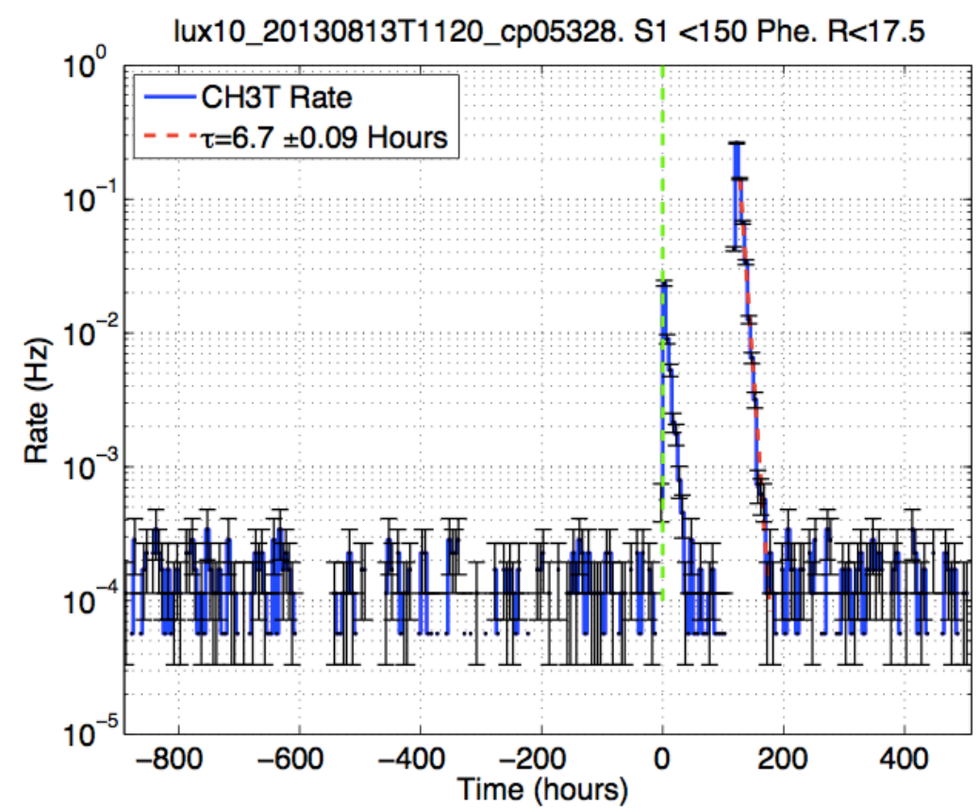

Tritiated Methane Calibration

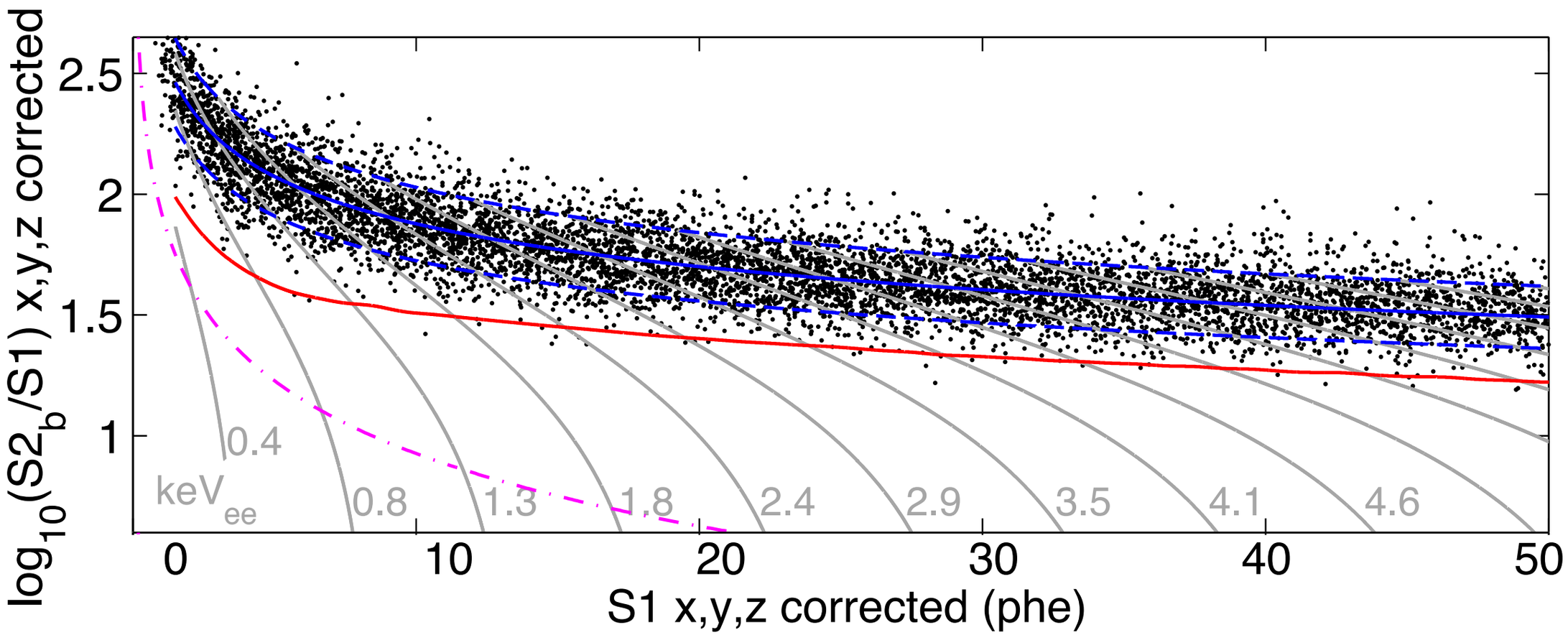

Energy Scale

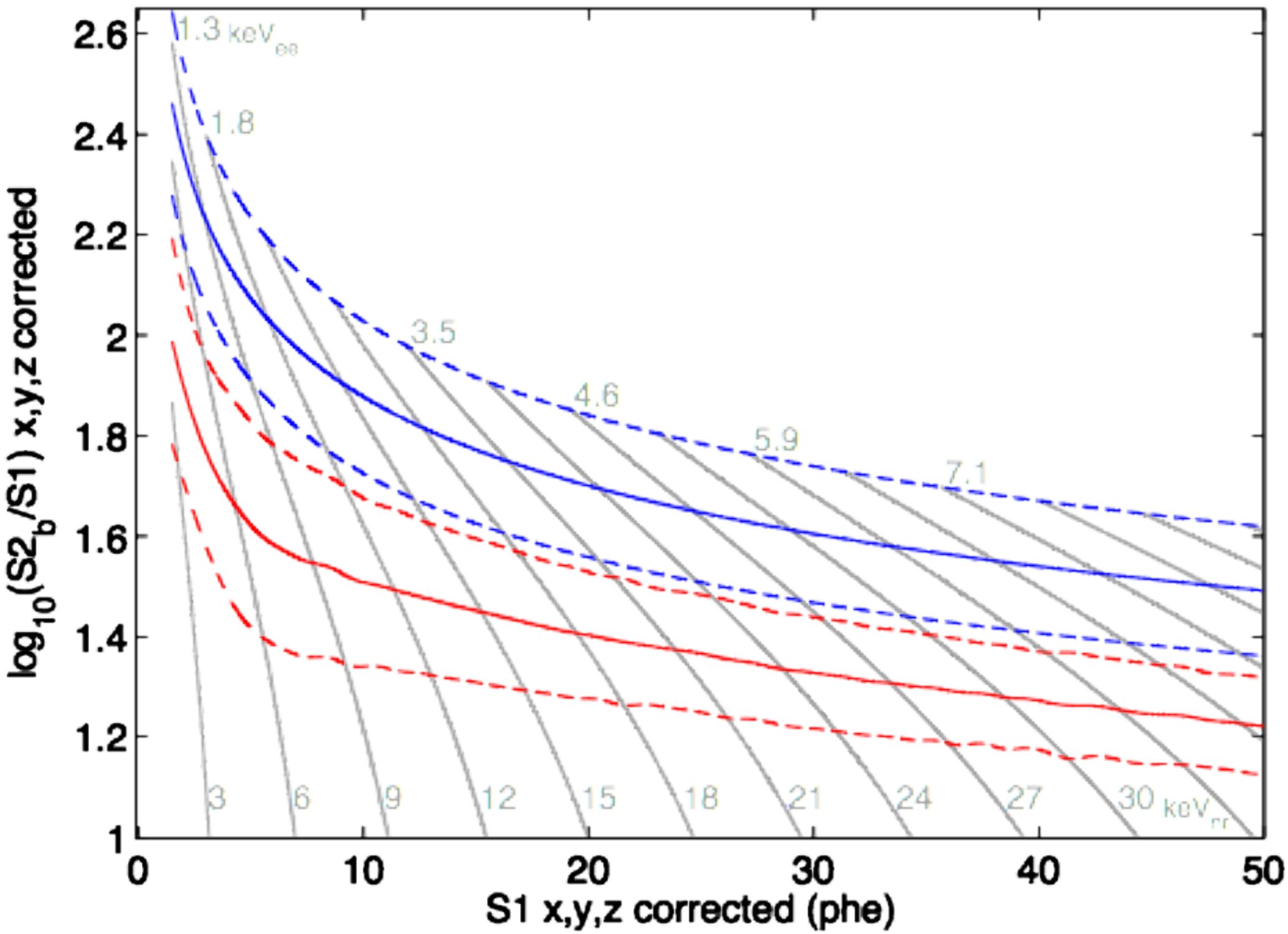

AmBe, ^{252}Cf Neutron Source Calibrations

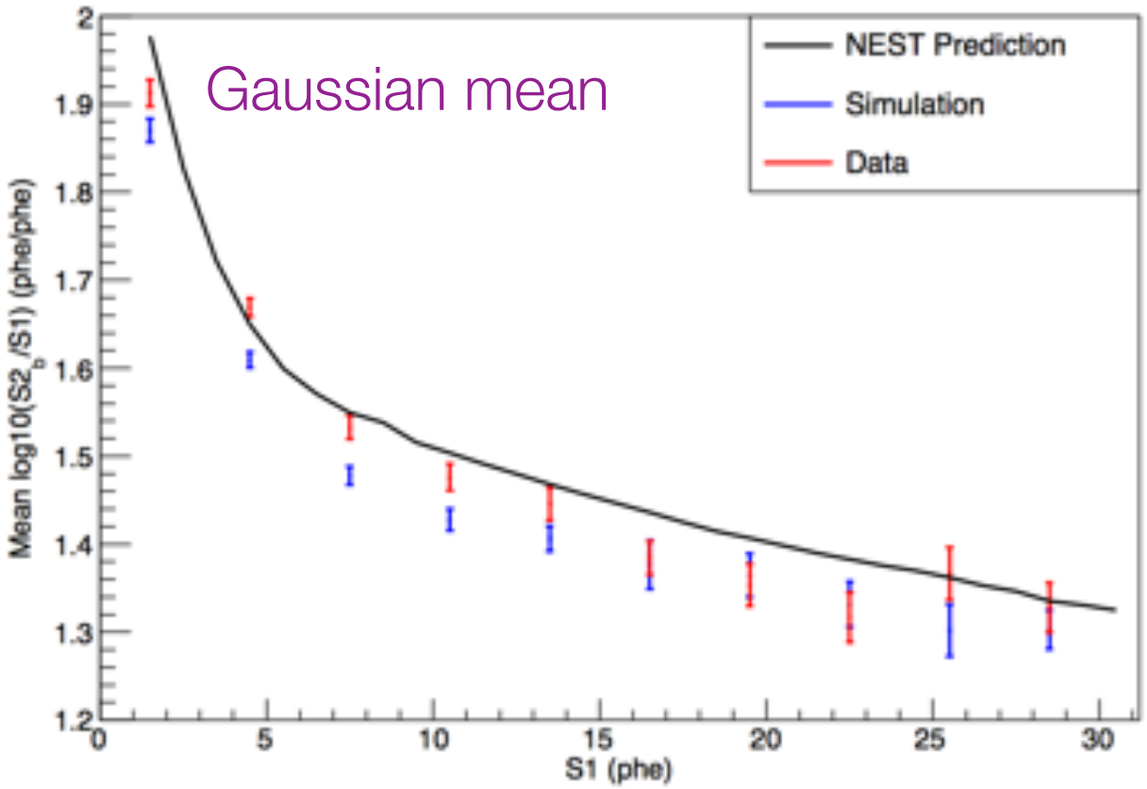

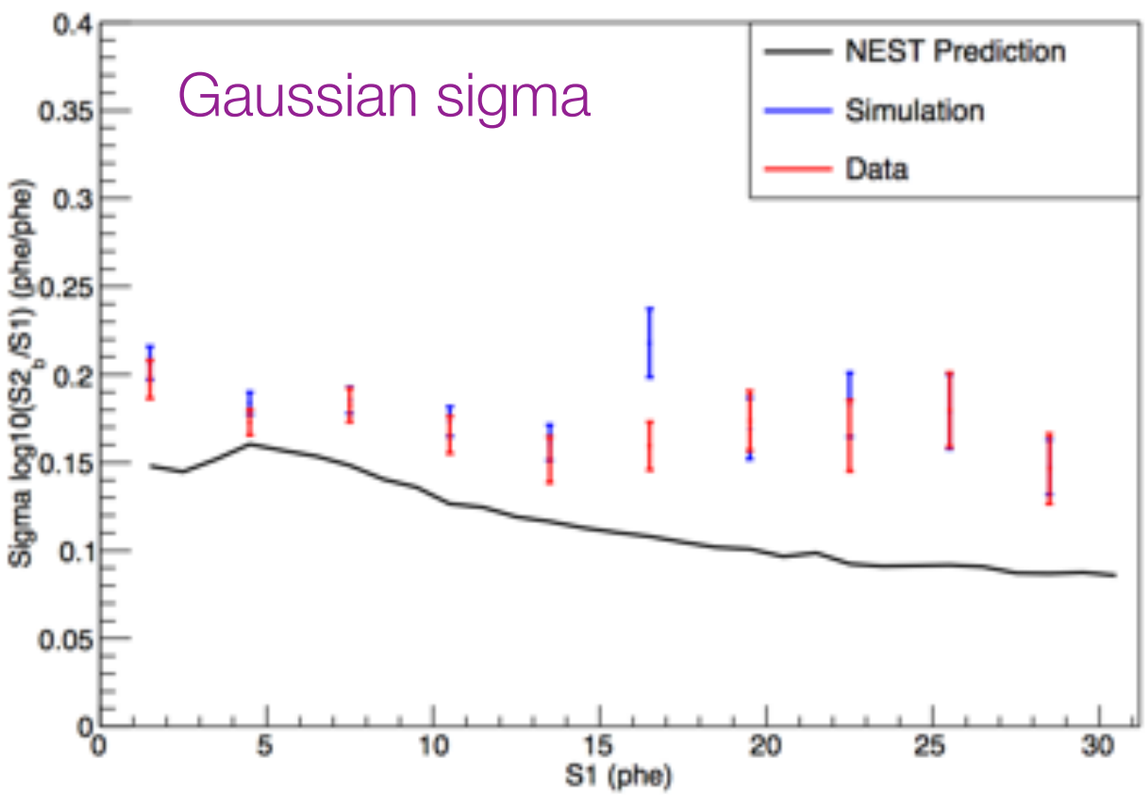

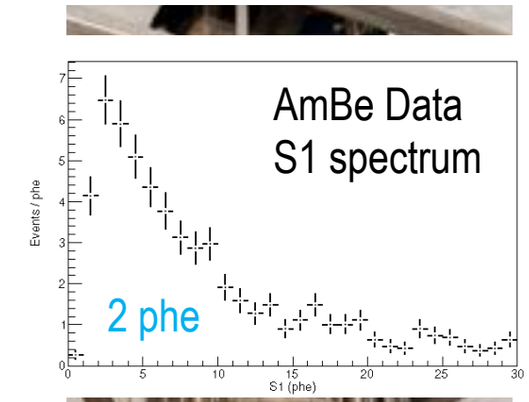

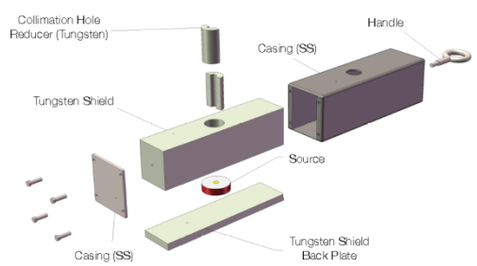

Simulation contains ER event, neutron interactions present in real detector.

Differences used to back-correct NR band calculation.

AmBe, ^{252}Cf Neutron Source Calibrations

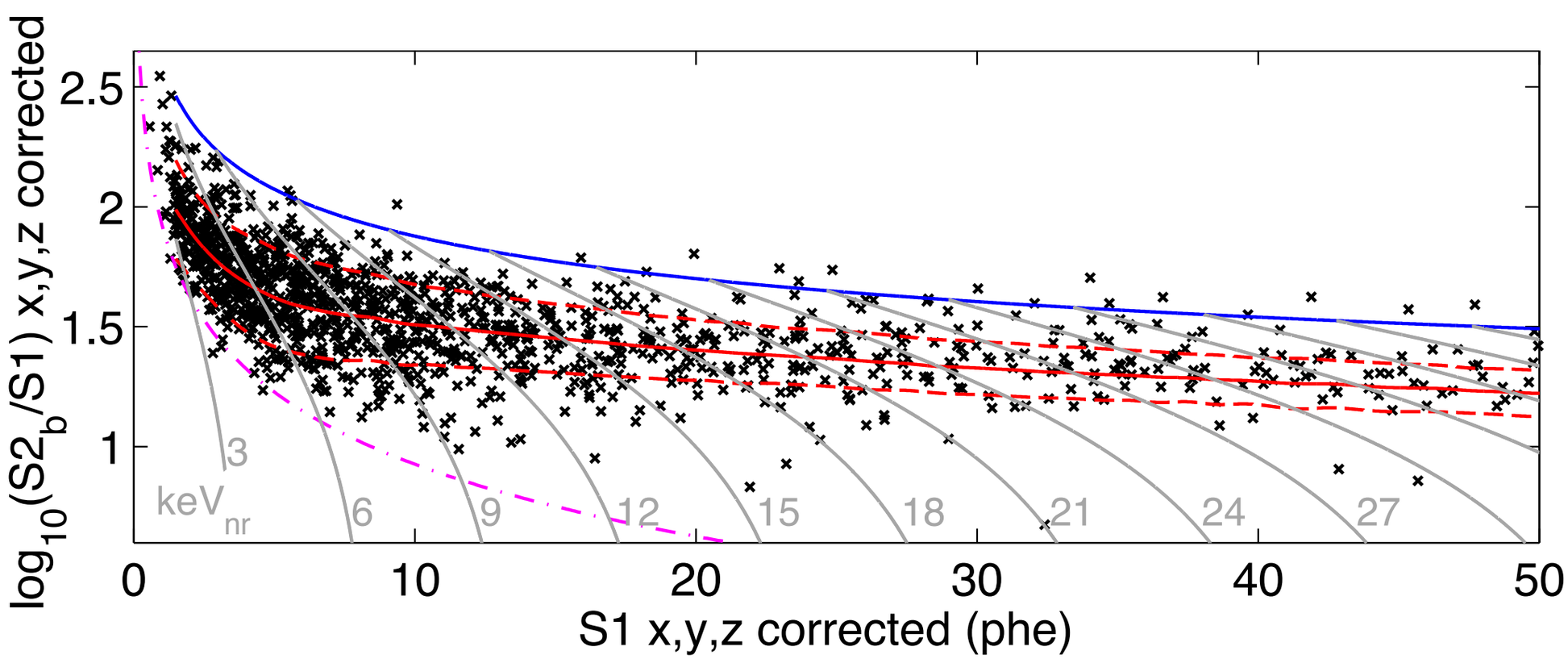

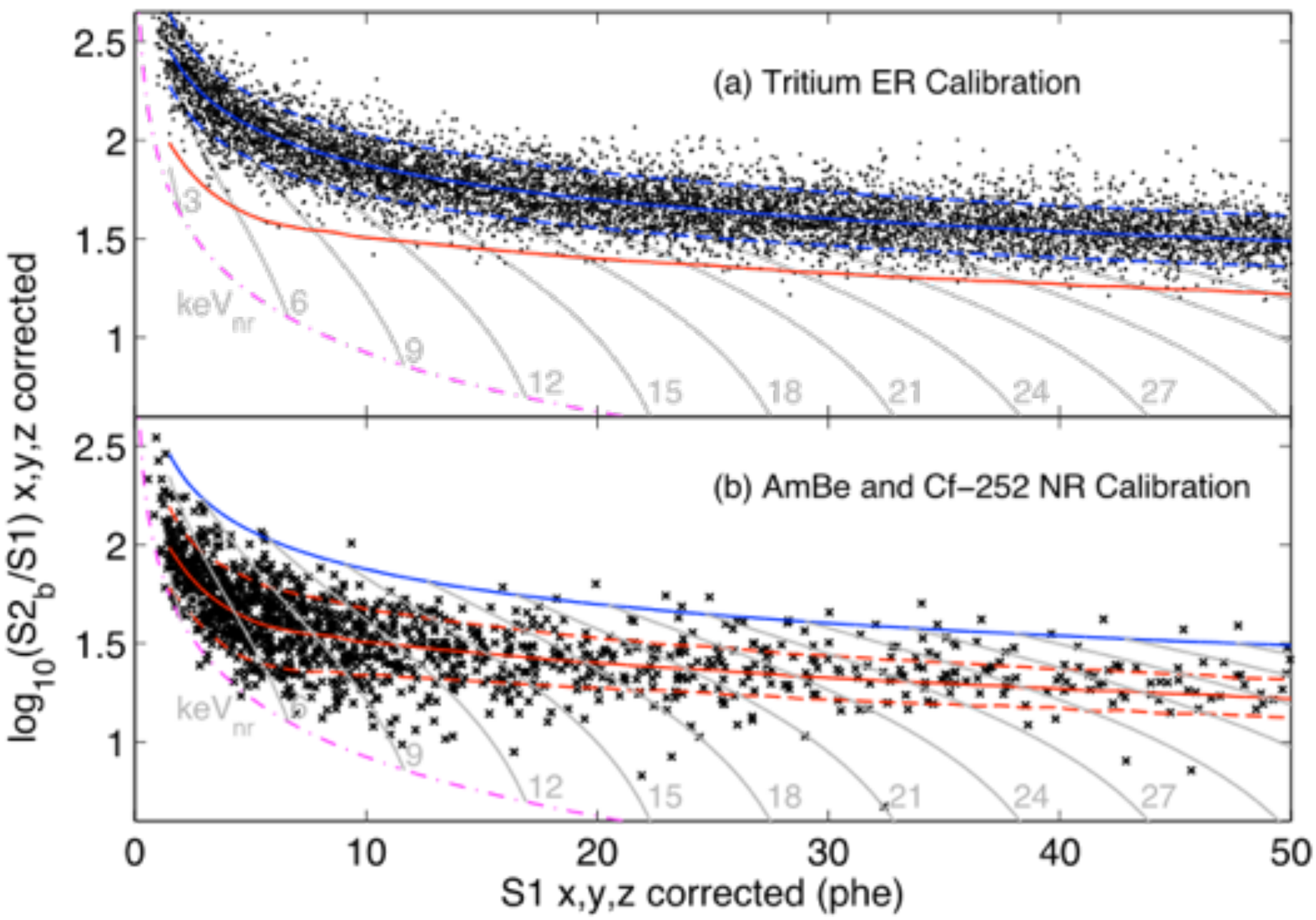
(a) Tritium ER Calibration
(b) AmBe and Cf−252 NR Calibration
keV_nr
3
6
9
12
15
18
21
24
27
2.5
2
1.5
1
0
10
20
30
40
50
log10(S2b/S1) x,y,z corrected
S1 x,y,z corrected (phe)

Electron Recoil Discrimination

Average discrimination from 2-30 S1 photoelectrons
measured to be 99.6% (with 50% nuclear recoil acceptance)

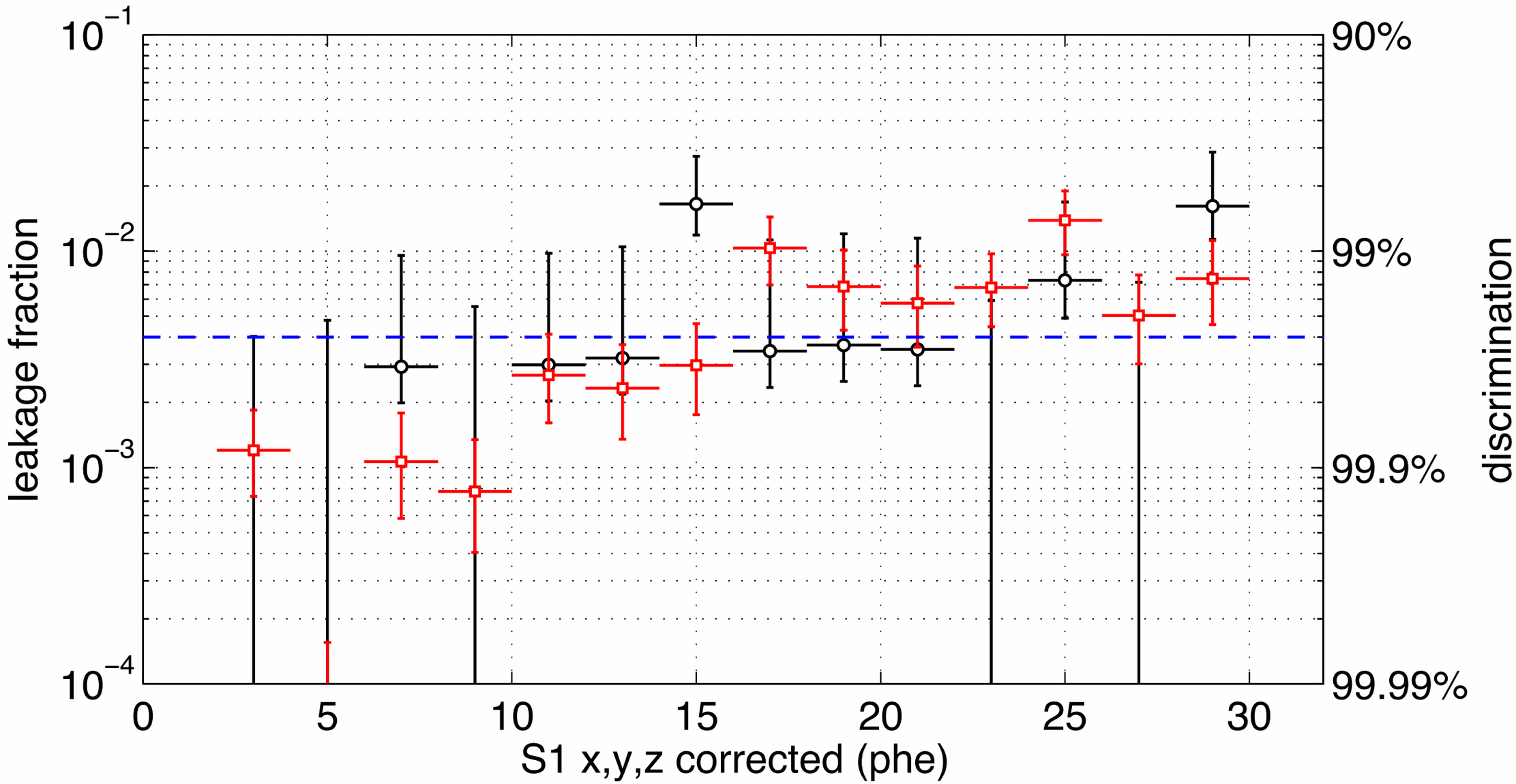

Black circles show leakage from counting events from the calibration data.
Red circles show projections of Gaussian fits below the nuclear recoil band mean.

Several independent estimates of total efficiency

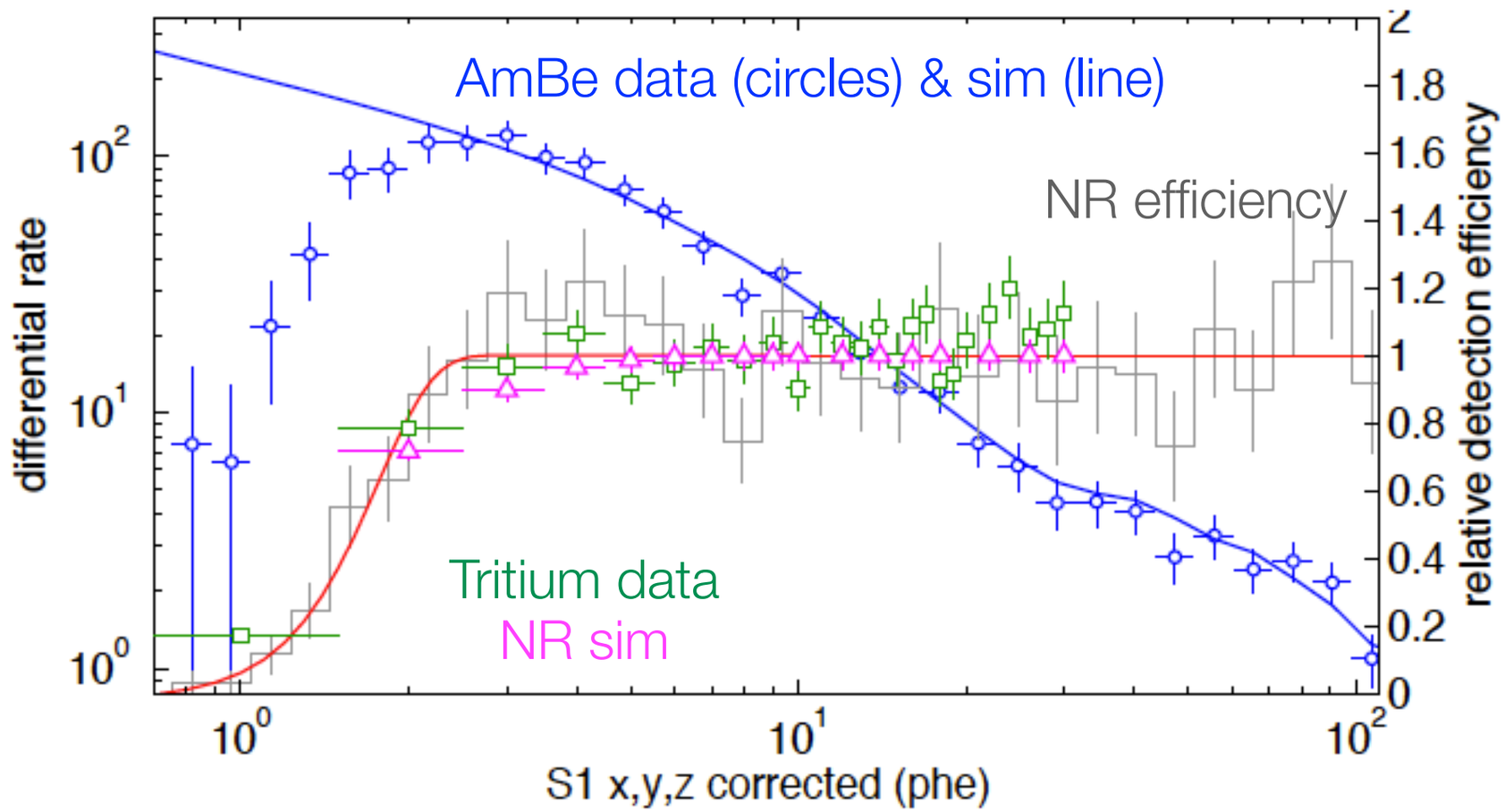

We find good agreement between the data and simulation-estimated efficiencies.

D.S. Akerib et al., Nucl. Instr. Meth. A **675**, 63 (2012)

WIMP Detection Efficiency - True Recoil Energy

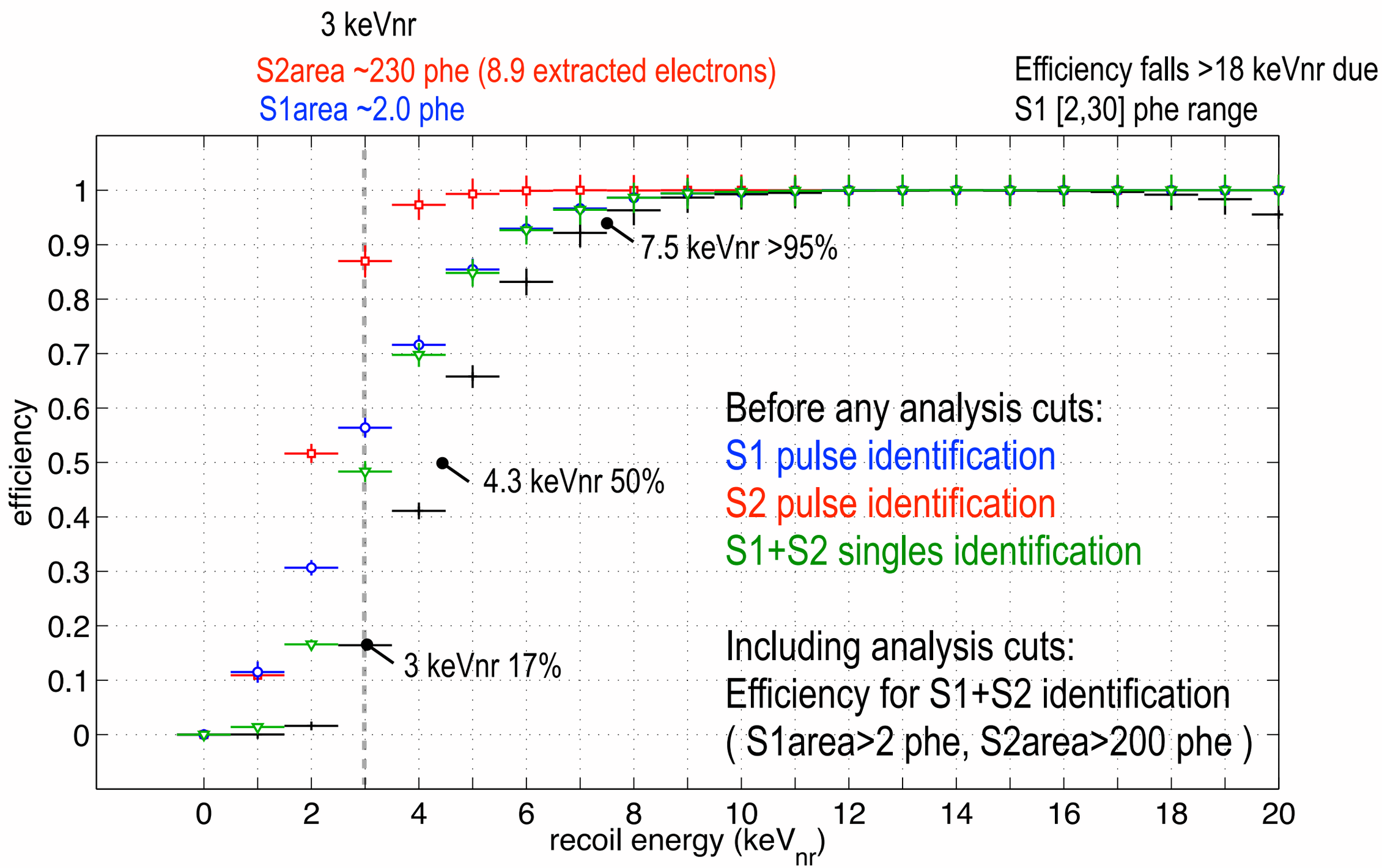

True Recoil Energy equivalence based on LUX 2013 Neutron Calibration/NEST Model

Efficiency of pulse finding and selection

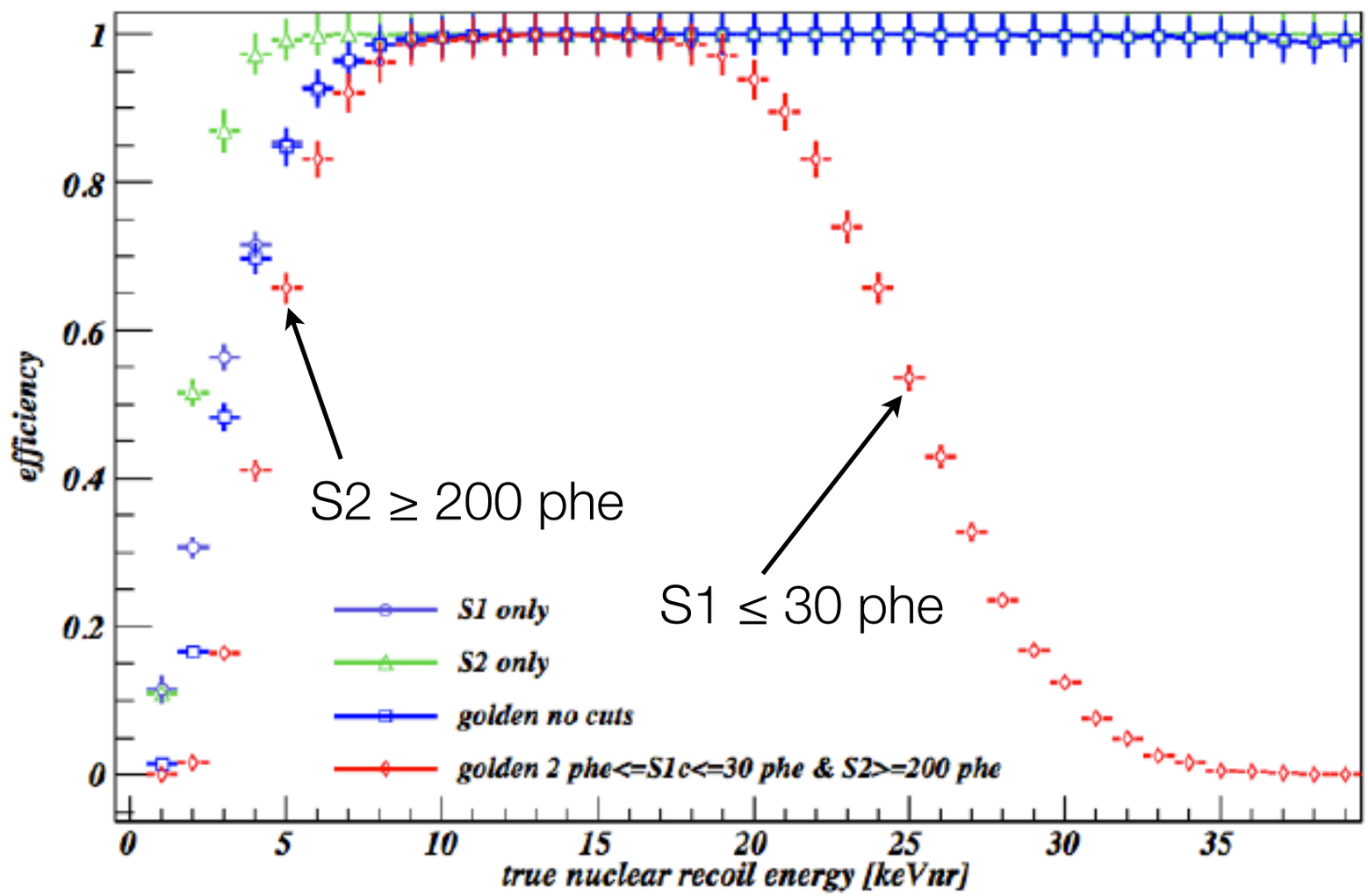

LUX High Energy Gamma Background in 220 kg

- Full gamma Spectrum, excluding region ±2 cm from top/bottom grids

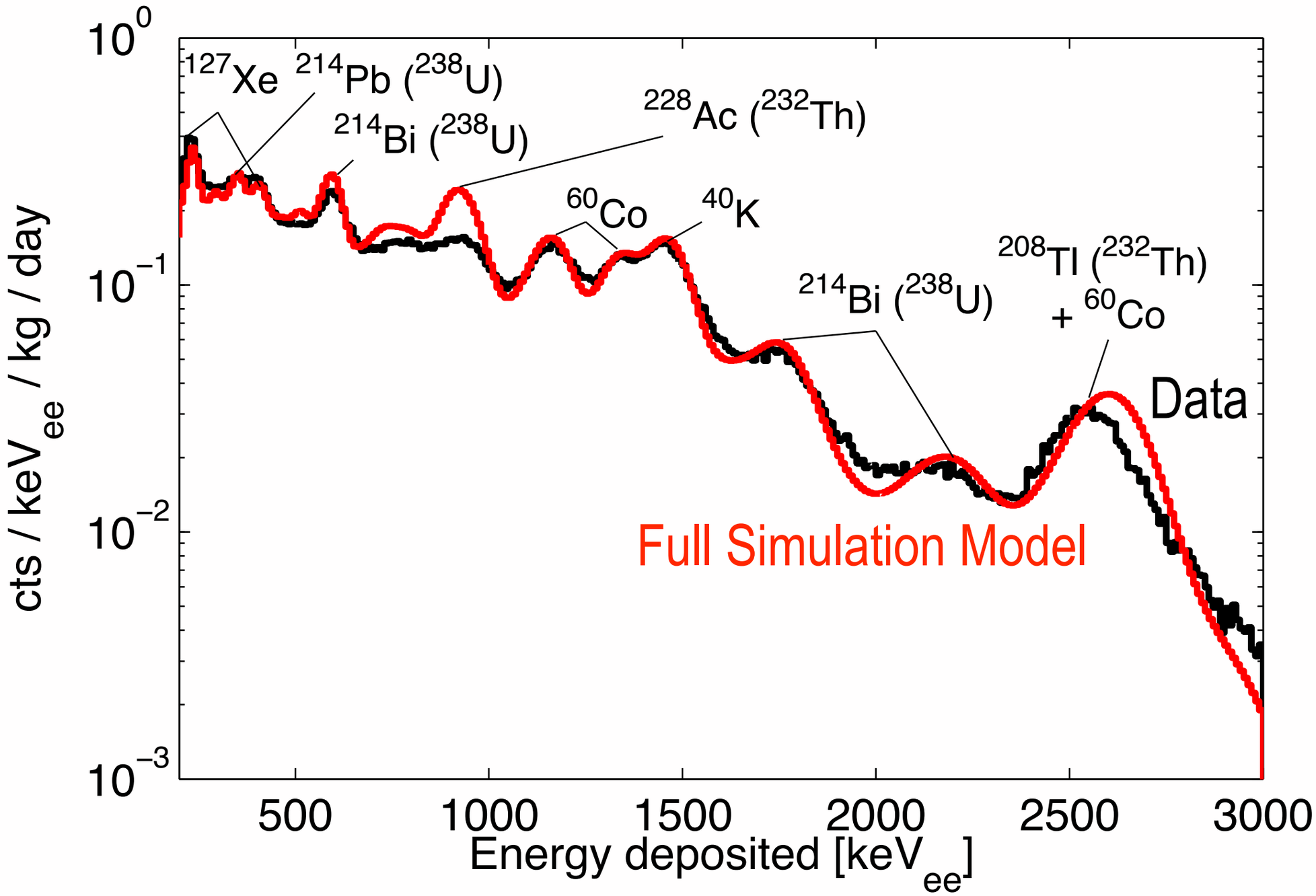

Total Electron Recoil Event Rate <5 keVee

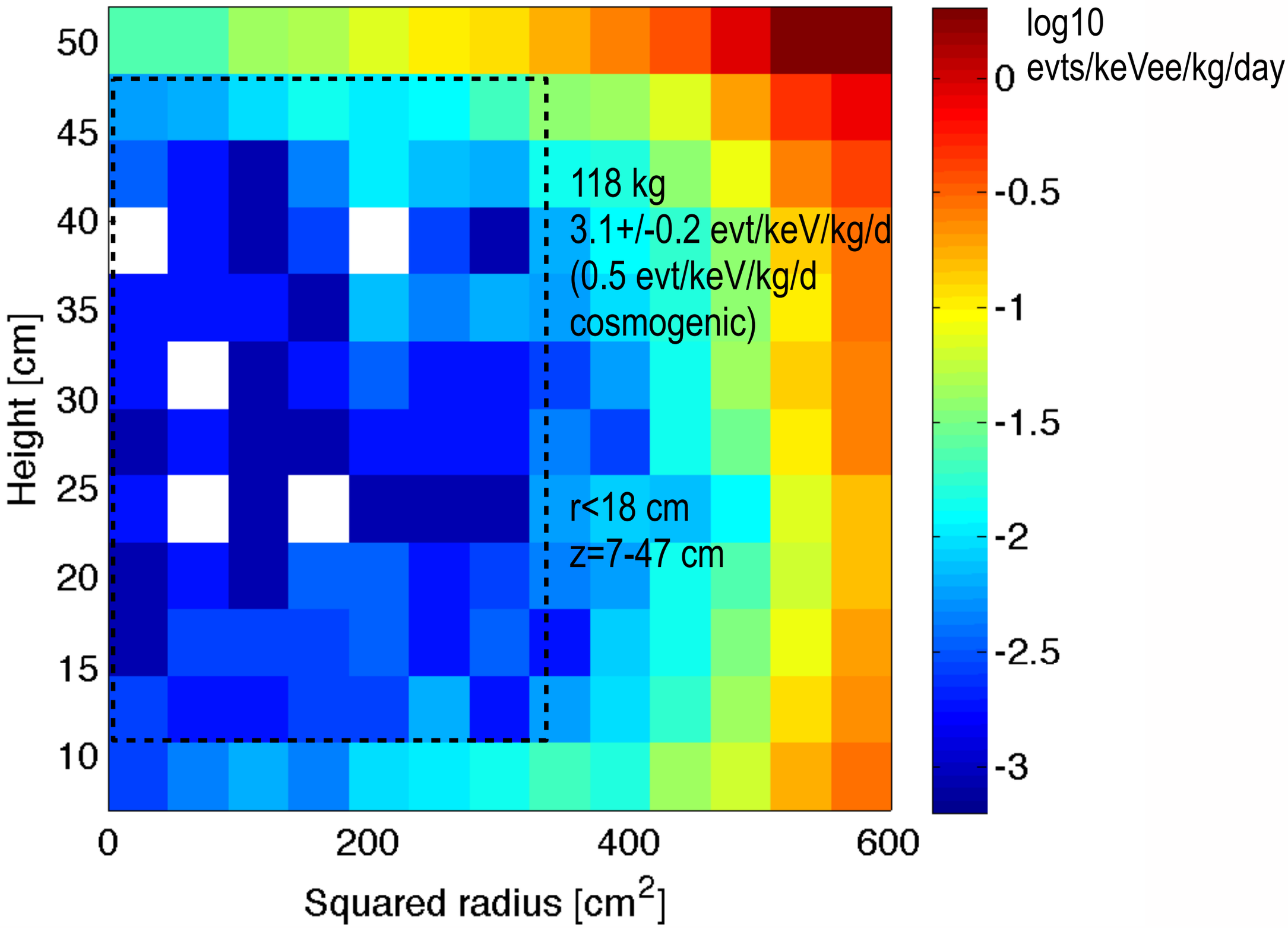

And it continues to get quieter - Xe Cosmogenic Activity cools (last 44 days)

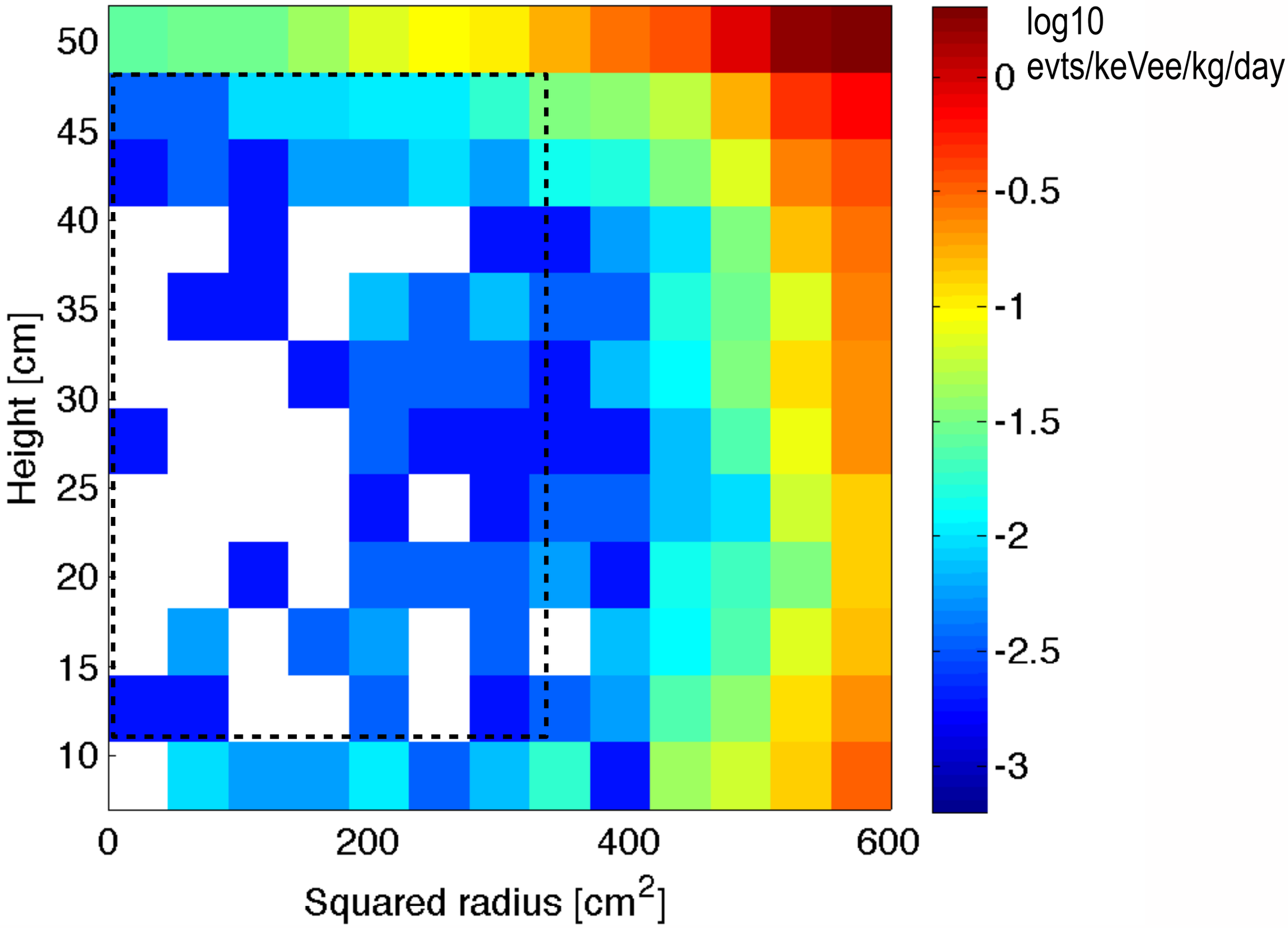

^{127}Xe Electron Capture - Simulation

Background: x-ray in center of detector after full escape of decay gamma

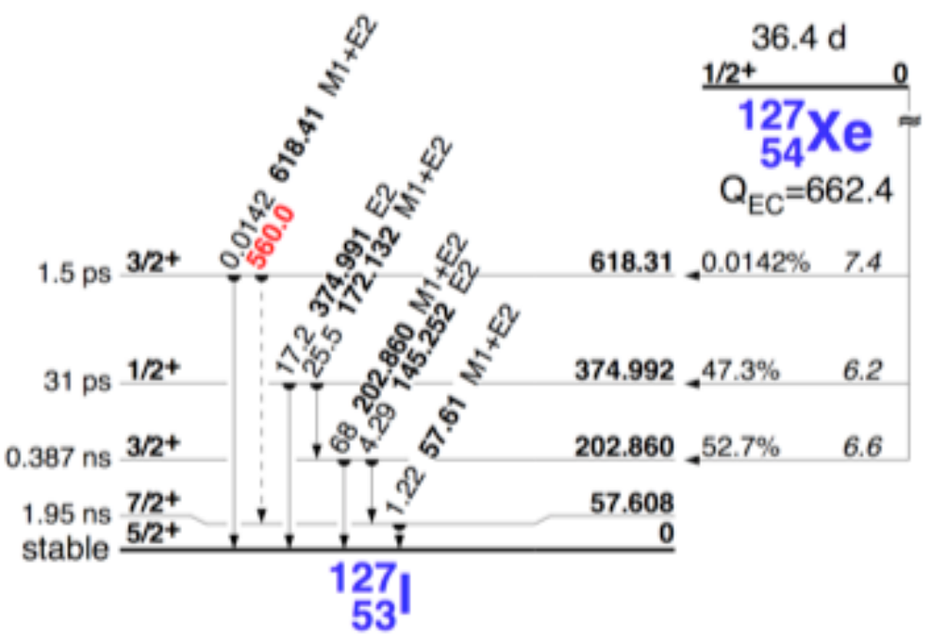

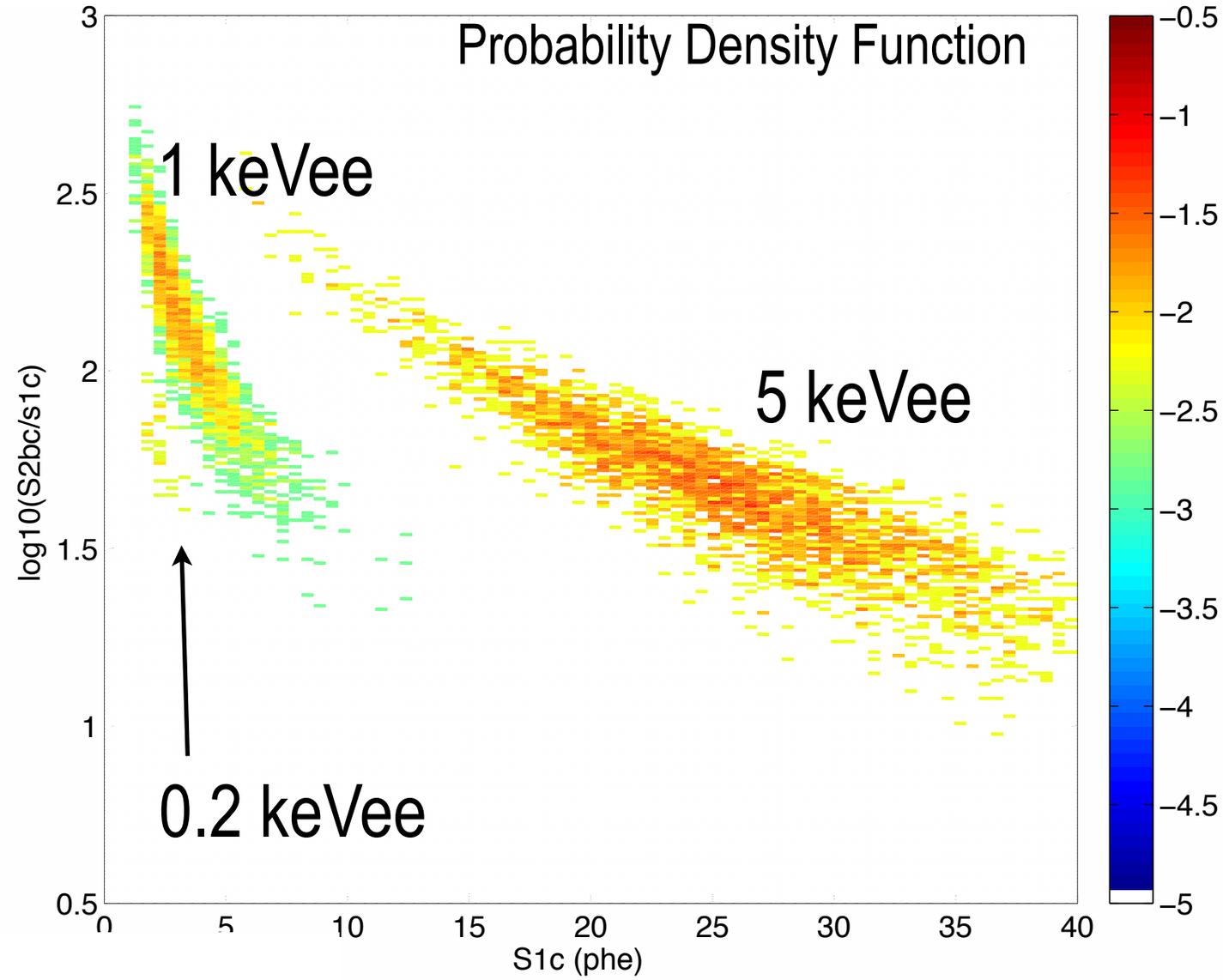

Energy released via cascade x-rays, or Auger electrons. Total binding energy shown, and also expected EC probability from that shell

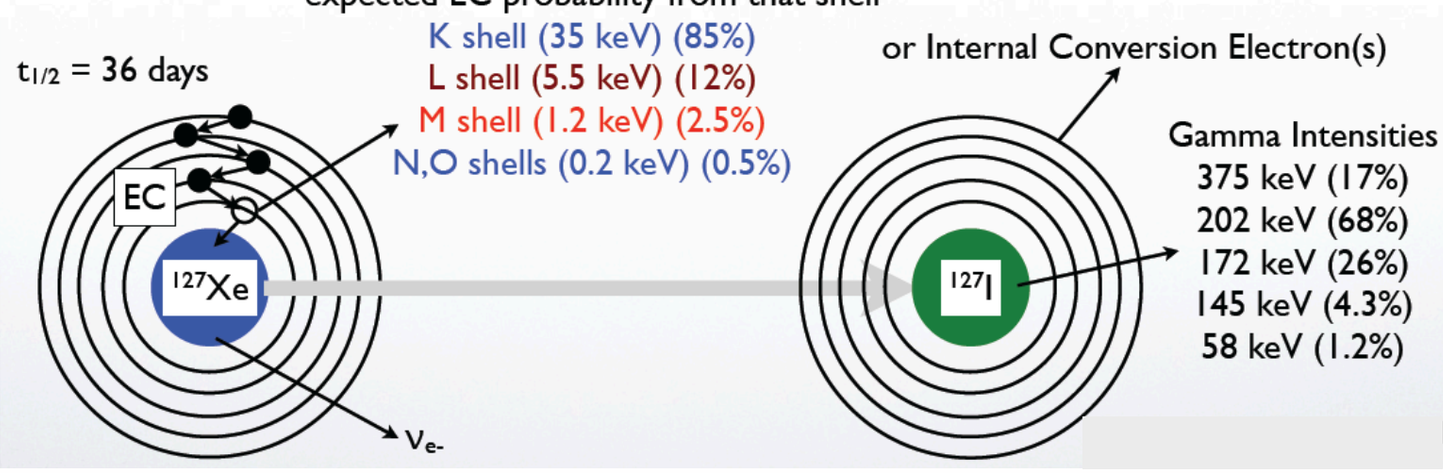

Electron capture from S-wave orbital,

$p+e^- \rightarrow n+\nu_e$

Cut	Explanation	Events Remaining
All Triggers	S2 Trigger >99% for S2>200 phe	83,673,413
Detector Stability	Cut periods of excursion for Xe Gas Pressure, Xe Liquid Level, Grid Voltages	82,918,901
Single Scatter Events	Identification of S1 and S2. Single Scatter cut.	6,585,686
S1 energy	Accept 2-30 phe (low energy <5 keVee,<25 keVnr)	26,824
S2 energy	Accept 200-3300 phe	20,989
S2 Electron Trains	Cut if >100 phe outside S1+S2 identified. (0.8% drop in livetime.)	19,796
Drift Time Cut away from grids	Cutting away from cathode and gate regions, 60 < drift time < 324 us	8731
Fiducial Volume	Radius < 18 cm, 38 < drift time < 305 us, 118 kg fiducial	160

Simulated WIMP Signals for 85 days, 118 kg

- Pick a mass of 1000 GeV and cross section at the existing XENON100 90% CL Sensitivity 1.9×10^{-44} cm^2 - Would expect 9 WIMPs in LUX Search

Conservatively assume no signal generated for recoils < 3 keVnr to reflect lowest energy for which NR calibration is available.

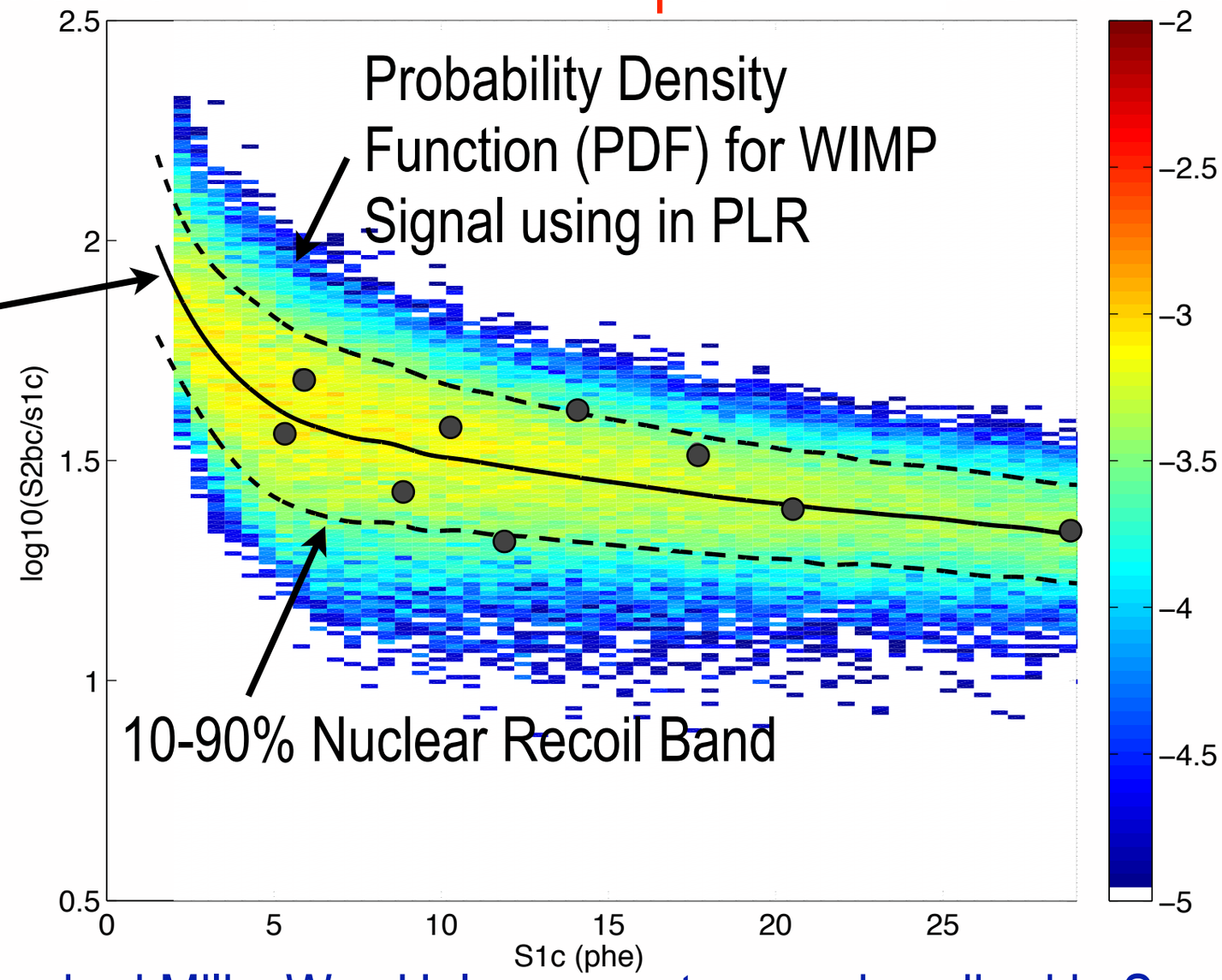

- PDF assumes Standard Milky Way Halo parameters as described in Savage, Freese, Gondolo (2006) v_0=220 km/s, v_{escape} = 544 km/s, ρ_0 = 0.3 GeV/c^2, v_{earth} = 245 km/s
  - Helm Form Factor.

Simulated WIMP Signals for 85 days, 118 kg

- At a mass of 8.6 GeV and cross section favored CDMS II Si (2012) cross section 2.0×10^{-41} cm^2 - Expect 1550 WIMPs in LUX Search

Conservatively assume no signal generated for recoils < 3 keVnr to reflect lowest energy for which NR calibration is available.

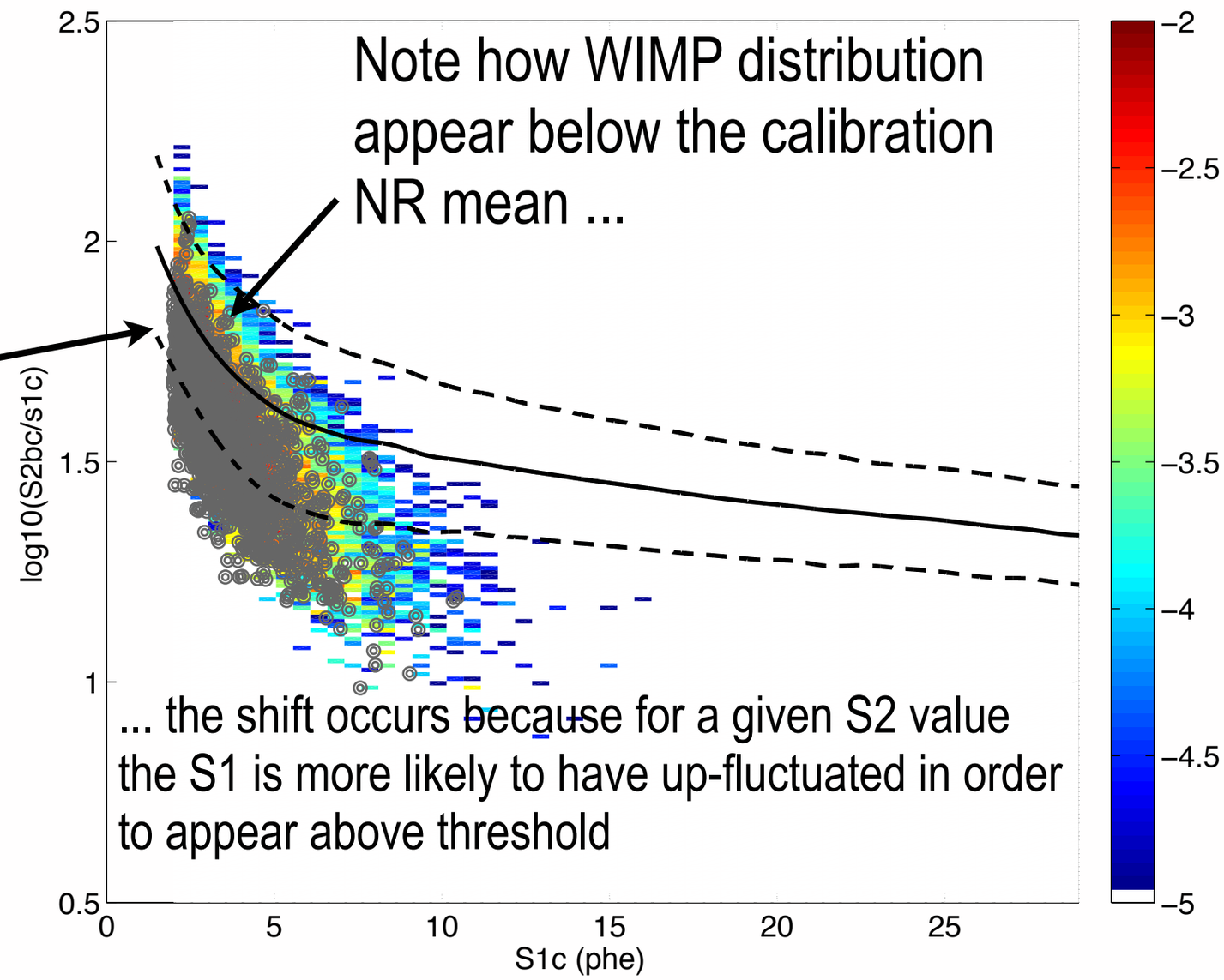

- The shift in the WIMP PDF downwards improves the effective ER event leakage fraction

Position of Low Energy Events in 85 day Exposure

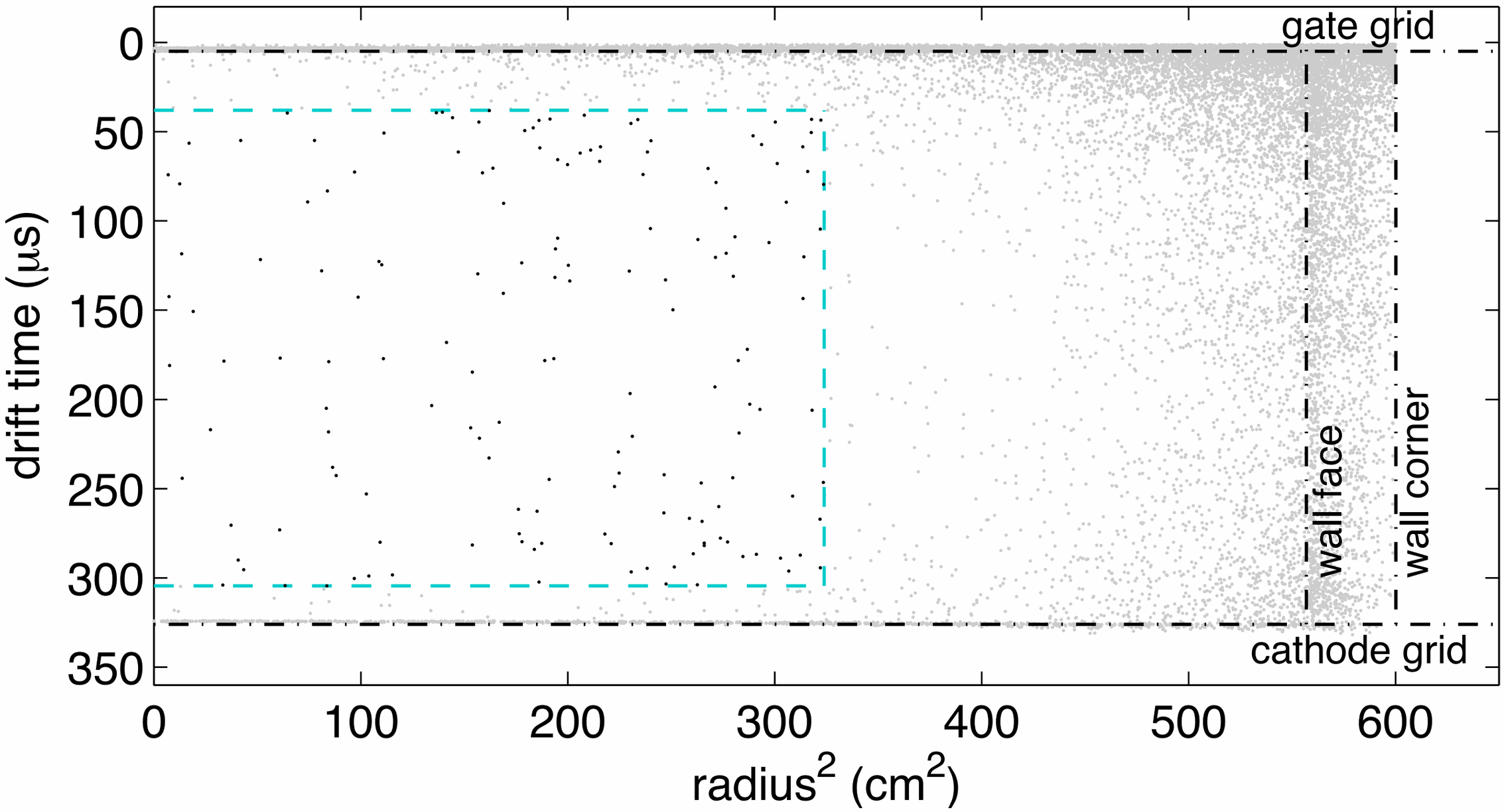

LUX WIMP Search, 85 live-days, 118 kg

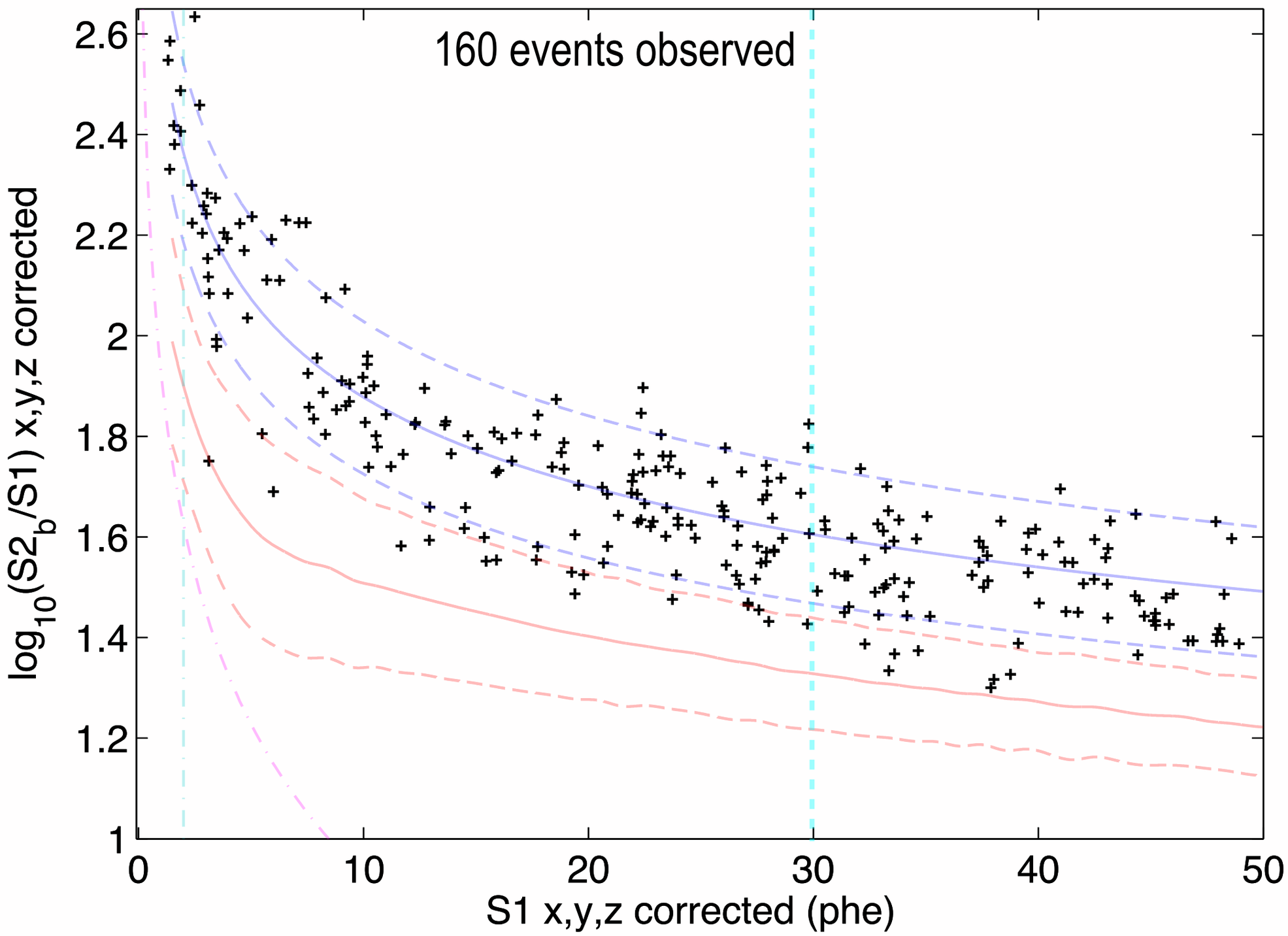

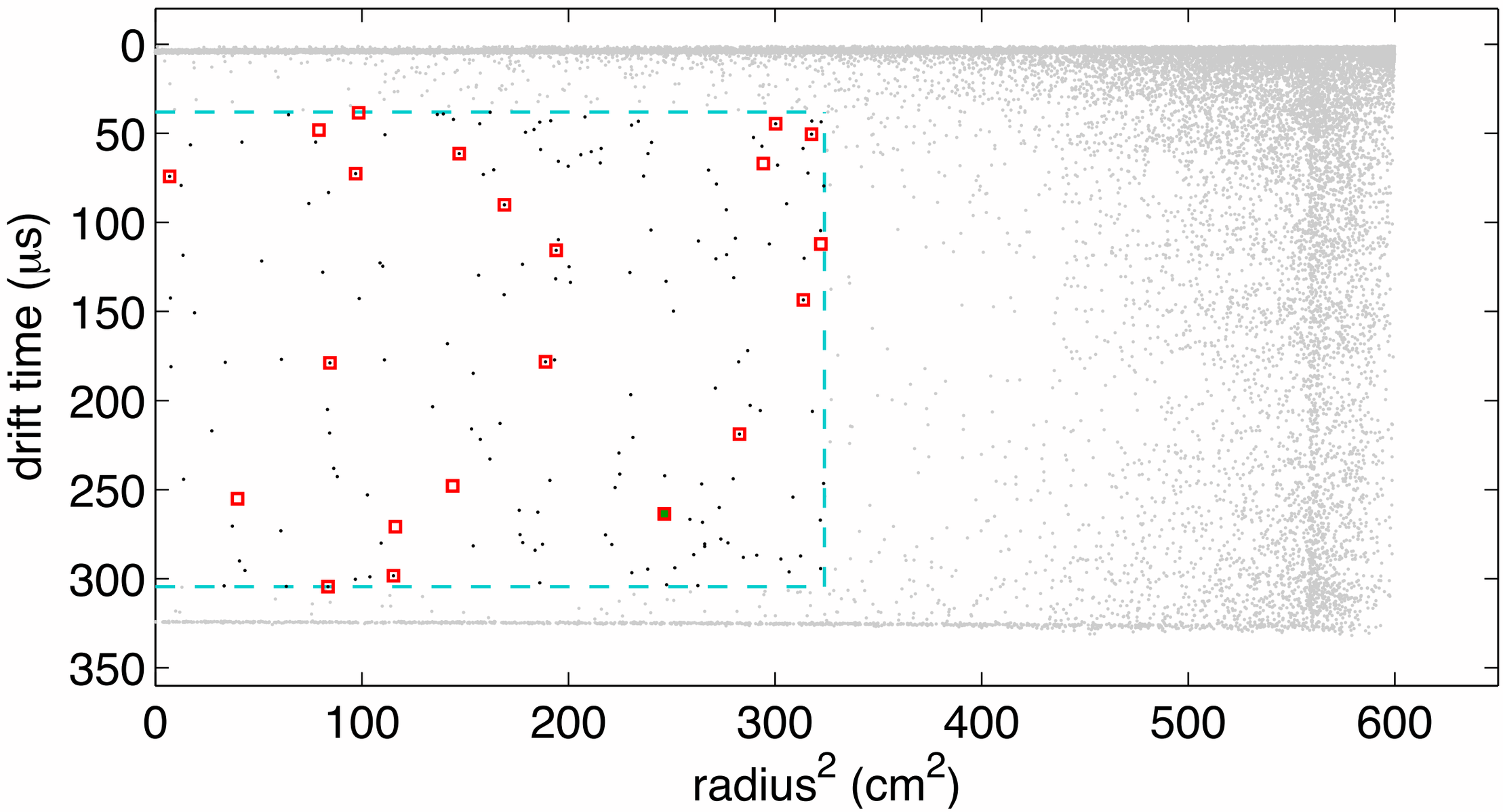
0
50
100
150
200
250
300
350
drift time (μs)
0
100
200
300
400
500
600
radius^2 (cm^2)

LUX WIMP Search, 85 live-days, 118 kg

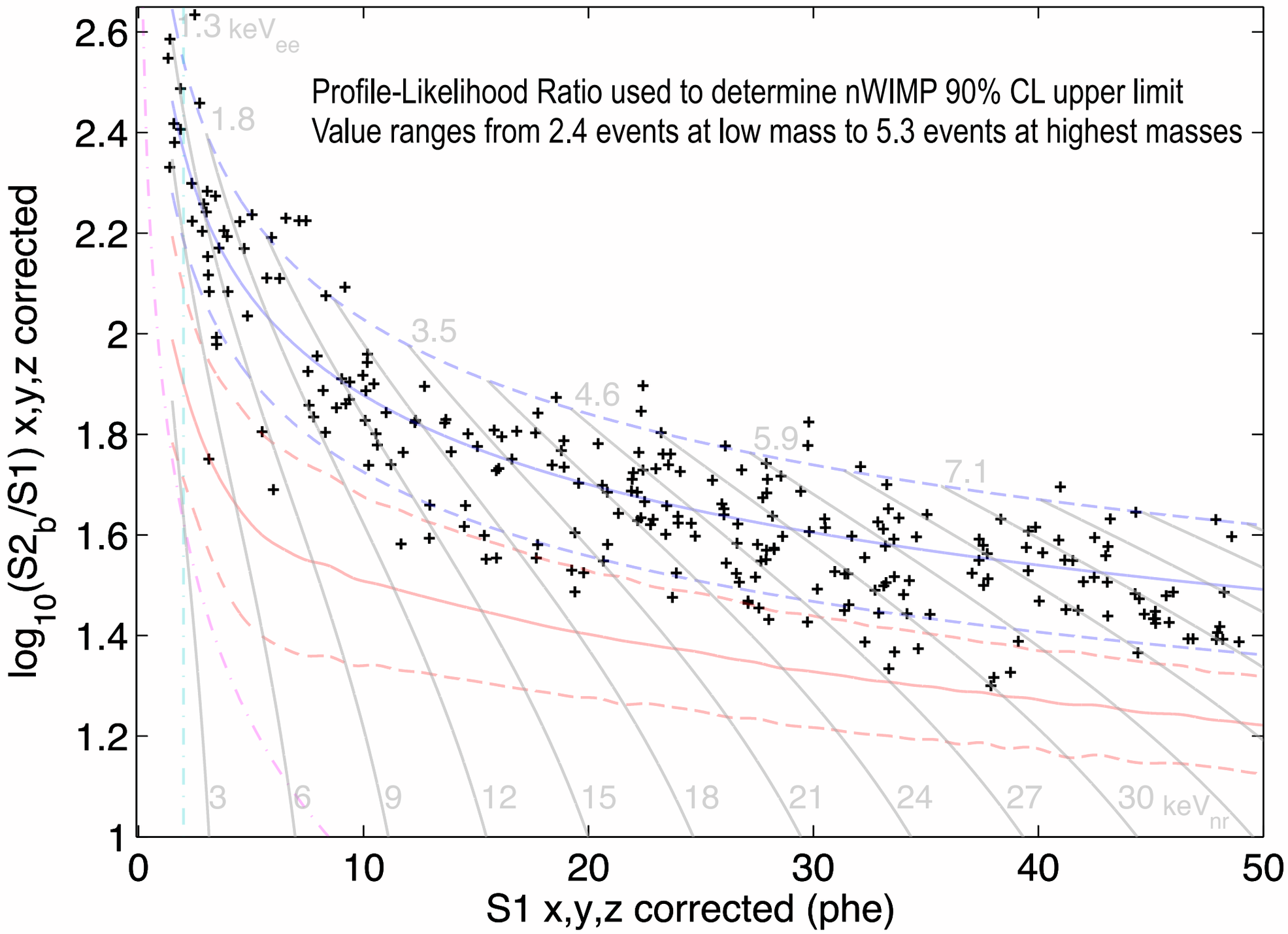

Use an extended likelihood

$$\mathcal{L}_{WS} = \frac{e^{-N_s - N_{Compt} - N_{Xe-127} - N_{Rn222}}}{\mathcal{N}!} \prod_{i=1}^{\mathcal{N}} N_s P_s(\boldsymbol{x}; \boldsymbol{\sigma}, \boldsymbol{\theta_s}) + N_{Compt} P_{ER}(\boldsymbol{x}; \boldsymbol{\theta_{Compt}}) + N_{Xe-127} P_{ER}(\boldsymbol{x}; \boldsymbol{\theta_{Xe-127}}) + N_{Rn} P_{ER}(\boldsymbol{x}; \boldsymbol{\theta_{Rn}})$$

Discriminant between ER/NR

Energy

Discriminant against external/internal radiation

Observables: $\mathbf{x} = (S1, \log_{10}(S2/S1), r, z)$

Parameter of interest: N_s

Nuisance parameters: N_{Compt}, $N_{Xe\text{-}127}$, $N_{Rn/Kr\text{-}85}$

Gaussian constrain to within 30% of the predicted rates

Predicted WIMP scattering

$$\frac{dR}{dE_R} = N_T \frac{\rho_\chi}{M_\chi} \int_{v_{min}}^{\infty} v f_\oplus(\vec{v}, \vec{v}_e) \frac{d\sigma}{dE_R} d^3v$$

C. McCabe, Phys. Rev. D, **82**, 023530 (2010)

$$\frac{d\sigma}{dE_R} = \frac{1}{2v^2} \frac{M_N \sigma_n}{\mu_{ne}^2} \frac{(f_p Z + f_n(A-Z))^2}{{f_n}^2} F^2(E_R)$$

Use standard isothermal halo model with cutoff

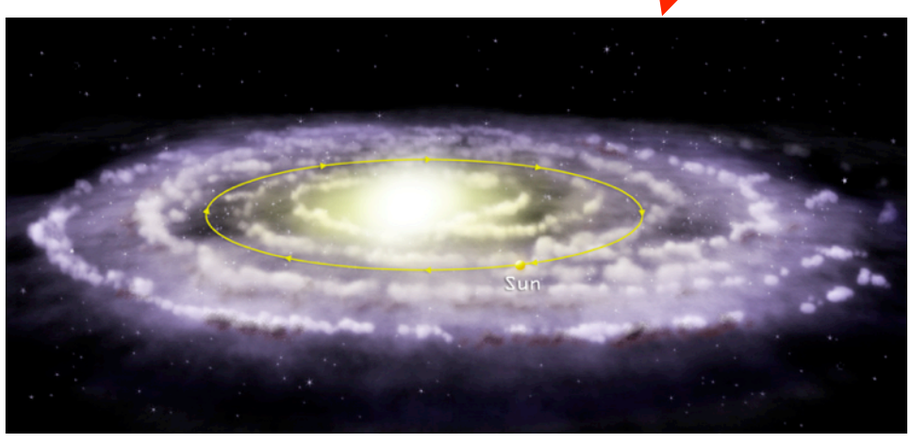

Use Helm form factor

$$F^2(E_R) = \left(\frac{3j_1(qR)}{qR}\right)^2 e^{-q^2 s^2}$$

$$R = \sqrt{r^2 - 5s^2}$$

Velocity of solar system in the galaxy: v_0 = 220 km/s

Velocity of earth around the sun: v_E = 245 km/s

Galactic escape velocity: v_{esc} = 544 km/s

Local dark matter density: ρ = 0.3 GeV/c^2/cm^3

WIMP signal model

$$P_s(log_{10}(S2/S1)|S1)P_s(E_{NR}(S1))P_s(r)P_s(z)$$

$$P_s(E_{NR}(S1)) = \varepsilon(S1)\frac{dR}{dE_{NR}}(\sigma_0, m_{wimp}, \boldsymbol{\theta_{dm}})\frac{dE_{NR}}{dS1}$$

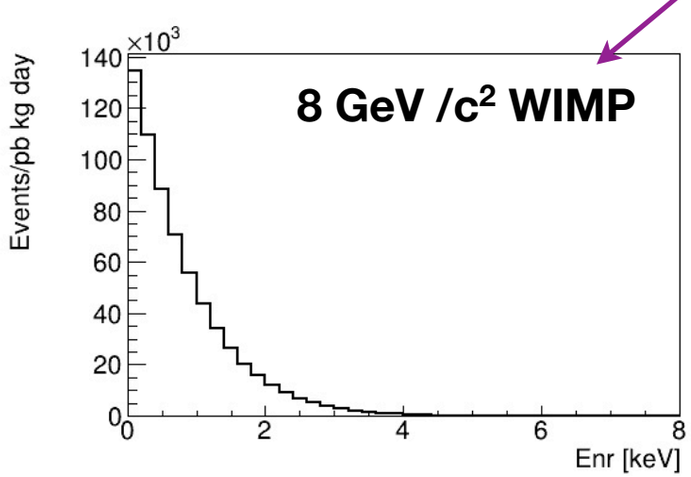

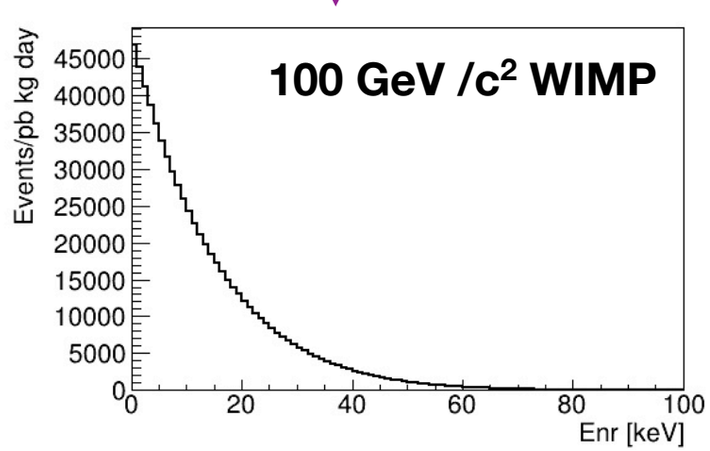

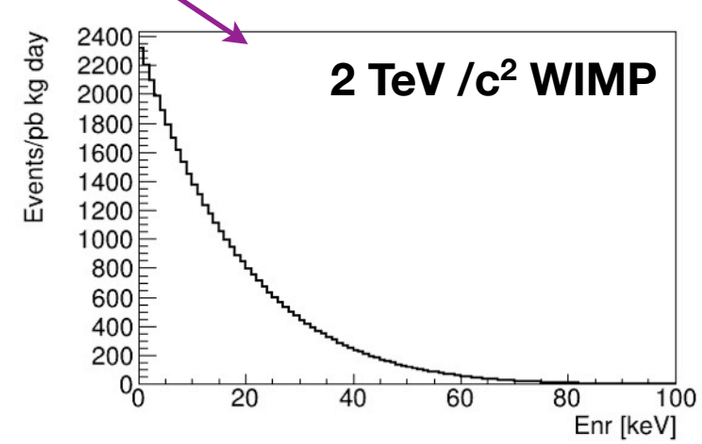

Use simulation in final model of WIMP signal

$$P_s(log_{10}(S2/S1)|S1)P_s(E_{NR}(S1))P_s(r)P_s(z)$$

Model as uniform in (r^2,z)

Use realistic simulation to model 2D pdf, includes resolution and efficiencies

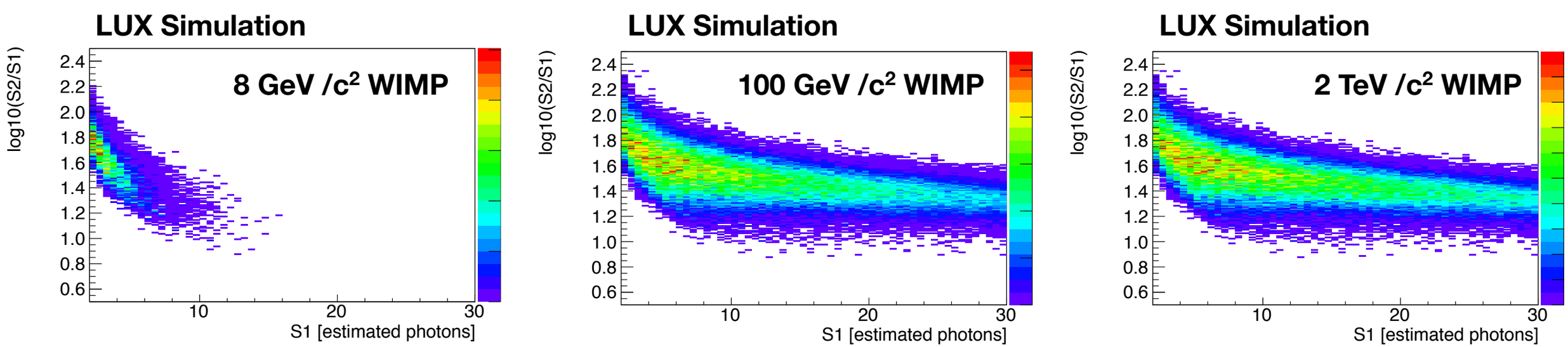

Radioactive materials model

$$P_{ER}(log_{10}(S2/S1)|S1)P_{Compton}(E_{ee}(S1))P_{Compton}(r,z)$$

Model as uniform in $E_{ee} \in [0.9, 5.1]$ keVee

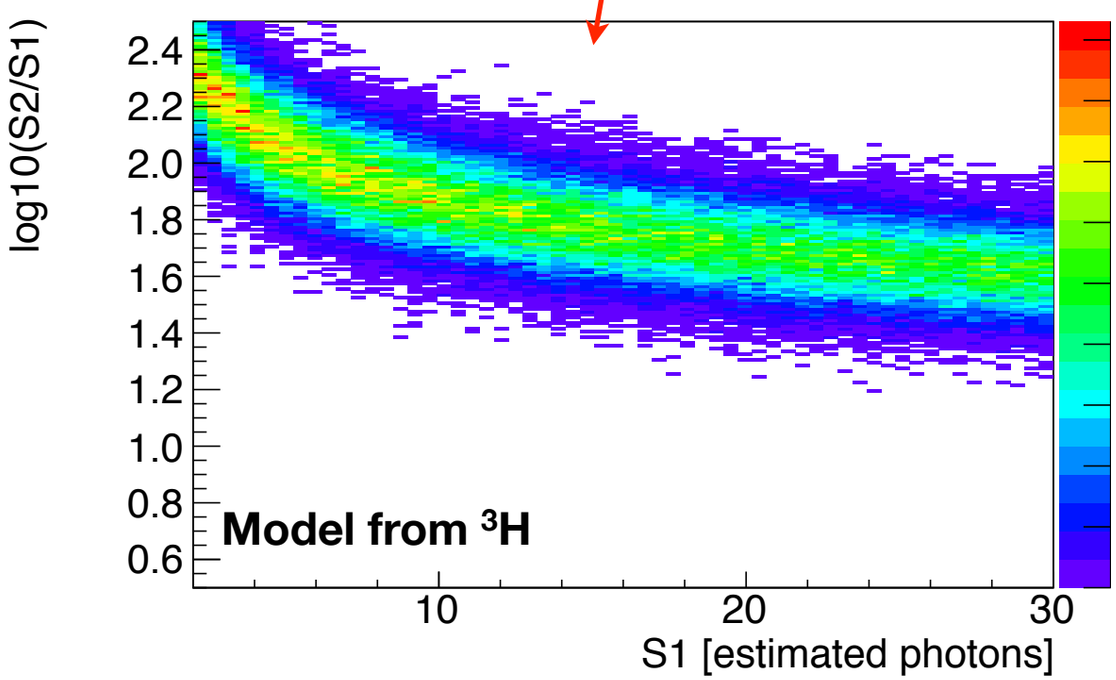

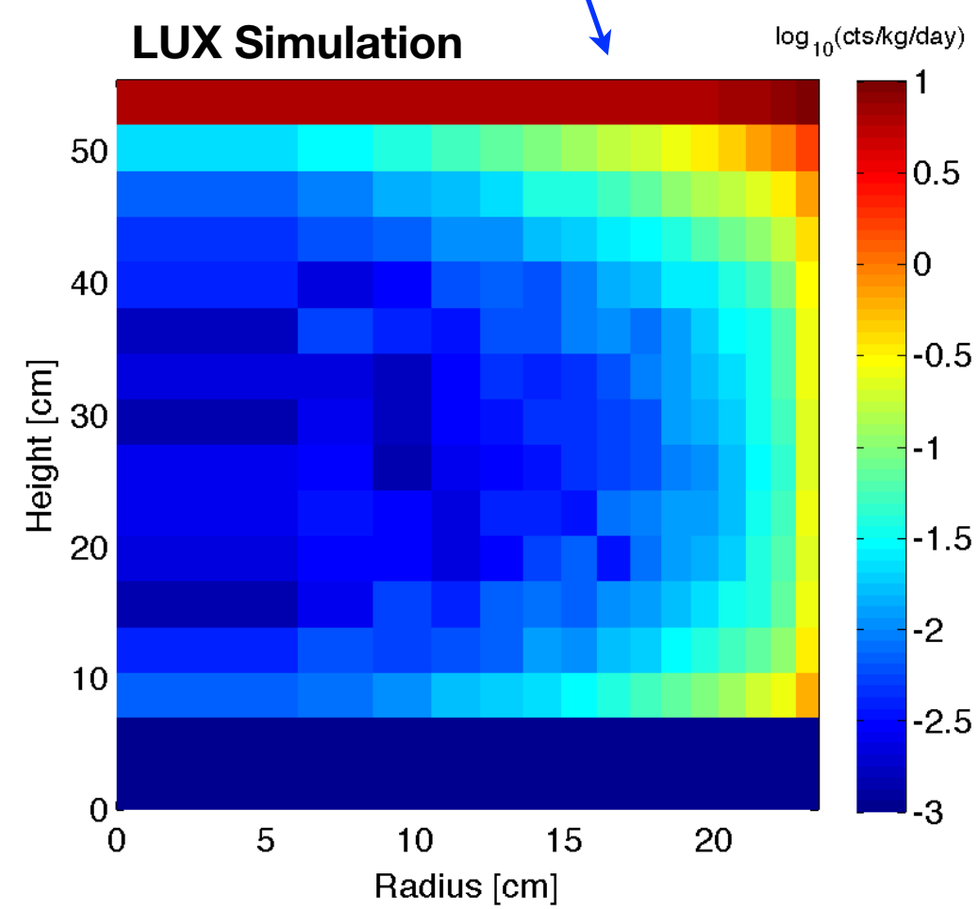

Predict 129 events in WIMP search data

^{127}Xe model

$$P_{ER}(log_{10}(S2/S1)|S1)P_{^{127}Xe}(E_{ee}(S1))P_{^{127}Xe}(r,z)$$

Again use simulation to model pdfs, includes resolution and efficiencies

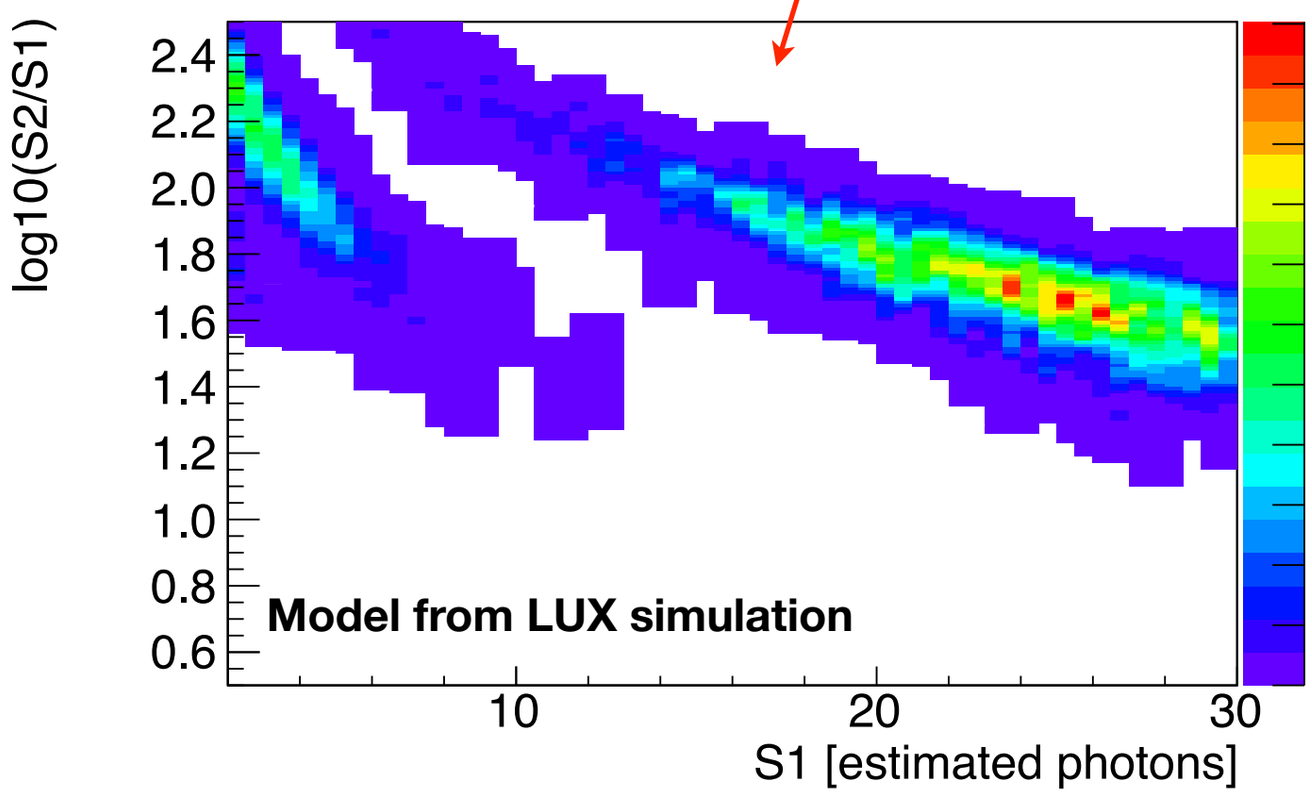

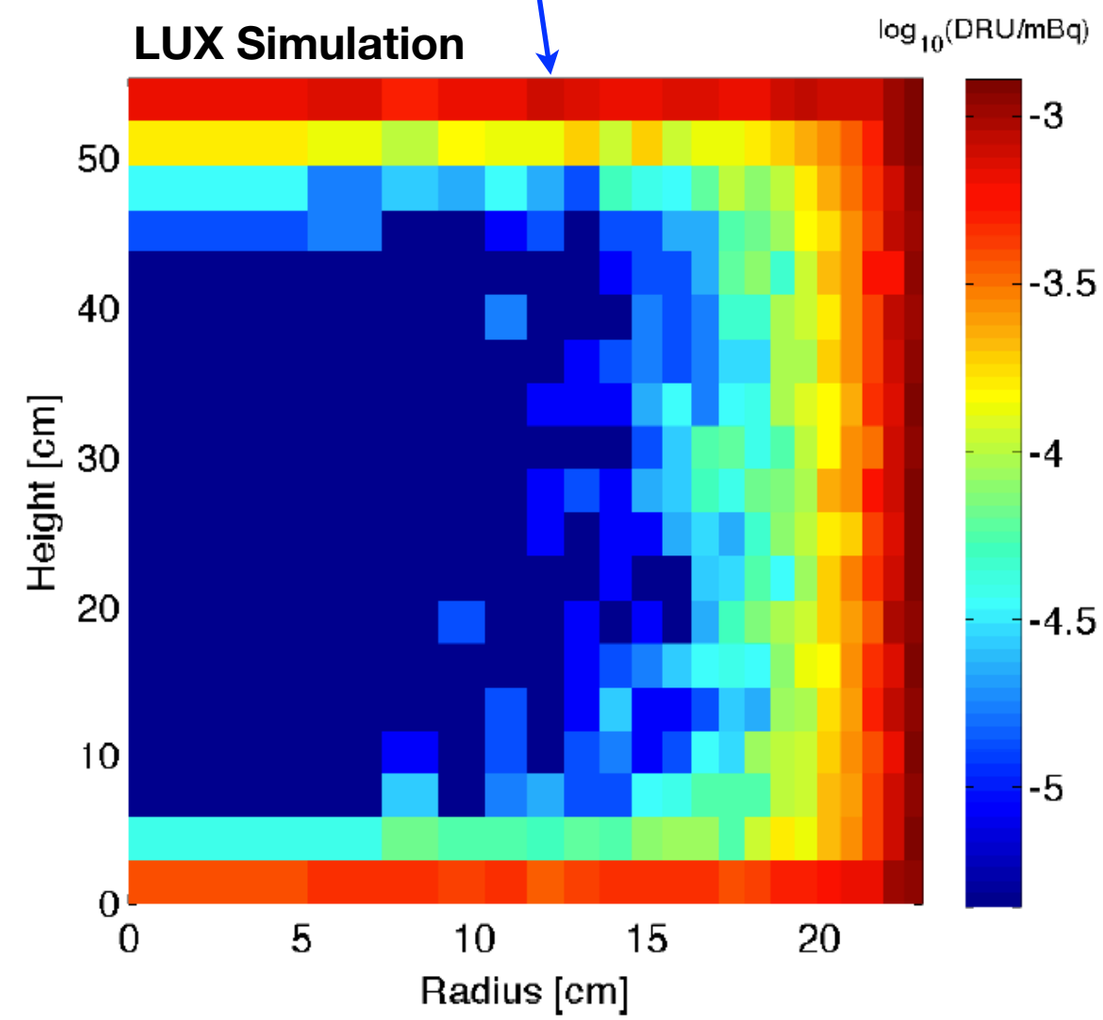

Predict 15 events in WIMP search region

$^{214}Pb/^{85}Kr$ background

$$P_{ER}(log_{10}(S2/S1)|S1)\,P_{Rn}(E_{ee}(S1))\,P_{Rn}(r)P_{Rn}(z)$$

Model as uniform in $E_{ee} \in [0.9, 5.1]$ keVee

Model as uniform in (r^2,z)

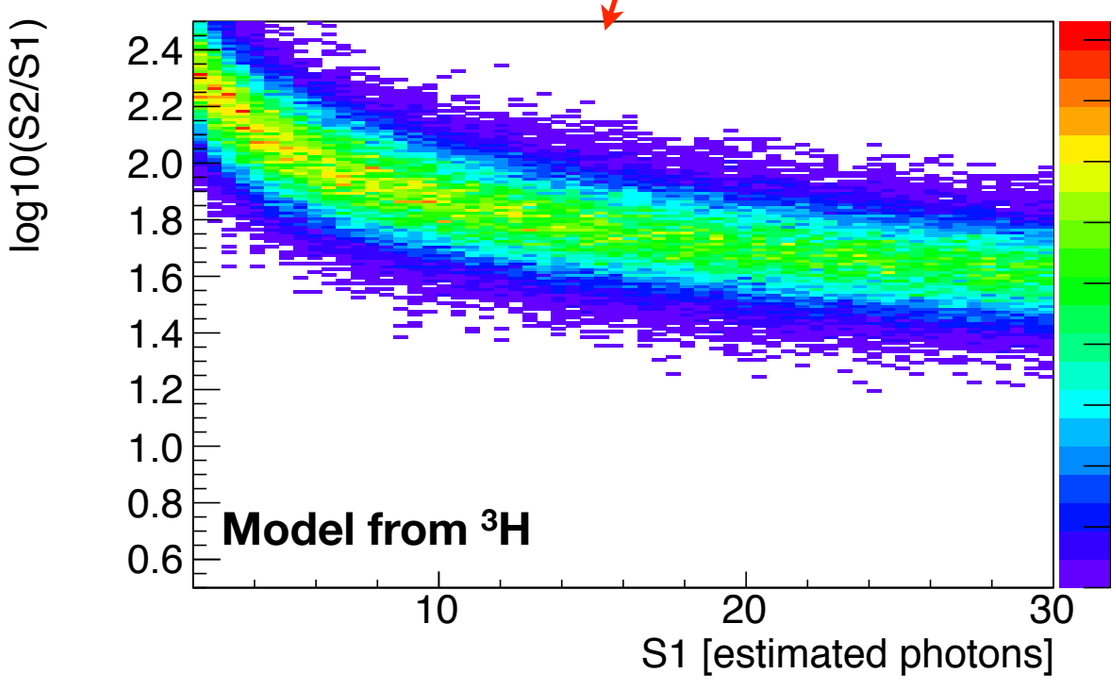

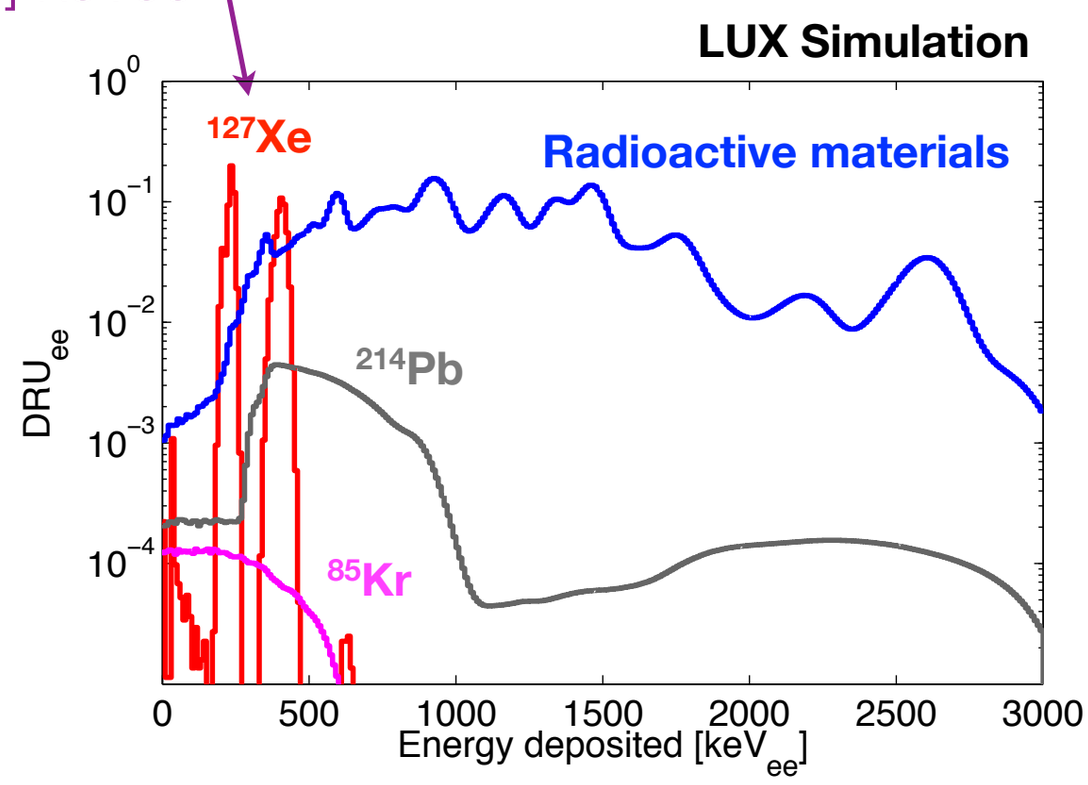

Predict 10 events in WIMP search region

Background Summary for 118 kg Fiducial

- Average levels over period April-August WIMP Search Run

Background Component	Source	10^{-3} x evts/keVee/kg/day
Gamma-rays	Internal Components including PMTS (80%), Cryostat, Teflon	$1.8 \pm 0.2_{stat} \pm 0.3_{sys}$
^{127}Xe (36.4 day half-life)	Cosmogenic 0.87 -> 0.28 during run	$0.5 \pm 0.02_{stat} \pm 0.1_{sys}$
^{214}Pb	222Rn	$0.11\text{-}0.22_{(90\%\ CL)}$
^{85}Kr	Reduced from 130 ppb to 3.5±1 ppt	$0.13 \pm 0.07_{sys}$
Predicted	Total	$2.6 \pm 0.2_{stat} \pm 0.4_{sys}$
Observed	Total	$3.1 \pm 0.2_{stat}$

Spin Independent Sensitivity

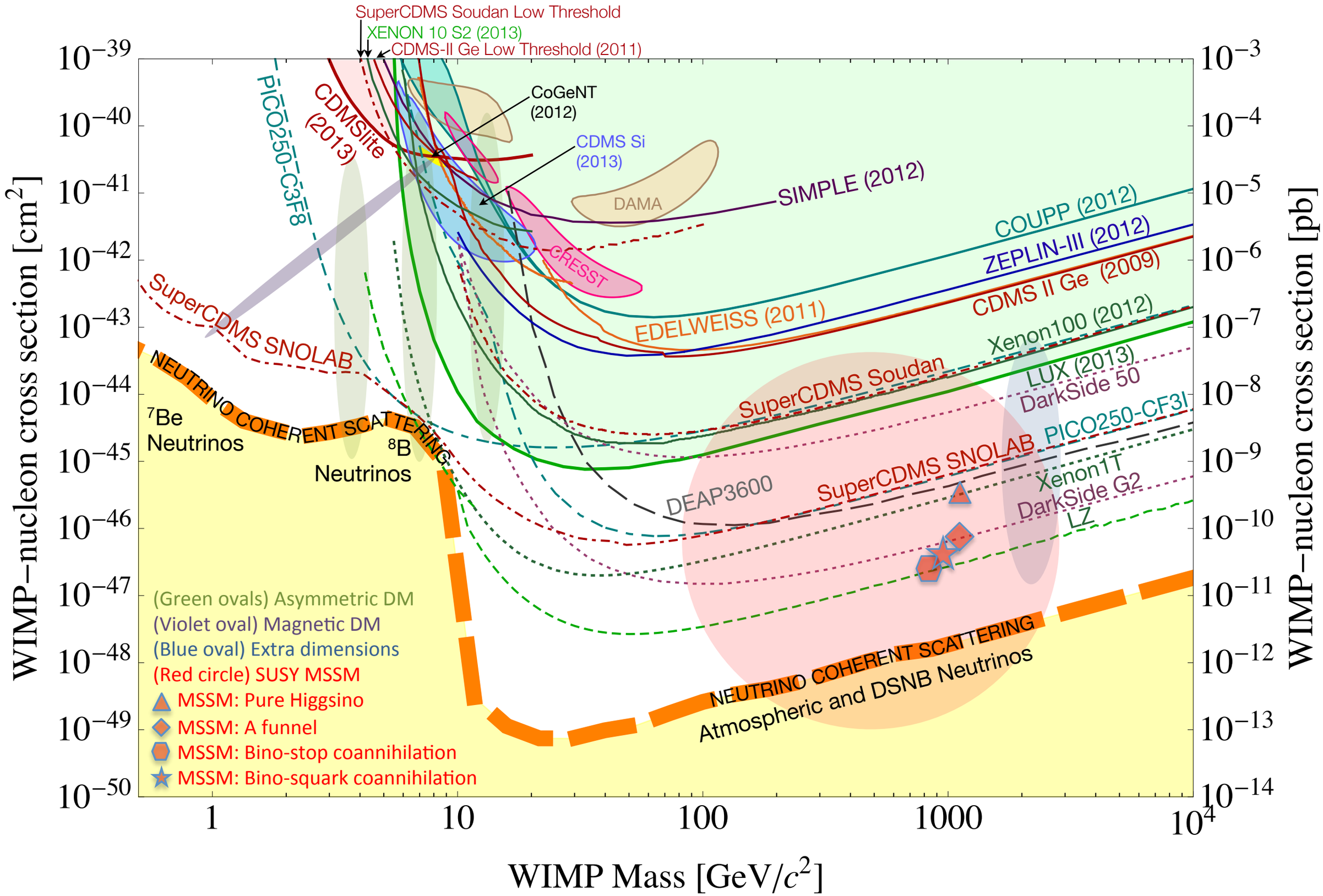

Spin Independent Sensitivity

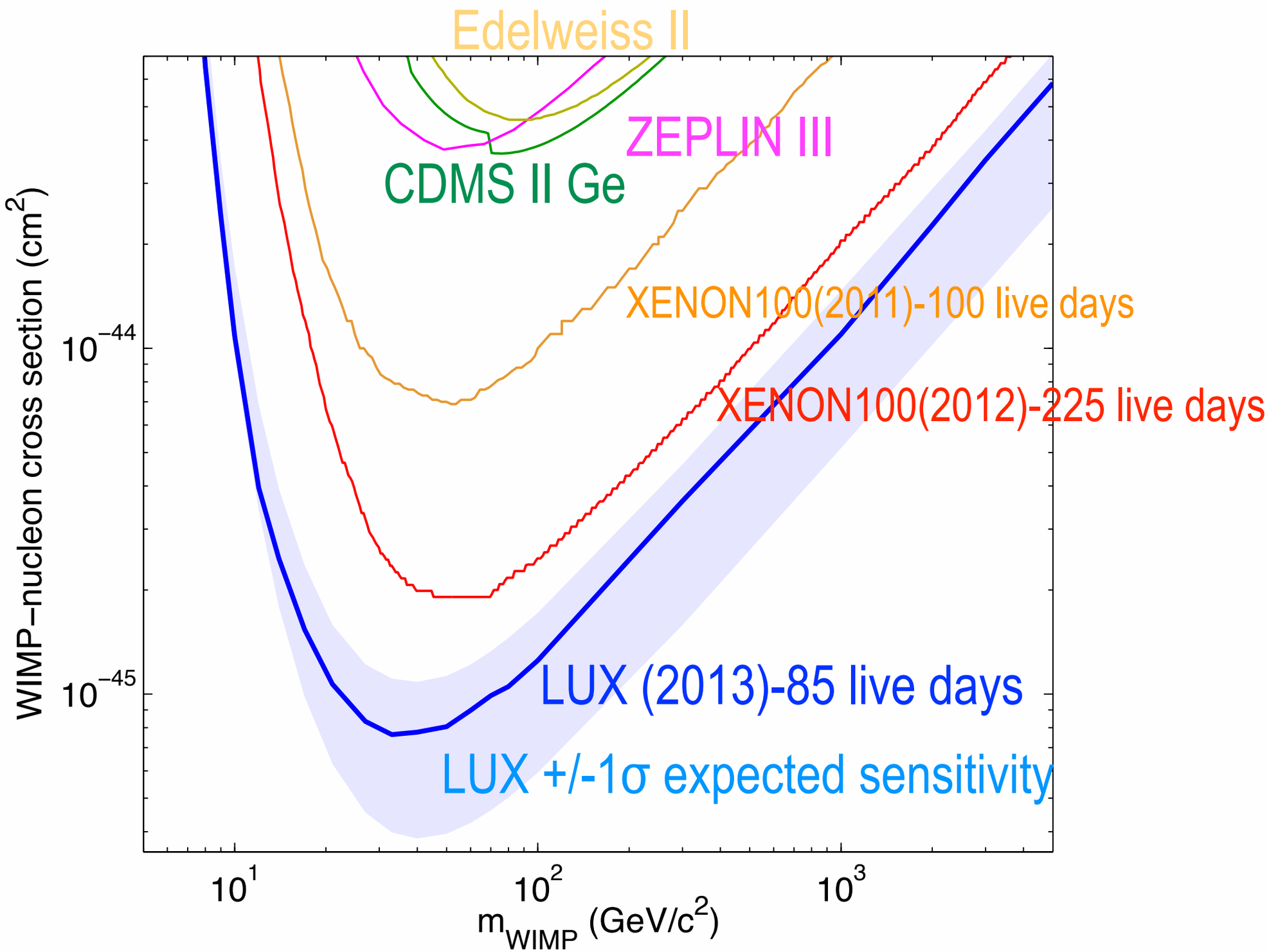

Spin Independent Sensitivity Plots

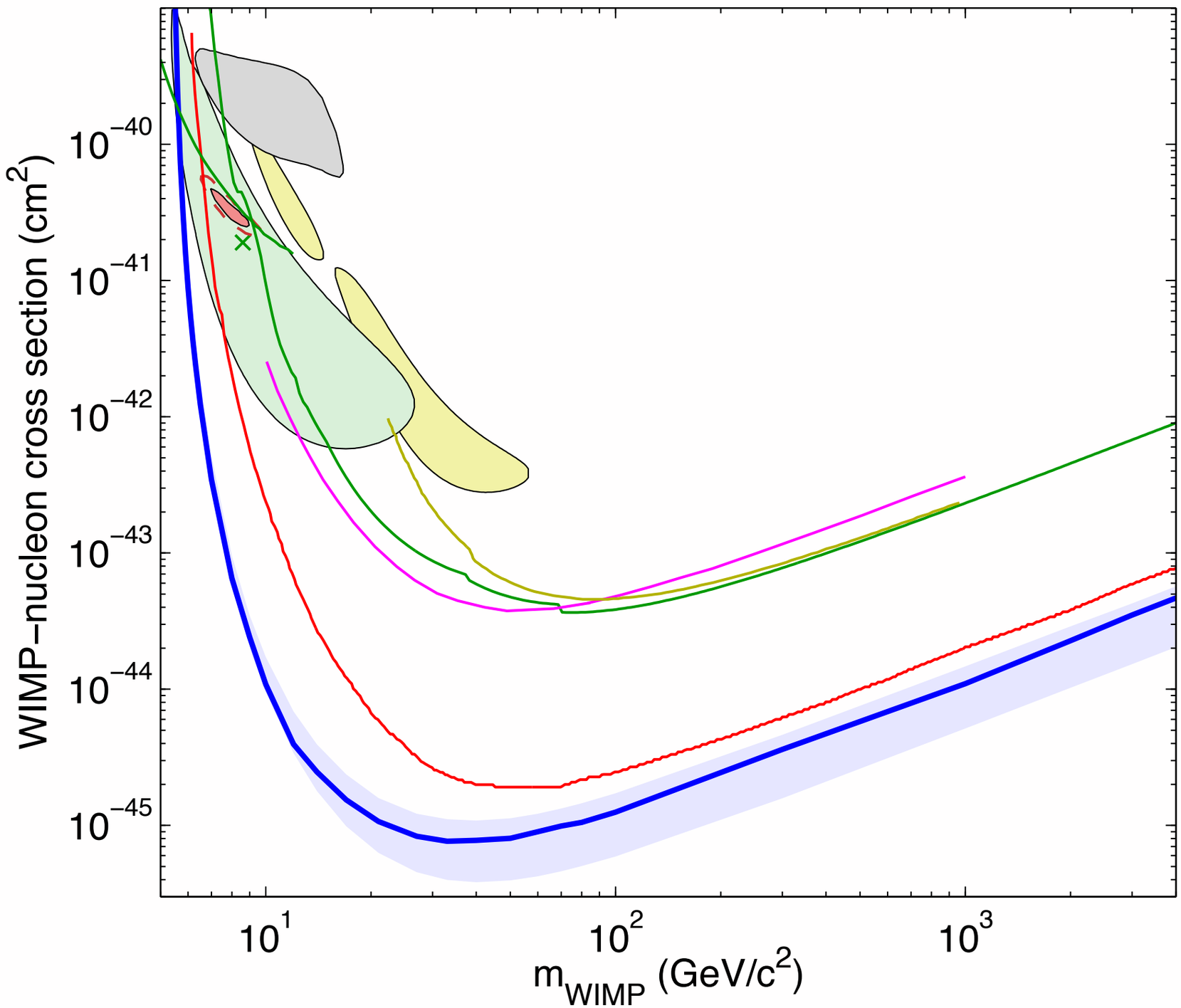

Low Mass Region

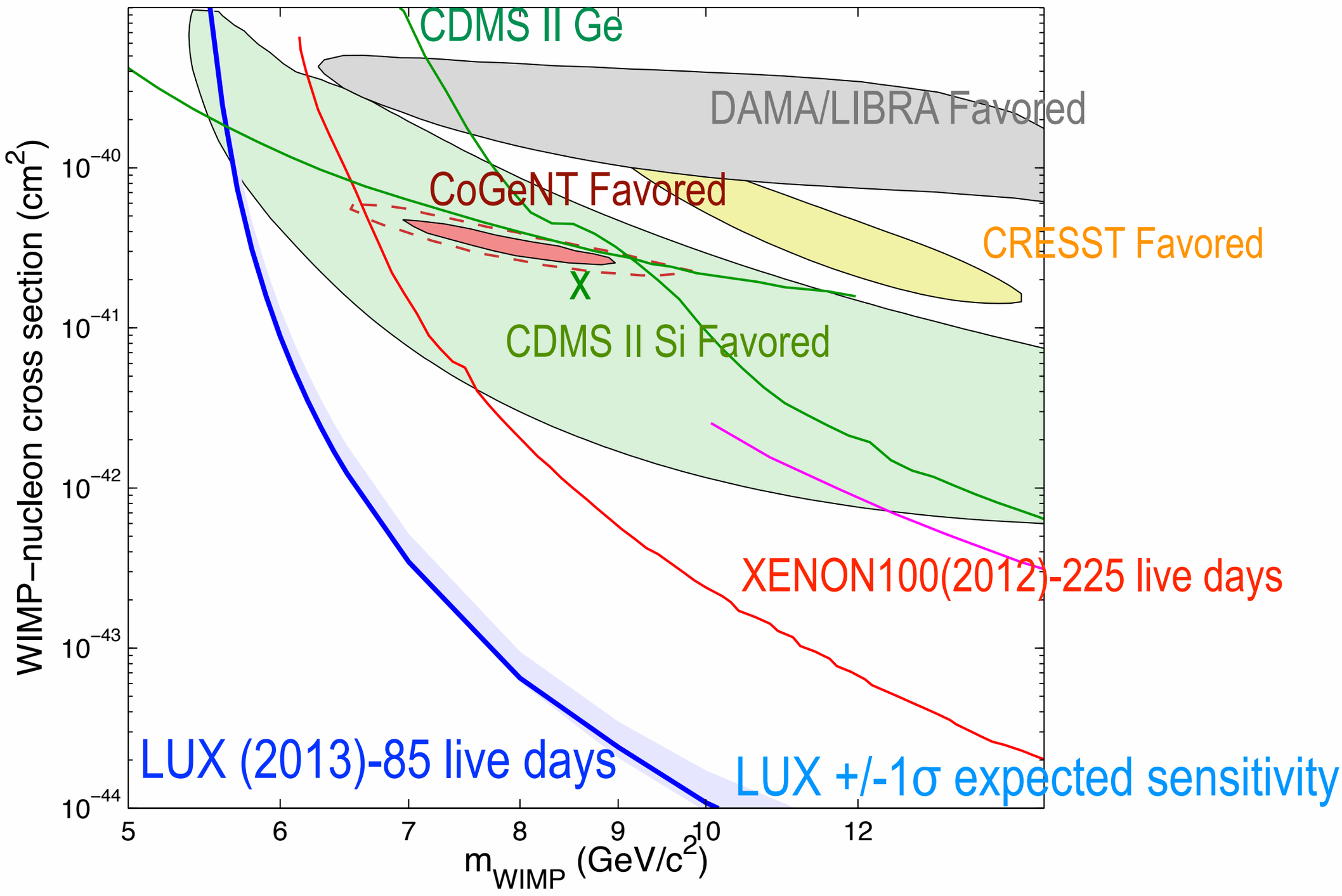

LUX WIMP Search, 85 live-days, 118 kg

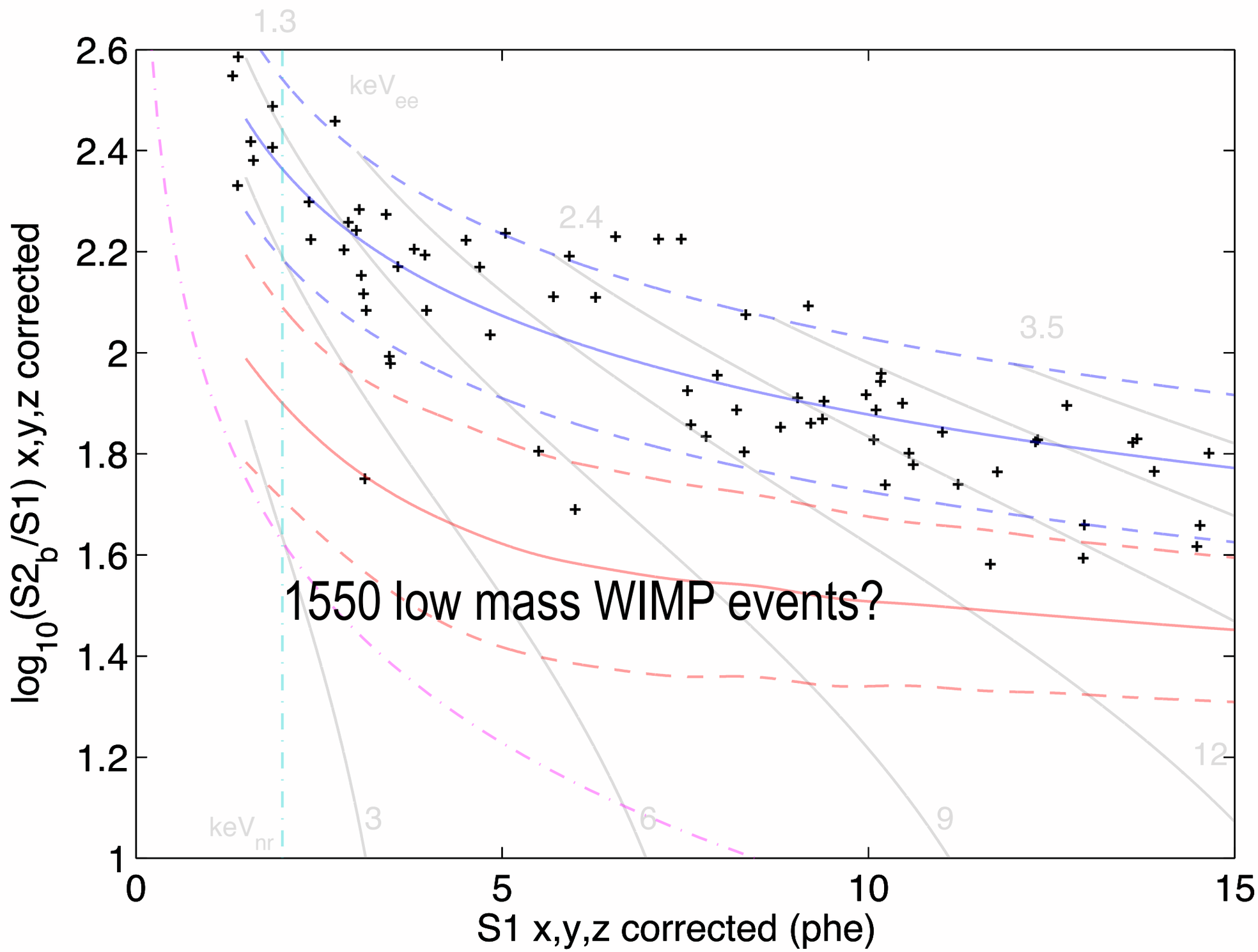

The Near-Term Future

- Detector work
- Additional calibrations
- Start (notional) year-long run

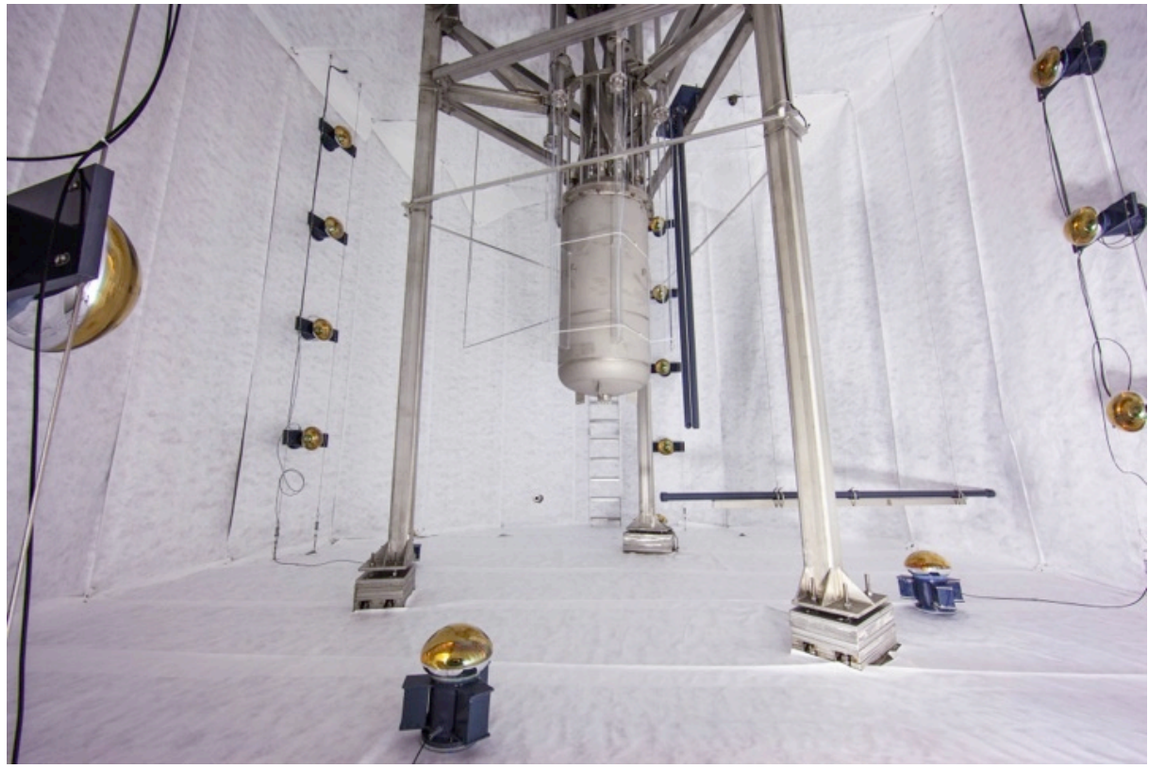

Next: LZ

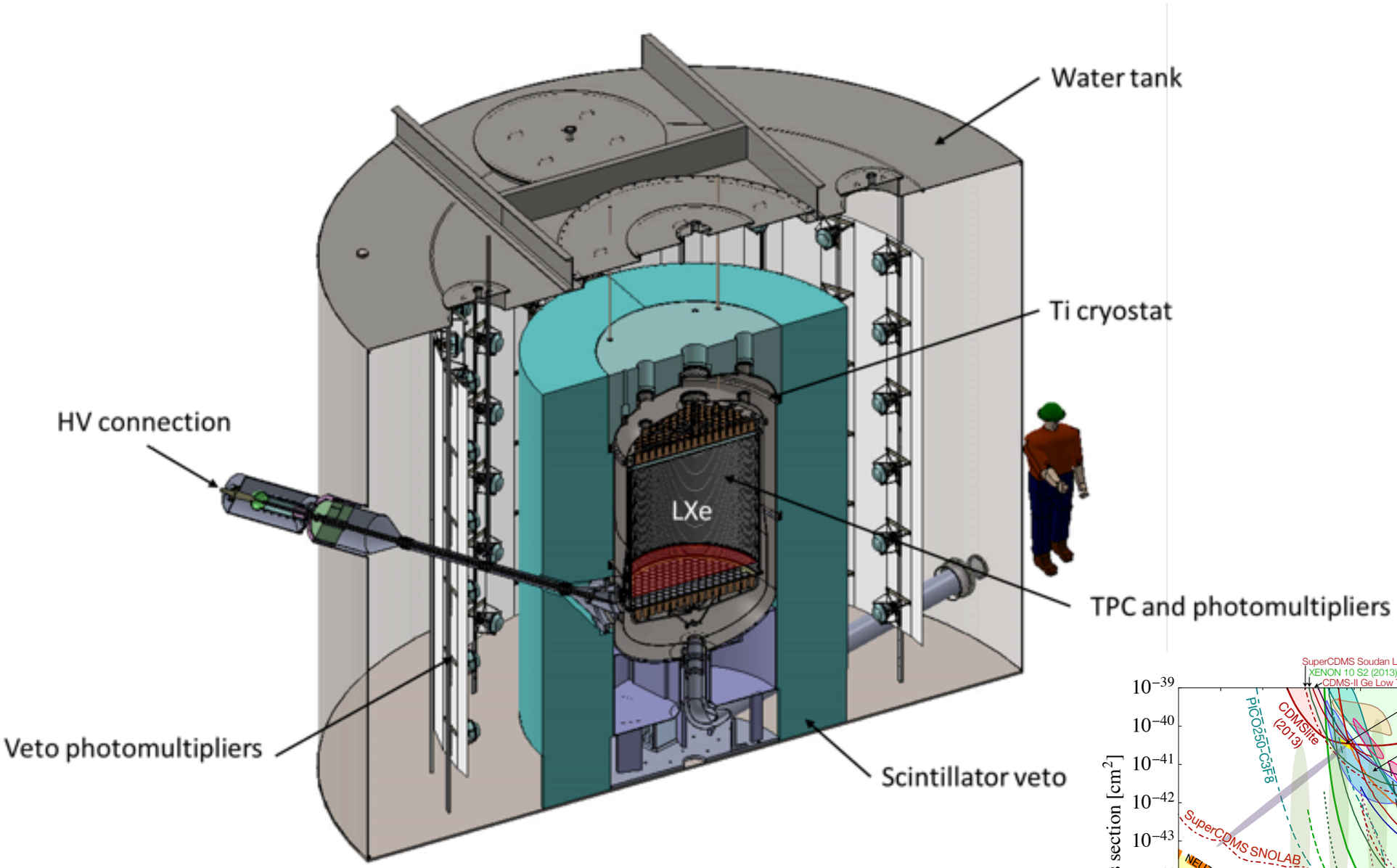
Water tank
Ti cryostat
HV connection
LXe
TPC and photomultipliers
Veto photomultipliers
Scintillator veto

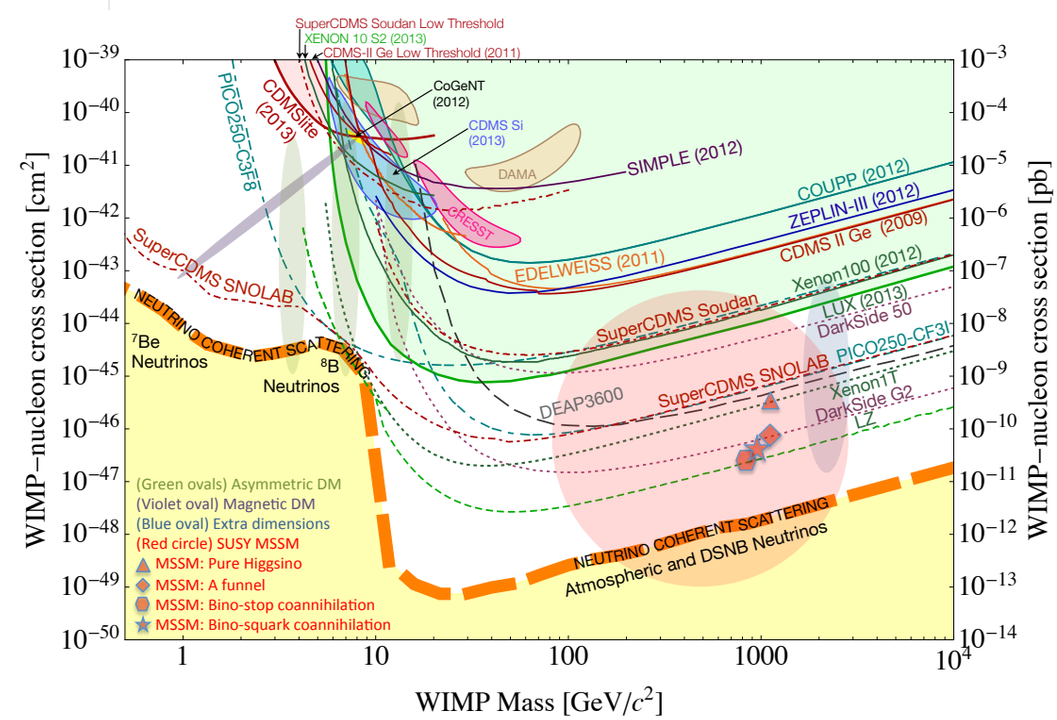
SuperCDMS Soudan Low Threshold
XENON 10 S2 (2013)
CDMS-II Ge Low Threshold (2011)
CoGeNT (2012)
CDMS Si (2013)
CDMSlite (2013)
PICO250-C3F8
DAMA
SIMPLE (2012)
COUPP (2012)
ZEPLIN-III (2012)
CDMS II Ge (2009)
CRESST
EDELWEISS (2011)
Xenon100 (2012)
LUX (2013)
DarkSide 50
SuperCDMS Soudan
SuperCDMS SNOLAB
PICO250-CF3I
Xenon1T
DarkSide G2
LZ
DEAP3600
NEUTRINO COHERENT SCATTERING
7Be Neutrinos
8B Neutrinos
Atmospheric and DSNB Neutrinos
(Green ovals) Asymmetric DM
(Violet oval) Magnetic DM
(Blue oval) Extra dimensions
(Red circle) SUSY MSSM
MSSM: Pure Higgsino
MSSM: A funnel
MSSM: Bino-stop coannihilation
MSSM: Bino-squark coannihilation
WIMP–nucleon cross section [cm^2]
WIMP–nucleon cross section [pb]
WIMP Mass [GeV/c^2]

MULBERRY

Dark Matter Experiment Has Detected Nothing, Researchers Say Proudly

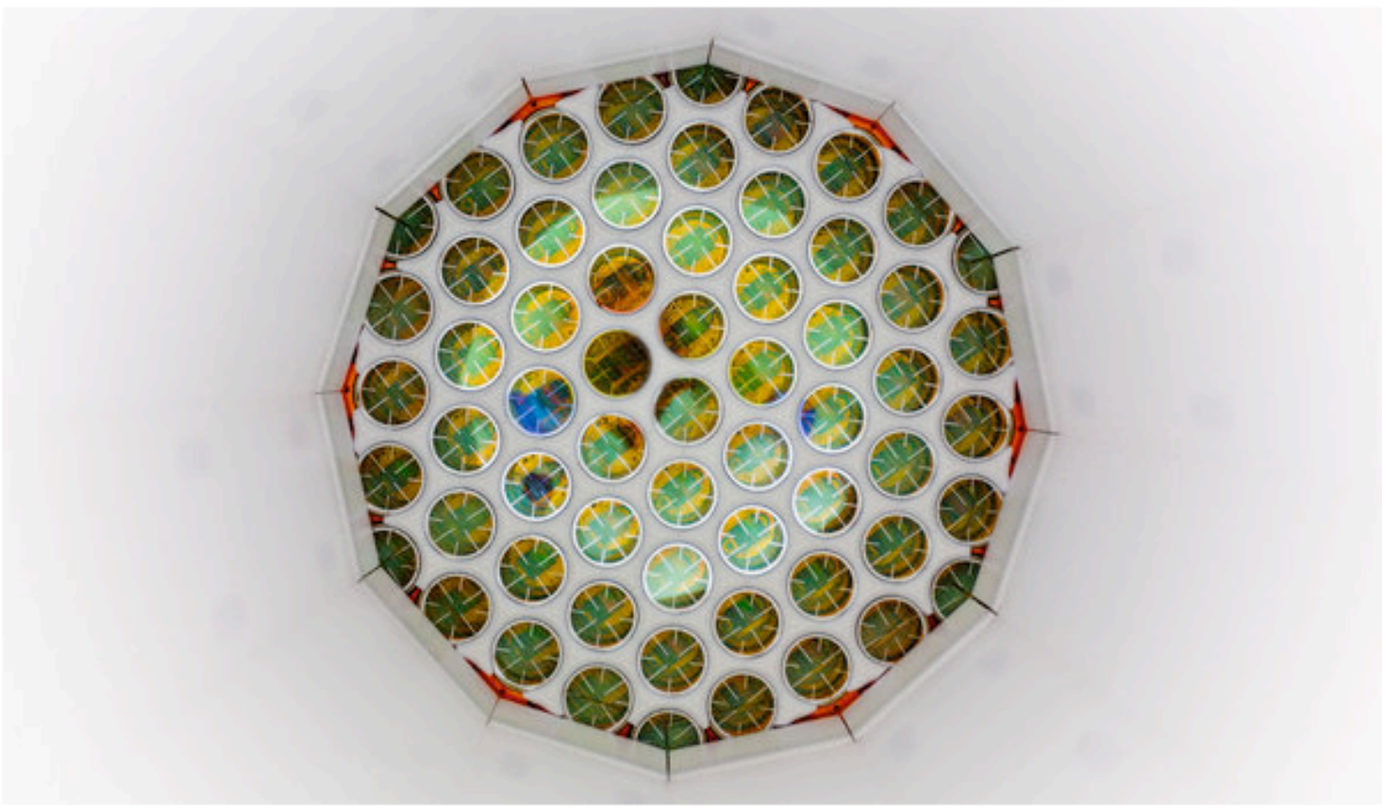

Matthew Kapust/South Dakota Science and Technology Authority

Inside the Large Underground Xenon dark matter detector.

By DENNIS OVERBYE
Published: October 30, 2013

The former Homestake Gold Mine in Lead, S.D., has a hallowed place in the history of physics as a spot where nothing happens.

Connect With Us on Social Media

It was there, in the 1970s, that Raymond Davis Jr. attempted to catch neutrinos, spooky subatomic particles

FACEBOOK
TWITTER
GOOGLE+
SAVE

LUX:

- Operating Well
- Detailed Calibrations
- Backgrounds Understood

Best is yet to come!